The Linnean Society of London
ZOOLOGICAL Journal of the Linnean Society

Osteology of the Late Cretaceous Argentinean sauropod dinosaur Mendozasaurus neguyelap: implications for basal titanosaur relationships

Journal:	*Zoological Journal of the Linnean Society*
Manuscript ID	ZOJ-07-2017-3052.R2
Manuscript Type:	Original Article
Keywords:	Gondwana < Palaeontology, Mesozoic < Palaeontology, Sauropodomorpha < Taxa, Dinosauria < Taxa, phylogeny < Phylogenetics, Evolution, Cretaceous < Palaeontology

Abstract: The titanosaurian sauropod dinosaur Mendozasaurus neguyelap is represented by several partial skeletons from the Upper Cretaceous Sierra Barrosa Formation in Mendoza Province, Argentina. A detailed revision allows us to firmly establish its position within Titanosauria, as well as enabling an emended diagnosis. New remains demonstrate that the presacral vertebrae of Mendozasaurus were not unusually short anteroposteriorly, with this compression instead resulting from taphonomic crushing. Mendozasaurus was incorporated into an expanded version of a titanosauriform-focussed phylogenetic data matrix, along with several other contemporaneous South American titanosaurs. The resultant data matrix comprises 84 taxa scored for 423 characters and and our analysis recovers Mendozasaurus as the most basal member of a diverse Lognkosauria, including Futalognkosaurus and the gigantic titanosaurs Argentinosaurus, Notocolossus, Patagotitan and Puertasaurus. Lognkosauria forms a clade with Rinconsauria (Muyelensaurus + Rinconsaurus), with Epachthosaurus and Pitekunsaurus recovered at the base of this grouping. A basal lithostrotian position for this South American clade is well supported, contrasting with some analyses that have placed these taxa outside of Lithostrotia or closer to Saltasauridae. The sister clade to this South American group is composed of an array of near-global taxa, and supports the hypothesis that most titanosaurian clades were widespread by the Early–middle Cretaceous.

ABSTRACT

The titanosaurian sauropod dinosaur *Mendozasaurus neguyelap* is represented by several partial skeletons from a single locality within the Coniacian (lower Upper Cretaceous) Sierra Barrosa Formation in the south of Mendoza Province, northern Neuquén Basin, Argentina. A detailed revision of *Mendozasaurus*, including previously undocumented remains from the holotype site, allows us to more firmly establish its position within Titanosauria, as well as enabling an emended diagnosis of this taxon. Autapomorphies include: (1) middle and posterior cervical vertebrae with tall and transversely expanded neural spines that are wider than the centra, formed laterally by spinodiapophyseal laminae that are not connected with the pre- or postzygapophyses; (2) anterior caudal vertebrae (excluding anteriormost) with ventrolateral ridge-like expansion of prezygapophyses; and (3) humerus with divided lateral distal condyle on anterior surface. New remains demonstrate that the presacral vertebrae of *Mendozasaurus* were not unusually short anteroposteriorly, with this compression instead resulting from taphonomic crushing. Comparative studies of articulated pedes of other taxa allow us to interpret that the pedal formula of *Mendozasaurus* was 2-2-2-2-0, based on disarticulated bones that form a right hind foot. *Mendozasaurus* was incorporated into an expanded version of a titanosauriform-focussed phylogenetic data matrix, along with several other contemporaneous South American titanosaurs. The resultant data matrix comprises 84 taxa scored for 423 characters and our phylogenetic analysis recovers *Mendozasaurus* as the most basal member of a diverse Lognkosauria, including *Futalognkosaurus* and the gigantic titanosaurs *Argentinosaurus*, *Notocolossus*, *Patagotitan* and *Puertasaurus*. Lognkosauria forms a clade with Rinconsauria (*Muyelensaurus* + *Rinconsaurus*), with *Epachthosaurus* and *Pitekunsaurus* recovered at the base of this grouping. A basal lithostrotian position for this South American clade is well supported, contrasting with some analyses that have placed these taxa outside of Lithostrotia or closer to Saltasauridae. The sister clade to this South American group is composed of an array of near-global taxa, and supports the hypothesis that most titanosaurian clades were widespread by the Early–middle Cretaceous.

ADDITIONAL KEYWORDS: Gondwana–Lithostrotia–Lognkosauria–Mendoza–Mesozoic–Neuquén Group–Sierra Barrosa Formation–Titanosauriformes

INTRODUCTION

The Cretaceous of South America records a diverse array of titanosauriform sauropod dinosaurs, including some of the largest and smallest sauropods to have ever lived (Powell, 2003; González Riga, 2010; Mannion & Otero, 2012; García *et al*., 2014; Lacovara *et al*., 2014; Jesus Faria *et al*., 2015; Carballido *et al*., 2017). Mendoza Province, situated in the western central region of Argentina, has thus far yielded four titanosauriform genera (*Mendozasaurus neguyelap* [González Riga, 2003], *Malarguesaurus florenciae* [González Riga, Previtera & Pirrone, 2009], *Quetecsaurus rusconii* [González Riga & Ortiz David, 2014], and *Notocolossus gonzalezparejasi* [González Riga *et al*., 2016]), as well as indeterminate remains (Wilson, Martinez & Alcober, 1999) and trackways (including *Titanopodus mendozensis*; González Riga & Calvo, 2009; González Riga, 2011; González Riga *et al*., 2015) attributed to this clade. These sauropod-bearing deposits span much of the Late Cretaceous (González Riga & Astini, 2007).

Mendozasaurus neguyelap was the first dinosaur to be named from Mendoza, and is represented by several partial skeletons collected by the lead author from a single locality in the south of the province (Fig. 1), close to the border with Neuquén Province (González Riga, 2003, 2005; González Riga & Astini, 2007). Originally assigned to an unnamed stratigraphic unit within the Río Neuquén Subgroup (González Riga, 2003), the remains of *Mendozasaurus* were later ascribed to either the Portezuelo or Plottier Formation (see González Riga & Astini, 2007). However, following stratigraphic revision of the Neuquén Group, including subdivision of the Portezuelo Formation (Garrido, 2010), the position of *Mendozasaurus* has now been constrained to the middle–upper Coniacian Sierra Barrosa Formation (see González Riga & Ortiz David, 2014). The study of the *Mendozasaurus* quarry (Fig. 2) was one of the first taphonomic analyses to be published on Cretaceous dinosaurs from Argentina (González Riga & Astini, 2007). It interpreted the accumulation of several individuals as an 'overbank bone assemblage', highlighting the potential of crevasse splay facies as important sources of paleontological data in Cretaceous meandering fluvial systems.

Calvo *et al*. (2007) described *Futalognkosaurus dukei* from the upper Turonian–Coniacian Portezuelo Formation of Neuquén Province, close to the border with Mendoza Province, and thus spatiotemporally close to the locality yielding *Mendozasaurus*. Their phylogenetic analysis recovered *Futalognkosaurus* as the sister taxon to *Mendozasaurus*, leading these authors to erect the new clade Lognkosauria. Hypotheses regarding the phylogenetic position of *Mendozasaurus* have almost all been based on iterations of data matrices published by González Riga (2003) and Carballido *et al*. (2011a, b). Nearly all analyses agree on a titanosaurian placement, and most of those that have also incorporated *Futalognkosaurus* have recovered it as the sister taxon to *Mendozasaurus*, forming the clade Lognkosauria. The exceptions to this are: (1) the analysis of Carballido *et al*. (2011b), in which *Mendozasaurus* and *Futalognkosaurus* were recovered in a polytomy with all other titanosaurs; (2) the parsimony analysis of Gorscak and O'Connor (2016), in which the two were not closely related (see also Gorscak *et al*., 2017); and (3) that of Carballido *et al*. (2017), in which several taxa were recovered as more closely related to *Futalognkosaurus* than *Mendozasaurus*, resulting in a diverse Lognkosauria. Early iterations of the González Riga (2003) data matrix recovered Lognkosauria as the sister taxon to the late Early Cretaceous African lithostrotian *Malawisaurus* (Calvo *et al*., 2007; Calvo, González Riga & Porfiri, 2008a; González Riga *et al*., 2009; Coria *et al*., 2013). This position is similar to that

recovered in versions of the Carballido *et al*. (2011a) data matrix, in which Lognkosauria has been found to occupy a position either just outside of Lithostrotia (Carballido *et al*. 2012, 2017; Carballido & Sander, 2014; Lacovara *et al*., 2014), or as a basal member of this clade, clustering with other South American taxa (González Riga *et al*., 2016). However, subsequent analyses based on the González Riga (2003) data matrix have placed Lognkosauria in a more derived lithostrotian position. These analyses have grouped Lognkosauria either as a subclade within or sister taxon to the South American Rinconsauria (Gallina & Apesteguía, 2011; Gallina & Otero, 2015; Salgado, Gallina & Paulina Carabajal, 2015), or near to the saltasaurid radiation (González Riga & Ortiz David, 2014; see also the independent analyses of Gorscak and O'Connor, 2016), with a possible close relationship to *Alamosaurus* from the latest Cretaceous of North America (Tykoski & Fiorillo, 2016). As such, much uncertainty still surrounds the position of Lognkosauria within Titanosauria.

Here, we present a revised diagnosis and full description of *Mendozasaurus neguyelap* (Fig. 3), including previously undocumented remains. We also provide an independent analysis of its relationships with other titanosaurs, including testing the monophyly of Lognkosauria.

Institutional abbreviations: **IANIGLA**, Instituto Argentino de Nivología, Glaciología y Ciencias Ambientales, Colección de Paleovertebrados, Mendoza, Argentina; **MAU**, Museo Argentino Urquiza, Rincón de los Sauces, Neuquén, Argentina; **MCF**, Museo 'Carmen Funes', Neuquén, Argentina; **MLP**, Museo de La Plata, La Plata, Argentina; **MUCPv**, Museo de la Universidad Nacional del Comahue, Neuquén, Argentina; **PVL**, Fundacion Miguel Lillo, Universidad Nacional de Tucumán, San Miguel de Tucuman, Argentina; **UNCUYO-LD**, Universidad Nacional de Cuyo, Laboratorio y Museo de Dinosaurios, Mendoza, Argentina; **UNPSJB**, Universidad Nacional de la Patagonia ''San Juan Bosco'', Comodoro Rivadavia, Argentina.

Anatomical abbreviations: **ACDL**, anterior centrodiapophyseal lamina; **aEI**, average Elongation Index; **CDF**, centrodiapophyseal fossa; **CPOL**, centropostzygapophyseal lamina; **CPRL**, centroprezygapophyseal lamina; **lSPRL**, lateral spinoprezygapophyseal lamina; **PCDL**, posterior centrodiapophyseal lamina; **mSPRL**, medial spinoprezygapophyseal lamina; **POCDF**, postzygapophyseal centrodiapophyseal fossa; **PODL**, postzygodiapophyseal lamina; **POSDF**, postzygapophyseal spinodiapophyseal fossa; **PPDL**, paradiapophyseal lamina; **PRCDF**, prezygapophyseal centrodiapophyseal fossa; **PRDL**, prezygodiapophyseal lamina; **SDF**, spinodiapophyseal fossa; **SPDL**, spinodiapophyseal lamina; **SPOF**, spinopostzygapophyseal fossa; **SPOL**, spinopostzygapophyseal lamina; **SPRL**, spinoprezygapophyseal lamina; **TPOL**, intrapostzygapophyseal lamina; **TPRL**, intraprezygapophyseal lamina.

SYSTEMATIC PALEONTOLOGY

SAUROPODA MARSH, 1878
MACRONARIA WILSON & SERENO, 1998
TITANOSAURIFORMES SALGADO, CORIA & CALVO, 1997
TITANOSAURIA BONAPARTE & CORIA, 1993
LITHOSTROTIA UPCHURCH, BARRETT & DODSON, 2004

LOGNKOSAURIA CALVO *ET AL*., 2007

Phylogenetic definition: The least inclusive clade containing *Futalognkosaurus dukei* and *Mendozasaurus neguyelap* (Calvo *et al*., 2007).

Included species: *Argentinosaurus huinculensis*, *Drusilasaura deseadensis*, *Futalognkosaurus dukei*, *Mendozasaurus neguyelap*, *Notocolossus gonzalezparejasi*, *Patagotitan mayorum*, *Pitekunsaurus macayai*, *Puertasaurus reuili*, *Quetecsaurus rusconii*.

Revised diagnosis: Lognkosauria is supported by the following synapomorphies: (1) dorsoventral height of posterior-most cervical and anterior-most dorsal neural spines divided by posterior centrum height of 1.0 or greater (C19 [reversal]); (2) posterior cervical neural arches with deep spinodiapophyseal fossa at base of lateral surface of neural spine (C417); (3) dorsal half of posterior cervical neural spines laterally expanded as a result of expansion of the lateral lamina (C418); (4) lowest aEI value of anterior caudal centra less than 0.6 (C26 [reversal]); (5) base of scapular blade with a 'D'-shaped cross-section (C217); (6) distal end of radius mediolaterally wider than proximal end (C46); (7) ratio of mediolateral breadth of tibial condyle to breadth of fibular condyle of femur greater than 0.8 (C389 [reversal]); (8) proximal end to distal end maximum mediolateral width ratio of metatarsal V less than 1.6 (C74).

MENDOZASAURUS GONZÁLEZ RIGA, 2003

Type species: *Mendozasaurus neguyelap* González Riga, 2003

Holotype: Twenty-two mostly articulated caudal vertebrae (IANIGLA-PV 065/1–22), three anterior chevrons (IANIGLA-PV 065/23–25), and fragments of posterior chevrons (IANIGLA-PV 065/26–30).

Referred material: The following disarticulated bones were found associated with the holotype, including remains not mentioned in previous publications on *Mendozasaurus*: five cervical vertebrae (IANIGLA-PV 076/1–3; 076/5, 084/1); two dorsal vertebrae (IANIGLA-PV 76/4, 066); one thoracic rib (IANIGLA-PV 084/2); a right scapula (IANIGLA-PV 068); a right sternal plate (IANIGLA-PV 067); a left and right humerus (IANIGLA-PV 069/1–2); a right radius (IANIGLA-PV 070/2); a right ulna (IANIGLA-PV 070/1); six metacarpals (IANIGLA-PV 071/1–5, 154); a fragment of pubis (IANIGLA-PV 072); the proximal half of a right femur (IANIGLA-PV 073/1) and a left femur (IANIGLA-PV 073/4); one left (IANIGLA-PV 074/2) and three right tibiae (IANIGLA-PV 073/2–3, 074/1); a left and right fibula (IANIGLA-PV 074/3 and 074/4, respectively); a right astragalus (IANIGLA-PV 155); twelve metatarsals (IANIGLA-PV 077/1–5, 100/1–6, 153); ten pedal phalanges (IANIGLA-PV 077/6–12, 078/1–2, 079) and four osteoderms (IANIGLA-PV 080/1–2, 81/1–2).

Revised diagnosis: *Mendozasaurus neguyelap* can be diagnosed by seven autapomorphies (marked with an asterisk), as well as two local autapomorphies: (1) middle–posterior cervical vertebrae with tall and transversely expanded neural spines that are wider than the centra, with the lateral expansion formed by spinodiapophyseal laminae, without contribution from the pre- or postzygapophyses*; (2) anteriormost caudal neural spine dorsoventral height divided by centrum height >1.2; (3) anterior caudal vertebrae (excluding

anteriormost) with ventrolateral thickening of prezygapophyses*; (4) middle caudal centra with greatly reduced posterior condyles displaced dorsally*; (5) laterally compressed and anteroposteriorly elongated middle caudal neural spines, with the horizontal dorsal margin forming a 90° angle with the dorsal portion of the anterior margin in lateral view*; (6) humerus with divided lateral distal condyle on anterior surface; (7) second ridge on posterior surface of distal third of radius, parallel to main interosseous ridge*; (8) metacarpal I with ridge or tubercle on the dorsolateral margin at approximately two-thirds of length from proximal end*; (9) large subconical to subspherical osteoderms, lacking a cingulum*.

Locality and horizon: Arroyo Seco, south of Cerro Guillermo, Malargüe Department, Mendoza Province, Argentina (González Riga, 2003); upper levels of the Sierra Barrosa Formation, Río Neuquén Subgroup, Neuquén Group; middle–upper Coniacian, early Late Cretaceous (Garrido, 2010; González Riga & Ortiz David, 2014) (Figs 1, 2).

DESCRIPTION AND COMPARISONS

Nomenclature for vertebral laminae and fossae follows the standardized terminology of Wilson (1999) and Wilson *et al*. (2011), and serial variation in caudal vertebrae is demarcated using the scheme proposed by Mannion *et al*. (2013).

CERVICAL VERTEBRAE

Five cervical vertebrae are preserved (González Riga, 2005), including two that are described here for the first time (see Table 1 for measurements). A middle–posterior cervical vertebra (IANIGLA-PV 076/5) is relatively complete (Fig. 4), but the posterior end has been eroded away, and the element is still in its field jacket. It is probably the most anterior cervical vertebra preserved. IANIGLA-PV 076/3 preserves the centrum and lower part of the neural arch, including the right diapophysis, of a middle–posterior cervical vertebra, but it has been strongly compressed dorsoventrally (Fig. 5). IANIGLA-PV 076/2 preserves only a fragmentary neural spine and partial postzygapophysis. IANIGLA-PV 076/1 is a posterior cervical vertebra that is generally complete, but poorly preserved in places, and has undergone anteroposterior compression (Fig. 6). The fifth element (IANIGLA-PV 84/1) is probably one of the posteriormost cervical vertebrae (Fig. 7), and is less distorted than IANIGLA-PV 076/1. Apart from its eroded posterior surface, IANIGLA-PV 84/1 is largely complete. This latter cervical vertebra, as well as IANIGLA-PV 076/5 in particular, demonstrates that the cervical (and dorsal) centra of *Mendozasaurus* were not especially short anteroposteriorly, and that the apparently short length of the centrum of IANIGLA-PV 076/1 is best regarded as a taphonomic artefact. Below we describe all of the cervical vertebrae together, rather than individually, noting where there is morphological variation between elements.

All of the cervical centra are opisthocoelous and dorsoventrally compressed, with the height: width ratio varying between 0.86 in IANIGLA-PV 076/5 and 0.49 in IANIGLA-PV 84/1. The ventral surface of the centrum is transversely concave in between the parapophyses, flattening and becoming convex posteriorly. Whereas there is no ventral ridge on IANIGLA-PV 076/3 (Fig. 5E), there is a low, rounded midline ridge along the anterior half of the non-condylar centrum in IANIGLA-PV 076/5 and 076/1 (Fig. 6E). Although generally absent in

most macronarians, a small number of somphospondylans also preserve a ventral ridge in at least some cervical vertebrae, e.g. *Rapetosaurus* (Curry Rogers, 2009) and *Savannasaurus* (Poropat *et al*., 2016). All of the cervical centra lack ventral fossae and ventrolateral ridges. The lateral surface of the centrum is excavated by a fairly deep lateral pneumatic fossa, but this does not open into a foramen, and there are also no dividing ridges within the fossa. This 'simple' fossa is comparable to many somphospondylans, but it tends to be much shallower in those taxa (Upchurch, 1998; Curry Rogers, 2005), including *Futalognkosaurus* (Calvo *et al*., 2008b). A distinct ridge forms the dorsal margin of the lateral fossa. Parapophyses project laterally and, with the exception of the most posterior cervical vertebra preserved (IANIGLA-PV 84/1), quite strongly ventrally (Figs 4A, 6A), with those of IANIGLA-PV 076/1 similar to the condition in some euhelopodids (D'Emic, 2012) and diplodocoids (Mannion *et al*., 2013), as well as at least some other titanosaurs, e.g. *Isisaurus* (Jain & Bandyopadhyay, 1997), *Overosaurus* (Coria *et al*., 2013), *Patagotitan* (Carballido *et al*., 2017), and *Puertasaurus* (Novas *et al*., 2005). Unlike some saltasaurids (D'Emic, 2012), the parapophyses do not extend as far as the midlength of the centrum. As is the case in most derived titanosaurs (Upchurch, 1998; Curry Rogers, 2005), the dorsal surfaces of the parapophyses are unexcavated.

Relative to the height of the centrum, the neural arch of IANIGLA-PV 84/1 is dorsoventrally low in anterior view (Fig. 7C), consistent with the posterior cervical vertebrae of most derived somphospondylans (Bonaparte, González Riga & Apesteguía, 2006; Mannion *et al*., 2013). Both the anterior and posterior neural canal openings are subcircular. Centroprezygapophyseal laminae (CPRLs) are flat, mediolaterally wide sheets of bone that are not excavated or divided. The prezygapophyses are well separated from one another by a transversely elongate intraprezygapophyseal lamina (TPRL) that is mainly horizontal in anterior view (Fig. 7C), dipping only very gently towards the midline; in dorsal view it is U-shaped (Fig. 7B). Only in the posteriormost cervical vertebra (IANIGLA-PV 84/1) does the TPRL form the dorsal margin of the neural canal (Fig. 7C); in more anterior cervical vertebrae (see IANIGLA-PV 076/1) the anterior surface of the arch surrounding the neural canal is flat and featureless (Fig. 6A). The prezygapophyses are widely separated along their midline. Each prezygapophyseal articular surface is flat and faces mainly dorsally, but also medially and slightly anteriorly. They increase in anteroposterior length laterally, and extend a very short distance beyond the anterior margin of the condyle. In posterior view, the intrapostzygapophyseal lamina (TPOL) has a shallow, transversely wide U-shape, with no midline ventral ridge extending between it and the dorsal margin of the neural canal (Fig. 6C). The postzygapophyseal articular surfaces are flat and face mainly ventrally, but also laterally and very slightly posteriorly. There are no pre-epipophyses or epipophyses.

The diapophysis is supported from below by prominent anterior centrodiapophyseal (ACDL) and posterior centrodiapophyseal laminae (PCDL). The ACDL and PCDL form the margins of the centrodiapophyseal fossa (CDF), with the ventral margin of this fossa formed by the sharp ridge that delimits the dorsal margin of the lateral fossa of the centrum. A prezygodiapophyseal lamina (PRDL) and postzygodiapophyseal lamina (PODL) also contribute to the sheet-like diapophysis, with the dorsal surface of the latter tilted to face posterodorsally. The convex anterior border of the PRDL gives the diapophysis a 'wing'-shape in dorsal/ventral and anterior/posterior views (González Riga, 2005). The diapophyses project mainly laterally, but also curve slightly ventrally (e.g. Fig. 6A). An accessory lamina runs along the posterior surface of the neural arch, emanating from the posterior margin of the PCDL (Fig. 6A, E). A broken portion of the diapophysis of IANIGLA 076/5 reveals a

camellate internal tissue structure, as characterises the cervical and anterior dorsal vertebrae of *Galveosaurus* + Titanosauriformes (Wilson and Sereno, 1998; Mannion *et al*., 2013).

Although accentuated by crushing, the neural spine is anteroposteriorly short along its length, lacking bifurcation (Fig. 6F). It projects mainly dorsally, although we cannot be certain whether the anterior deflection of IANIGLA-PV 076/1 (Fig 6B, D) is a genuine feature. The neural spine is a dorsoventrally tall structure, exceeding twice the height of the centrum in IANIGLA-PV 076/1 (Fig. 6). Despite poor preservation, a midline prespinal ridge extends along most, or all, of the anterior surface of the neural spine of IANIGLA-PV 076/1 (Fig. 6A; see also González Riga, 2005), as is the case in the posterior cervical vertebrae of most somphospondylans (Salgado, Coria & Calvo, 1997; D'Emic, 2012), but is absent from the other preserved cervical neural spines, including IANIGLA-PV 84/1 (Fig. 7C). Robust lateral spinoprezygapophyseal laminae (lSPRLs) extend dorsomedially from the posterolateral corners of the prezygapophyses and extend along most of the spine (Fig. 6A). Although broken, there are also remnants of medial SPRLs (mSPRLs) at the base of the neural spine (Fig. 6A), which presumably must have merged with the prespinal lamina dorsally. The presence of paired SPRLs might represent an autapomorphy of *Mendozasaurus*, but we exclude it from our diagnosis because of the poor preservation in this region. Spinopostzygapophyseal laminae (SPOLs) form the posterolateral margins of a mediolaterally wide spinopostzygapophyseal (=postspinal) fossa (SPOF). The SPOLs are directly strongly dorsally, as well as being slightly medially deflected (Fig. 6C). There does not appear to be a postspinal ridge, but this region is poorly preserved.

On the lateral surface, at the base of the neural spine, there is a deep (but not sharp-lipped) spinodiapophyseal fossa (SDF) that is floored by the diapophysis, bounded anteriorly by the lSPRL, and posteriorly by the postzygapophysis (Figs 4B, 6D, 7A). Although many taxa have a SDF in their cervical vertebrae (González Riga, 2005; Wilson *et al*., 2011), the depth noted in *Mendozasaurus* otherwise appears to be restricted to the posterior cervical vertebrae of *Futalognkosaurus* (Calvo *et al*., 2008b), *Alamosaurus* (Tykoski & Fiorillo, 2016), and possibly *Isisaurus* (Jain & Bandyopadhyay, 1997). Within this fossa, a spinodiapophyseal lamina (SPDL) starts at the base of the spine and continues dorsally, where it is the sole contributor to the lateral expansion of the upper portion of the neural spine (Figs 4, 6). This lateral expansion means that the neural spine extends further laterally than the margins of the centrum, although it does not extend as far as the lateral margins of the prezygapophyses (González Riga, 2005). It also gives the neural spine a strongly convex dorsal margin in anterior view. Although this 'paddle'-shaped morphology has been described in the posteriormost cervical and anteriormost dorsal vertebrae of a number of somphospondylans (Bonaparte *et al*., 2006; Calvo *et al*., 2008b; D'Emic, 2012), the laminar contribution to the lateral expansion differs between taxa (González Riga, 2010; Gallina, 2011; Gallina & Apesteguía, 2015). Only in *Futalognkosaurus*, *Mendozasaurus*, *Quetecsaurus* (Gallina, 2011; González Riga & Ortiz David, 2014), and *Alamosaurus* (Tykoski & Fiorillo, 2016) is this known to be formed entirely by the SPDL, and *Mendozasaurus* is distinct in that this lateral expansion results in the neural spine being wider than the centrum.

DORSAL VERTEBRAE

Two dorsal vertebrae are preserved (IANIGLA-PV 076/4 and 066; see Table 1 for measurements). IANIGLA-PV 076/4 is interpreted as one of the anteriormost dorsal

vertebrae (González Riga, 2005). It preserves an incomplete neural arch, most of the neural spine, and the right diapophysis, although the posterior surface is largely incomplete. IANIGLA-PV 066 is complete, but it is poorly preserved in places, and has undergone some anteroposterior compression (Fig. 8). It is also from the anterior region of the dorsal series (suggested to be Dv3 by González Riga, 2005), evidenced by the position of the parapophysis on the dorsal half of the centrum and lower portion of the neural arch.

Although the anterior condyle of the centrum of IANIGLA-PV 066 has been worn (Fig. 8A), it was clearly strongly convex, as evidenced by the fairly deep posterior cotyle. The centrum is dorsoventrally compressed (width to height ratio=1.4), comparable to the anterior dorsal centra of several titanosaurs, including *Malawisaurus*, *Notocolossus*, *Opisthocoelicaudia*, and *Rapetosaurus* (Mannion *et al*., 2013; González Riga *et al*., 2016). Ventrally, the centrum is transversely convex, lacking ridges or fossae (Fig. 8E). A pneumatic foramen excavates the lateral surface of the dorsal half and anterior two-thirds of the centrum (Fig. 8B, D), although it does not ramify deeply. This foramen is posteriorly acute, and seems to be set within a fossa, as in many somphospondylans (Upchurch *et al*., 2004; Mannion *et al*., 2013). There are no ridges within either the fossa or foramen. The erosion of the anterior surface of the centrum reveals that the internal tissue structure is camellate.

On the lateral surface of the neural arch, the paradiapophyseal lamina (PPDL) and PCDL define a narrow, subtriangular CDF (Fig. 8B). The CPRLs are not bifid, but there are shallow, paired fossae dorsolateral to the neural canal opening on IANIGLA-PV 066. Similar excavations are present in the dorsal vertebrae of several other titanosaurs, including *Pitekunsaurus* (MAU-Pv-AG-446: PDM pers. obs. 2014) and *Rinconsaurus* (MAU-PV-CRS-05: PDM pers. obs. 2014). There is a large, deep, semi-circular shaped prezygapophyseal centrodiapophyseal fossa (PRCDF) limited by the CPRL, PRDL and PPDL (Fig. 8B). In anterior view, the TPRL is gently convex (Fig. 8A). Whereas the flat prezygapophyseal articular surfaces mainly face dorsally in IANIGLA-PV 076/4, they face dorsomedially and slightly anteriorly in IANIGLA-PV 066, tilted at approximately 40° to the horizontal, as is the case in most titanosaurs (Carballido *et al*., 2012).

Each CPOL has a free anterior margin as a result of excavation of its lateral surface, whereas the remainder of the posterior surface of the neural arch lacks ridges or fossae (Fig. 8C). The area above the posterior neural canal opening, in between the CPOLs, is shallowly excavated, and is divided by a ridge (González Riga, 2003) that has been broken and distorted. This was presumably a midline ridge that extended from the ventral midpoint of the V-shaped TPOL: a comparable feature is present in the anterior dorsal vertebrae of several other sauropods (Poropat *et al*., 2016), including the titanosaurs *Bonitasaura*, *Malawisaurus*, *Muyelensaurus*, and *Rapetosaurus* (Curry Rogers, 2005, 2009; Gallina & Apesteguía, 2011). The postzygapophyseal articular surfaces are flat and strongly tilted to face ventrolaterally. They have almost certainly been crushed anteriorly in IANIGLA-PV 066, so that they are extremely well separated along the midline; this has also resulted in the PODL being extremely short and barely discernible in this vertebra (Fig. 8D). Although the absence of a hyposphene characterises the middle–posterior dorsal vertebrae of Lithostrotia (Salgado *et al*., 1997; Upchurch, 1998), the two preserved dorsal vertebrae of *Mendozasaurus* are probably too anterior in the sequence to determine whether this structure was genuinely absent in this taxon.

Diapophyses project laterally and very slightly dorsally, and they are longer along their dorsal than ventral margins (Fig. 8A, C). They also expand slightly dorsoventrally towards their distal tips. Each diapophysis has a sub-triangular cross section, with the apex of this

triangle formed by the PCDL, and the other corners formed by the PODL and PRDL. As is the case in the cervical vertebrae, the PRDL extends laterally in IANIGLA-PV 076/4, whereas it is a reduced structure in IANIGLA-PV 066. It is not possible to determine whether an ACDL is genuinely absent. The posterior surface of the diapophysis lacks excavations.

The neural spine is anteroposteriorly compressed and projects primarily dorsally, and very slightly posteriorly (Fig. 8B, D). Dorsal to the postzygapophyses, the neural spine rapidly decreases in transverse width, before forming subparallel margins along the dorsal half, with a gently convex dorsal margin. In IANIGLA-PV 076/4, the neural spine appears to have small triangular aliform processes, which seem to be formed entirely by the SPOLs (Fig. 8C). Distinct midline prespinal and postspinal laminae begin at the base of the neural spine and extend until at least close to the spine apex (Fig. 8A, C), as is the case in most somphospondylans (Salgado *et al*., 1997; Curry Rogers, 2005; D'Emic, 2012; Mannion *et al*., 2013). Short, but distinct, spinoprezygapophyseal laminae (SPRLs) are present at the base of the neural spine (Fig. 8A). In IANIGLA-PV 076/4, these merge at spine midheight with the undivided SPDLs, resulting in a prominent fossa on the dorsal surface of the diapophysis, posterior to the prezygapophysis. In contrast, the SPRLs in IANIGLA-PV 066 are less robust and merge with the prespinal ridge a short distance up the spine. SPDLs form the anterolateral margins of the neural spine and remain separate from the prespinal lamina. The presence of SPDLs in anteriormost dorsal vertebrae is generally a feature restricted to lithostrotians and some diplodocoids (Salgado *et al*., 2007; D'Emic, 2012; Poropat *et al*., 2016). A well-developed postzygapophyseal spinodiapophyseal fossa (POSDF) is present between the SPDL and SPOL (González Riga, 2003). SPOLs are undivided and form the posterolateral margins of the neural spine; there also seems to be evidence for weakly developed epipophyses.

The shaft of a large thoracic rib (IANIGLA-PV 084/2) is preserved, demonstrating its plank-like cross-sectional shape. However, its incomplete nature means that we cannot determine its position in the dorsal sequence.

CAUDAL VERTEBRAE

A total of 22 caudal vertebrae are preserved (Fig. 9; see Table 2 for measurements). These comprise: (1) four anterior caudal vertebrae (IANIGLA-PV 065/1–4) that were found disarticulated (Fig. 9A–M); (2) a series of nine partially articulated anterior–middle caudal vertebrae (IANIGLA-PV 065/5–13) (Fig. 9N–T, AC–AD); (3) a series of six articulated middle–posterior caudal vertebrae (IANIGLA-PV 065/14–19) (Fig. 9U–AD); and (4) three disarticulated posterior caudal vertebrae (IANIGLA-PV 065/20–22) (González Riga, 2003). Although they do not form a continuous series, these 22 caudal vertebrae are described as Cd I–XXII below. Rather than providing a complete description of each caudal vertebra, we record anatomical features the first time that they can be observed, and then document how they change along the sequence.

Cd I is fairly complete, but has undergone anteroposterior crushing, with most of the anterior surface eroded (Fig. 9A–D). It is from the anteriormost region of the tail, although it is not the first caudal vertebra. The centrum is strongly procoelous, as is the case in the anterior caudal vertebrae of all lithostrotian titanosaurs, as well as a number of other eusauropod taxa (Salgado *et al*., 1997; Upchurch, 1998; Whitlock, D'Emic & Wilson, 2011; Mannion *et al*., 2013). A small central depression excavates the posterior condylar surface (González Riga, 2003). Although the ventral surface is not well preserved, it is clearly

transversely convex, and seems to lack ridges or fossae. No fossa or foramen excavates the lateral surface of the centrum, in contrast to the anterior caudal vertebrae of many diplodocoids (Upchurch, 1998), and a small number of titanosauriforms (D'Emic, 2012; Mannion *et al*., 2013). Caudal ribs are situated on the upper part of the lateral surface of the centrum and extend onto the neural arch. They project posterolaterally, as is the case in most titanosauriforms (Mannion & Calvo, 2011), although their extension beyond the posterior margin of the non-condylar centrum might be an artefact of anteroposterior crushing (see Cd II). In anterior view, the caudal ribs are triangular, tapering distally (Fig. 9A), in contrast to the wing-like caudal ribs that characterise the anteriormost caudal vertebrae of most diplodocoids (Upchurch, 1998; Whitlock *et al*., 2011). The ventral margins of the caudal ribs are dorsally deflected along their medial sections in anterior view, but become close to horizontal laterally. The posterior surface of the neural arch, ventrolateral to each postzygapophysis, forms a large, sharp-lipped postzygapophyseal centrodiapophyseal fossa (POCDF; Fig. 9D). Postzygapophyses have flat to very mildly concave articular surfaces that face ventrolaterally. Each postzygapophysis is supported ventrally by a dorsomedially directed CPOL that also forms the lateral and dorsal margins of the posterior neural canal opening. There is no hyposphene, an absence that characterises most somphospondylans (Upchurch, 1998; Mannion *et al*., 2013). A sharp PRDL is present, and there are remnants of a PODL on the right side. A sharp-lipped SDF is present above the PODL on the lateral surface of the neural spine (González Riga, 2003), a feature that also characterises several other titanosaurs, including *Alamosaurus*, *Dongyangosaurus*, *Futalognkosaurus*, and *Malawisaurus* (Wilson, 2002; Whitlock *et al*., 2011). The neural spine projects mainly dorsally, and slightly posteriorly. It is tall relative to the centrum height (ratio of 1.25), contrasting with most other titanosauriforms, although similar ratios are present in *Futalognkosaurus* (Calvo *et al*., 2008b: fig. 16) and *Saltasaurus* (Powell, 2003: pl. 33). There is no SPDL, but the SPRL and SPOL merge along the dorsal half of the neural spine to form a laterally thickened apex. A similar morphology is present in the anterior caudal vertebrae of several other titanosaurs, including *Futalognkosaurus* and *Malawisaurus* (González Riga *et al*., 2009). The presence of the SPRL on the lateral surface of the neural spine, ventral to this lateral thickening, appears to be a result of the anteroposterior crushing of the caudal vertebra: this lateral extent is otherwise known only in diplodocoids (Wilson, 2002). It could be argued that the SPRL is actually a SPDL, as interpreted by Carballido *et al*. (2017), but there seems to be a clear change in orientation at the prezygapophyseal level between the lower part of this lamina (our PRDL) and the upper part (our SPRL), even accounting for crushing. As such, we regard both *Mendozasaurus* and *Futalognkosaurus* (MUCPv-323: PDM pers. obs. 2009; contra Carballido *et al*., 2017) as lacking a SPDL in anterior caudal vertebrae. In contrast, *Patagotitan* seems to have a continuous lamina extending from the caudal rib up to the neural spine, and we agree with Carballido *et al*. (2017) in identifying this as a SPDL. The SPOLs of Cd I of *Mendozasaurus* form the posterolateral margins of the neural spine, with a postspinal fossa in between. A ridge-like midline postspinal lamina is present and seems to extend for most of the spine length, although dorsally it becomes transversely widened and more rugose. The dorsal margin of the neural spine lacks the trifid morphology that characterises the anterior caudal vertebrae of several somphospondylans (D'Emic *et al*., 2013), including *Futalognkosaurus* (Calvo *et al*., 2008b).

Cd II preserves most of the centrum and the base of the arch, including the prezygapophyses, but has been transversely compressed (Fig. 9E–G). It reveals that the internal tissue structure of the vertebra is non-camellate, contrasting with the camellae that

pneumatise the anteriormost caudal vertebrae of several lithostrotians (Wilson, 2002; Mannion *et al*., 2013). Caudal ribs project posterolaterally, but do not extend beyond the posterior margin of the non-condylar centrum, contrasting with the condition in the titanosaurs *Andesaurus* (Mannion & Calvo, 2011) and *Notocolossus* (González Riga *et al*., 2016), as well several basal titanosauriforms (Mannion & Calvo, 2011; D'Emic, 2012; Mannion *et al*., 2013). There is a tubercle on the dorsal surface of the caudal rib (D'Emic *et al*., 2013), approximately at the midpoint between the prezygapophysis and the distal end of the rib (Fig. 9E, F). A comparable feature has previously been noted in several other somphospondylan taxa, including *Baurutitan*, *Epachthosaurus*, and *Huabeisaurus* (Martínez *et al*., 2004; Kellner, Campos & Trotta, 2005; D'Emic *et al*., 2013), but is also present in a wider array of eusauropods (Poropat *et al*., 2016). The prezygapophyses project anterodorsally and extend well beyond the anterior margin of the centrum.

Cd III lacks the posterior surface of the neural arch and spine, and the latter is also incomplete dorsally (Fig. 9H–J). It demonstrates the presence of a midline prespinal lamina, in addition to well-developed SPRLs. Only the right half of the vertebra of Cd IV is preserved, although the neural spine is largely complete (Fig. 9K–M). A sharp-lipped POCDF remains present (González Riga, 2003). There is a prominent tubercle ('SPRL-process' *sensu* D'Emic *et al*., 2013) on the dorsal margin of the SPRL, close to the prezygapophysis (González Riga, 2003), that is best observed in lateral view (Fig. 9L; note that this feature might also be subtly present on Cd III). A comparable, though often less prominent, tubercle is present in several other titanosauriforms, including *Alamosaurus*, *Giraffatitan*, and *Saltasaurus* (González Riga, 2003; D'Emic & Wilson, 2011; D'Emic, 2012). The neural spine of Cd IV projects posterodorsally. In this regard, *Mendozasaurus* differs from *Epachthosaurus*, in which there is a reverse shift, from posterodorsally- to vertically-oriented neural spines in the anteriormost caudal vertebrae (Martínez *et al*., 2004). In anterior view, the neural spine of Cd IV of *Mendozasaurus* is transversely expanded dorsally.

Cd V is complete apart from the neural spine, but is heavily distorted, such that the vertebra is strongly sheared anteriorly. The centrum is procoelous, the caudal ribs curve posterolaterally, and a POCDF is present, as in preceding caudal vertebrae. The ventrolateral surfaces of the prezygapophyses are thickened, a feature that continues into at least the next few caudal vertebrae (Cd VI–VIII), in which this thickening becomes a prominent swelling (Fig. 9H, I, N). A similar feature is present in the anterior caudal vertebrae of *Diplodocus*, although in that taxon the expansion forms a distinct ridge (Tschopp, Mateus & Benson, 2015). We consider this as a convergent feature and regard the swelling as an autapomorphy of *Mendozasaurus*. Cd VI (Fig. 9N–Q) and Cd VII (Fig. 9R) are less deformed than Cd V, although Cd VII is missing the right side of the centrum, the right prezygapophysis, and the posterior condyle. Both vertebrae demonstrate the retention of a small, rugose tubercle on the dorsal surface of the SPRL. In Cd VII, the neural spine is reduced to a simple, transversely compressed plate that projects dorsally and posteriorly.

The centrum of Cd VIII is the first caudal vertebra that lacks strong procoely, with a concave anterior articular surface (Fig. 9S), and an irregularly concave posterior surface that is slightly convex dorsally (Fig. 9T). In the middle and posterior centra, the posterior articular surfaces are practically planar, with the exception of the reduced condyles that are dorsally displaced (González Riga, 2003). This morphology is different to most lithostrotians (e.g. *Narambuenatitan* [Filippi, García & Garrido, 2011]; *Rinconsaurus* [Calvo & González Riga, 2003]; *Overosaurus* [Coria *et al*., 2013]), in which a prominent condyle is retained (Fig. 10). There are no excavations or ridges on the lateral surface of the centrum of Cd VIII of

Mendozasaurus, and its ventral surface is transversely convex. As such, the caudal centra of *Mendozasaurus* lack the ventrolateral ridges and midline hollow that characterise many somphospondylans and diplodocoids (Upchurch, 1998; Wilson, 2002; Mannion *et al*., 2013). The caudal ribs (= transverse processes) curve posterolaterally, although they do not extend as far as the posterior margin of the centrum. In contrast, *Notocolossus* exhibits well-developed and ventrally curved transverse processes (González Riga *et al*., 2016: fig. 3). The prezygapophyses of Cd VIII of *Mendozasaurus* project anteriorly and slightly dorsally, and extend well beyond the anterior margin of the centrum. Cd IX is very incomplete and poorly preserved, and the centrum of Cd X has a small posterior convexity that is dorsally restricted.

Cd XI and Cd XII are fairly complete and articulated, although the former is poorly preserved and more distorted than the latter. The posterior articular surface of the centrum of Cd XII is irregular, and caudal ribs are absent on both vertebrae, with the exception of a very small bulge-like process around the arch-centrum junction. As such, we regard these as some of the first middle caudal vertebrae (Fig. 9AD). Anterodorsally projecting prezygapophyses extend well beyond the anterior margin of the centrum. There is a shallow fossa on both lateral surfaces at the base of arch, ventrolateral to the postzygapophyses. The anterior margin of the neural spine is subvertical; unfortunately, the posterior margin is incomplete. Cd XIII is missing most of the anterior half of the centrum and the left prezygapophysis. The dorsal half of the posterior articular surface of the centrum of Cd XIII is gently convex, whereas the ventral half is concave. As in the middle caudal vertebrae of other titanosauriforms (Calvo & Salgado, 1995), the neural arch is restricted to the anterior half of the centrum.

The ventrolateral surfaces of the anteriorly projecting prezygapophyses lack a raised ridge-like expansion in Cd XIV and subsequent caudal vertebrae. In lateral view, the anterior margin of the neural spine is vertical, the dorsal margin is horizontal, and the posterior margin slants such that it faces posteroventrally. This morphology was described by González Riga (2003: fig. 5) as an autapomorphic character of *Mendozasaurus* and is considered valid herein. Some titanosaurs exhibit laterally compressed and anteroposteriorly elongated middle caudal neural spines, including *Andesaurus*, *Dreadnoughtus*, *Epachthosaurus, Malawisaurus* and *Narambuenatitan* (Fig. 10). However, the shape of this neural spine is different to that of *Mendozasaurus*. The neural spines of *Epachthosaurus* form an obtuse angle at their anterodorsal corner (Fig. 10D) (Martínez *et al*. 2004: fig. 8). In *Andesaurus* (Fig. 10E) and *Malawisaurus* (Fig. 10F), the anterodorsal corner is rounded and the dorsal margin is slightly convex (Jacobs *et al*., 1993: fig. 2; Mannion & Calvo, 2011: fig. 6). In *Narambuenatitan* (Fig. 10G), the dorsal border is not horizontal: it is higher posteriorly (Filippi *et al*., 2011: fig. 9). Finally, in *Dreadnoughtus* (Fig. 10B) the shape of the neural spine is different to that of *Mendozasaurus* and changes along the caudal series (Lacovara *et al*., 2014: supp. fig. 1). In the anteriormost middle caudal vertebrae (Cd XI–XVII) of *Dreadnoughtus*, the anterodorsal border is sharply pointed and anteriorly projected, extending, in some cases, beyond the anterior margin of the centrum. In contrast, from Cd XVIII–XXII, the neural spines of *Mendozasaurus* are posteriorly orientated.

Cd XVI of *Mendozasaurus* (Fig. 9U–X) has a shallow prespinal fossa at the base of the neural spine (Fig. 9U). Chevron facets are incomplete in Cd XVI, but the posterior ones are prominent structures that are widely separated from one another along the midline. Cd XVIII (Fig. 9Y–AB) and subsequent caudal vertebrae (Cd XIX–XXII) are from the posterior region of the tail. In these vertebrae, a prominent, anteroposteriorly elongate ridge is

retained at the arch-centrum junction, and the posterior articular surface of the centrum still has a dorsally restricted convexity.

CHEVRONS

Three fairly complete chevrons (IANIGLA-PV 065/23-25) from the proximal part of the tail are preserved (Fig. 11; see Table 3 for measurements), as well as four fragments (IANIGLA-PV 065/26–30). Although it is not possible to directly match them to particular caudal vertebrae, these probably belong to the series of nine partially articulated anterior–middle caudal vertebrae (Cd V–XIII). All three chevrons are proximally unbridged, as characterises most macronarians (Upchurch, 1995), and their proximal articular surfaces have a midline furrow, such that they are separated into distinct anterior and posterior portions (González Riga, 2003). This proximal morphology also characterises the titanosaurs *Aeolosaurus* (Powell, 1987; Santucci & Arruda-Campos, 2011), *Epachthosaurus* (UNPSJB-PV 920: PDM & SFP pers. obs. 2013), and *Maxakalisaurus* (Kellner *et al*., 2006), as well as some euhelopodids (D'Emic, 2012). Haemal canal depth is between 40–45% of total chevron proximodistal height, as is the case in many other titanosauriforms (Wilson, 2002; Mannion *et al*., 2013).

The lateral surfaces of the proximal rami lack ridges, such as those seen in some titanosaurs (e.g. *Alamosaurus*, *Epachthosaurus*, and *Saltasaurus*; Poropat *et al*., 2016), although these ridges are not always present in the anteriormost chevrons. There are also no ridges on the lateral surfaces of the transversely thin distal blades of the chevrons of *Mendozasaurus*, but sharp anterior and posterior midline ridges are present. In lateral view, the distal blade curves posteriorly, with only a subtle anteroposterior expansion occurring distally, and it has a convex distal margin.

SCAPULA

The right scapula (IANIGLA-PV 068; see Table 4 for measurements) is here described with the long axis of the scapular blade oriented horizontally (Fig. 12A, B). The acromion (proximal plate) is damaged dorsally and anteroventrally, and the dorsal margin of the blade is missing at its very distal end (Fig. 12A). Although incomplete, the coracoid articular surface does not seem to have been strongly tilted posteriorly, relative to the long axis of the scapular blade, contrasting with the condition observed in many diplodocoids (Tschopp *et al*., 2015), several derived titanosaurs (Wilson, 2002), and a number of taxa close to the titanosaurian radiation, e.g. *Ligabuesaurus* (Bonaparte *et al*., 2006). As in other somphospondylans (Wilson, 2002), the glenoid is bevelled medially. The acromial ridge is an anteroposteriorly wide, rounded ridge that posteriorly bounds the excavated lateral surface of the acromion (Fig. 12A). There is no fossa or excavation posterior to the acromial ridge, such as that seen in a number of neosauropods (Upchurch *et al*., 2004). As preserved, the posterodorsal margin of the acromion is straight. Although damaged, there is evidence for a ventral process at the posterior end of the acromion (D'Emic, Wilson & Williamson, 2011). A comparable feature is present in several other titanosauriforms (Fig. 13), e.g. *Alamosaurus* (D'Emic *et al*., 2011), *Chubutisaurus* (Carballido *et al*. 2011b), *Dreadnoughtus* (Ullmann & Lacovara, 2016), *Ligabuesaurus* (Bonaparte *et al*., 2006) and *Paralititan* (Smith *et al*., 2001).

The lateral surface of the scapular blade is dorsoventrally convex, forming a rounded ridge that is ventrally biased (Fig. 12A). This ridge fades out at approximately midlength of

the scapular blade, from which point the lateral surface is relatively flat. In contrast, the medial surface of the scapular blade is gently concave dorsoventrally. As such, the cross section at the base of the scapular blade is closest to the 'D'-shape of most eusauropods, differing from the subrectangular shape that characterises many somphospondylans (Wilson, 2002), although taxa such as *Diamantinasaurus* (Poropat *et al*., 2015a), *Ligabuesaurus* (Bonaparte *et al*., 2006), *Opisthocoelicaudia* (Borsuk-Białynicka, 1977), and *Patagotitan* (Carballido *et al*., 2017), also have this D-shaped cross section. The scapular blade is transversely thicker ventrally than dorsally at its base, a morphology that has also been reported in other titanosaurs (e.g. *Alamosaurus*; D'Emic *et al*., 2011). There are no ridges on the medial surface of the proximal portion of the distal blade (Fig. 12B), differing from those seen in a small number of derived titanosaurs (Sanz *et al*., 1999). There is also no ventral process towards the anterior end of the scapular blade, in contrast with some somphospondylans, e.g. *Alamosaurus* and *Euhelopus* (D'Emic *et al*., 2011; D'Emic, 2012; Mannion *et al*., 2013). The scapular blade expands dorsoventrally towards its distal end, and its ventral margin is concave in lateral view.

STERNAL PLATE

The preserved sternal plate (IANIGLA-PV 067; Fig. 12C) is a right, rather than left element, as originally identified (González Riga, 2003). Its lateral margin is incomplete, meaning that it was probably more strongly concave than it presently appears (see Table 4 for measurements). The medial margin is convex, and there is a prominent ridge at the anterior end of the ventral surface, situated on the lateral margin. A similar ridge is present in a wide range of eusauropods (Sanz *et al*., 1999; Upchurch *et al*., 2004; Poropat *et al*., 2016). As noted by González Riga (2003), the posterior margin is straight in dorsal view, lacking the convexity that characterises the sternal plates of most sauropods. *Mendozasaurus* shares this posterior morphology with a small number of other titanosaurs, including *Alamosaurus* and *Malawisaurus* (González Riga, 2003). Assuming that the sternal plate is from the same individual as the two humeri (see below), the ratio between its maximum length and the proximodistal length of the humerus is between 0.75–0.78, similar to other derived titanosaurs, e.g. *Alamosaurus* and *Opisthocoelicaudia* (Upchurch, 1998).

HUMERUS

A right (IANIGLA-PV 069/1) and a left (IANIGLA-PV 069/2) humerus, probably from the same individual, are preserved (Fig. 14; see Table 4 for measurements). Both are relatively complete: the right humerus is better preserved (Fig. 14A–F), whereas the left humerus is slightly less distorted (Fig. 14G–J).

The humerus is relatively slender throughout its length, with low ratios for the mediolateral widths of the proximal (<0.35), midshaft (<0.15), and distal ends (<0.30), relative to that of the proximodistal length of the humerus. As such, the humerus of *Mendozasaurus* is closer in morphology to the humeri of taxa like *Ligabuesaurus* and *Rapetosaurus*, rather than the robust forelimb elements that characterise many saltasaurids (Curry Rogers, 2005), as well as titanosaurs such as *Diamantinasaurus* (Poropat *et al*., 2015a) and *Dreadnoughtus* (Ullmann & Lacovara, 2016). If the femur (IANIGLA-PV 073/4) is from the same individual as the two humeri, then *Mendozasaurus* has a low humerus to femur length ratio of between 0.72 and 0.75, similar to basal eusauropods and a small

number of derived titanosaurs, such as *Jainosaurus* (Wilson, Barrett & Carrano, 2011) and *Opisthocoelicaudia* (Borsuk-Białynicka, 1977). However, other titanosaurian taxa have higher ratios, e.g. *Rapetosaurus* (0.80 [Curry Rogers, 2009]), *Dreadnoughtus* (0.84 [Lacovara *et al*., 2014]) and *Epachthosaurus* (0.85 [Martínez *et al*., 2004]), which might suggest that the humeri of *Mendozasaurus* are from a smaller individual than the femora.

There is no strong degree of torsion between the proximal and distal ends, and the proximal margin is gently convex in anterior view (Fig. 14B, G), lacking the well-developed process for *M. supracoracoideus* that creates a sinuous outline in some titanosaurian taxa (Upchurch, 1998; González Riga, 2003; González Riga *et al*., 2009; González Riga & Ortiz David, 2014). As is typical in most somphospondylans (Wilson, 2002; Mannion *et al*., 2013), the proximolateral corner is square-shaped. The proximomedial corner forms an acute, triangular projection, similar to that illustrated in *Paralititan* (Smith *et al*., 2001: fig. 2a), and previously considered an autapomorphy of *Angolatitan* by Mateus *et al*. (2011). The humerus of *Mendozasaurus* lacks the extreme proximomedial expansion that characterises that of *Notocolossus* (González Riga *et al*., 2016). As is the case in other titanosauriforms (Poropat *et al*., 2016), the proximal end is asymmetrical, with no notable expansion of the lateral margin relative to the shaft.

The humeral head extends onto the posterior surface as a prominent projection in *Mendozasaurus*, although crushing has obscured its morphology. There is no ridge along the lateral margin of the proximal third of the posterior surface, such as that recognised in several titanosaurs (e.g. *Epachthosaurus*, *Notocolossus* and *Saltasaurus* [González Riga *et al*., 2016; Poropat *et al*., 2016]). Although there is some evidence for such a ridge on the right humerus, this has been caused by crushing; the left humerus confirms its absence. As in many titanosauriforms (Upchurch, Mannion & Taylor, 2015), a prominent bulge for *M. scapulohumeralis anterior* is present, but there is no equivalent site for *M. latissimus dorsi*, the presence of which seems to characterise saltasaurids (Otero, 2010; D'Emic, 2012). Although the latter muscle scar was considered present in *Patagotitan* (Carballido *et al*., 2017), we interpret this as more likely to represent the site for *M. scapulohumeralis anterior* based on comparisons with other titanosauriforms.

The deltopectoral crest of the right humerus projects strongly medially, but this has been almost certainly accentuated by crushing. That of the left humerus projects anteromedially and is likely to be closer to the genuine orientation of the deltopectoral crest. A medially deflected deltopectoral crest characterises many titanosauriforms (Mannion *et al*., 2013). Distally, the deltopectoral crest doubles in mediolateral thickness, a feature previously recognised in some saltasaurids (Wilson, 2002), but that is also present in several more basal titanosaurs (Fig. 15), including the Argentinean taxa *Muyelensaurus* (MAU-PV-LL-70: PDM pers. obs. 2014), *Narambuenatitan* (MAU-PV-N-425: PDM pers. obs. 2014) and *Rinconsaurus* (MAU-PV-CRS-47: PDM pers. obs. 2014). A tubercle for attachment of the *M. coracobrachialis* is present on the anterior surface of the proximal third. At midshaft, the humerus has an elliptical cross section, with a mediolateral to anteroposterior width ratio of approximately 2.0. The lateral margin of the midshaft is straight in anterior view.

The lateral half of the anterior surface of the distal end has a clearly divided condyle (Fig. 14C, G, H). In this regard, *Mendozasaurus* differs from nearly all other titanosaurs in which this condyle is undivided (D'Emic, 2012; Mannion *et al*., 2013), with the exception of *Diamantinasaurus* (Poropat *et al*., 2015a), with which it shares this reversal to the plesiomorphic sauropod state. We regard this feature as a local autapomorphy of *Mendozasaurus*. A well-developed supracondylar fossa is bound by medial and lateral ridges

on the posterior surface of the distal end (Fig. 14E, J), as is the case in most somphospondylans (Mannion & Calvo, 2011). The undivided distal articular surface does not expand strongly onto the anterior surface of the humerus, contrasting with the condition in some saltasaurids (Wilson, 2002). There is some bevelling of the distal end, with the medial condyle extending further distally than the lateral one. Comparable bevelling is present in the humeri of at least some other titanosaurs, including *Saltasaurus* (PVL 4017-63: PDM & SFP pers. obs. 2013) and *Neuquensaurus* (MLP CS 1050: PDM pers. obs. 2013).

Radius

The right radius (IANIGLA-PV 070/2; Fig. 16A–D) is complete aside from a portion of the medial half of the shaft, but is broken into two pieces, and has undergone some distortion, particularly at the proximal end, as well as anteroposterior compression (see Table 4 for measurements).

In anterior view (Fig. 16B), the lateral margin is concave, whereas the medial margin is gently sinuous. Although distorted, the proximal end clearly becomes anteroposteriorly narrow medially, forming a distinct medial projection. The element is too crushed and damaged to determine whether a ridge for attachment of *M. biceps brachii* and *M. brachialis inferior* (see Upchurch *et al*., 2015) was present on the medial surface of the proximal end.

A posterolateral ridge extends along most of the radius length (Fig. 16D), beginning a short distance from the proximal end, as is the case in many titanosaurs, as well as a few more basal taxa (Curry Rogers, 2005; Mannion *et al*., 2013). There is evidence for a second, parallel ridge along the distal third of the posterior surface, medial to the posterolateral ridge, with a shallow groove separating the two ridges (Fig. 16D). Although some other titanosauriform taxa also possess two ridges, in those taxa the second ridge is either restricted to the anterolateral margin (e.g. *Diamantinasaurus*; Poropat *et al*., 2015a) or to the distal quarter of the radius (e.g. *Muyelensaurus*; MAU-PV-LL-71: PDM pers. obs. 2014). As such, the presence of a second ridge along the distal third of the radius is tentatively regarded as an autapomorphy of *Mendozasaurus*.

Although distorted, the distal end was clearly bevelled, with this bevelling restricted to the lateral two-thirds of the distal surface; however, poor preservation means that it is not possible to determine the angle of bevelling. A gentle concavity is situated on the posterior margin of the distal end (Fig. 16D), approximately equidistant from the medial and lateral margins. The distal end is also mediolaterally wider than the proximal end, a feature that *Mendozasaurus* shares with several macronarians (Curry Rogers, 2005; Mannion *et al*., 2013), including the titanosaurs *Patagotitan* (Carballido et al., 2017) and *Rapetosaurus* (Curry Rogers, 2009).

Ulna

The right ulna (IANIGLA-PV 070/1; Fig. 16E–H) is missing the proximal and distal articular surfaces, as well as a large amount of the posterior surface of the proximal third (with no posterior process preserved) (see Table 4 for measurements). As such, it is not possible to determine the nature of the olecranon process, or whether the articular surface of the anteromedial process was concave. The anteromedial and anterolateral processes form a

right angle to one another in proximal view, with a well-developed radial fossa. All three proximal processes continue distally as rounded ridges.

Distally, the ulna is posteriorly expanded, as is the case in most sauropods, but contrasting with several titanosauriforms with unexpanded distal ulnae, e.g. *Alamosaurus*, *Giraffatitan*, and *Saltasaurus* (D'Emic, 2012; Mannion *et al*., 2013). There is a very gentle fossa on the anteromedial surface of the distal end, for reception of the radius. In distal view, the ulna has a subtriangular or semi-circular outline, with a flat anteromedial margin. A similar morphology has been documented in several other titanosaurs, including *Diamantinasaurus*, *Epachthosaurus*, and *Saltasaurus* (Upchurch *et al*., 2015).

METACARPUS

A total of six metacarpals are preserved (Figs 17, 18; see Table 5 for measurements). IANIGLA-PV 071/1–5 potentially represent metacarpals I–V of manüs of one individual (Figs 17, 18A–AC), although all of them have undergone crushing. There is also a metacarpal of a smaller individual (IANIGLA-PV 154; Fig. 18AD–AI). The position of several elements within the manus is also revised, with three of the four metacarpals originally described by González Riga (2003) re-identified. All metacarpals are described as if held horizontally, with the long axis of the distal end oriented transversely. No carpal or manual phalangeal elements are preserved. Although we cannot rule out that their absence might be preservational, the titanosaurian affinities of *Mendozasaurus* mean that it probably genuinely lacked these elements in vivo.

If we assume that IANIGLA-PV 071/1–5 are from a single individual, then metacarpal IV would be the longest metacarpal in the manus, with metacarpals I–III subequal in length, and metacarpal V the shortest. This would be potentially autapomorphic, as in other sauropods one of metacarpals I–III is the longest in the manus (Curry Rogers, 2005; Poropat *et al*., 2015b); however, because of uncertainty in the number of individuals, we regard this as only a tentative autapomorphy of *Mendozasaurus*, pending the discovery of an articulated manus. Although the metacarpals are distorted, the metacarpus clearly would have formed a semi-tubular, 'U'-shaped outline in proximal view (Fig. 17)

There are two elements that can definitely be identified as metacarpal I from the left manus (IANIGLA-PV 071/4 [Fig. 18A–E], and 154 [Fig. 18AD–AI]). Metacarpal I has a D-shaped outline in proximal view (Fig. 18D, AE), with a mildly concave ventrolateral margin and a dorsolateral projection. The proximal and distal ends are twisted relative to one another. There is no lateral bowing of the metacarpal in dorsal view, contrasting with the morphology observed in the titanosaurs *Andesaurus* and *Argyrosaurus* (Apesteguía, 2005). At approximately two-thirds of the length from the proximal end, the dorsolateral margin forms a proximodistally short, sharp ridge or tubercle (Fig. 18E) that we consider an autapomorphy of *Mendozasaurus*. In distal view, the metacarpal is dorsoventrally taller along its lateral half, and the ventral margin is gently concave (Fig. 18C, AI). The distal end is not bevelled relative to the long axis of shaft, and there are no distinct distal condyles. As in nearly all titanosauriforms (Salgado *et al*., 1997; D'Emic, 2012), the distal articular surface does not extend onto the dorsal surface in any of the metacarpals.

Only one metacarpal II is preserved (IANIGLA-PV 071/3; Fig. 18F–K), and it is from a right manus. The proximal end is incomplete dorsally, and the element has undergone more deformation than the other metacarpals. The metacarpal decreases in dorsoventral height distally, and its ventral margin is dorsally bowed, although the latter might be a

preservational artefact. A rounded, ventral ridge extends distally from the proximal end, and is deflected medially; it disappears a short distance before the distal end. There is also evidence for a tubercle on the dorsomedial margin of the distal end, but this area is poorly preserved. In distal view, the metacarpal is slightly dorsoventrally taller along its medial margin, and overall has a transversely elongate, trapezoidal outline. None of the metacarpals possess the ventral 'channel'-like concavities described in *Argyrosaurus* (Mannion & Otero, 2012).

IANIGLA-PV 071/1 (Fig. 18L–Q) is a right metacarpal III (illustrated by González Riga & Astini [2007] as metacarpal IV?). In proximal view, the metacarpal is wedge-shaped (Fig. 18O). The apex of this triangular shape continues distally as a laterally deflected ventral ridge, situated on the ventrolateral margin at the distal end. In distal view, the metacarpal has a trapezoidal outline, with medially slanted margins, and a very mildly concave ventral margin (Fig. 18M).

In proximal view, the left metacarpal IV (IANIGLA-PV 071/2; Fig. 18R–W) seems to have a dorsoventrally tall 'T'-shape (Fig. 18V), lacking the 'chevron'-shape that characterises this element in brachiosaurids (D'Emic, 2012) and some other sauropods (Mannion *et al*., 2013). The ventral part of this 'T'-shape continues as a ridge along the proximal two-thirds of the ventral surface. Although poorly preserved and probably slightly incomplete distally, there is a dorsomedial flange along the distal third. In distal view (Fig. 18U), the metacarpal has a transversely elongate trapezoidal outline, similar to *Epachthosaurus* (Poropat *et al*., 2016) with a mildly concave lateral margin.

The left metacarpal V (IANIGLA-PV 071/5; Fig. 18X–AC) has a compressed 'D'-shape in proximal view, with the flat margin of this 'D' facing ventromedially (Fig. 18X). A ventral ridge extends distally from the proximal end and is deflected medially along its length; it becomes increasingly low and rounded distally, and is present until at least close to the distal end (the very distal end of the ventral surface is incomplete). Although this does not form a medially-biased flange-like swelling, such as that observed in *Andesaurus* and *Epachthosaurus* (Apesteguía, 2005; Mannion & Calvo, 2011; Poropat *et al*., 2016), it might have been affected by crushing. A dorsomedial flange is present along the distal half (Fig. 18AB), similar to that present in *Muyelensaurus* (MAU-PV-LL-152: PDM pers. obs. 2014) and *Petrobrasaurus* (MAU-Pv-PH-449: PDM pers. obs. 2014); although this feature is less prominent in *Mendozasaurus*, this might just be a result of dorsoventral crushing. In distal view, the metacarpal decreases in dorsoventral height towards its medial margin, with this reduction entirely restricted to the ventral margin (Fig. 18AB).

FEMUR

Two femora are preserved (IANIGLA-PV 073/1 and 073/4; Fig. 19; see Table 6 for measurements). Only the proximal half of the right femur (IANIGLA-PV 073/1) is preserved (Fig. 19G) and has undergone anteroposterior compression. The left femur (IANIGLA-PV 073/4) is complete, although it is slightly crushed and a little poorly preserved in places (Fig. 19A–F).

The femoral head projects mainly medially, lacking the dorsal deflection that characterises some sauropods (Upchurch *et al*., 2004; Curry Rogers, 2005). There is no evidence for a longitudinal ridge (*linea intermuscularis cranialis*) on the anterior surface of the shaft, contrasting with several derived titanosaurs (Otero, 2010; D'Emic, 2012; Poropat *et al*., 2015a). In contrast to brachiosaurids and several additional taxa (Mannion *et al*.,

2013), the well-developed fourth trochanter is not visible in anterior view. As in nearly all eusauropods (Upchurch, 1998), it is restricted to the medial margin of the posterior surface. Its distal tip is situated at approximately midlength of the femur. The lateral margin of the proximal end is deflected medially relative to the lateral margin of the shaft (González Riga, 2003). This is the condition in most basal macronarians, but several derived titanosaurs lack this medial deflection (Mannion *et al*., 2013). A trochanteric shelf appears to be present, a feature *Mendozasaurus* shares with most titanosaurs, as well as some taxa outside of Titanosauria (Otero, 2010; Mannion *et al*., 2013).

At midshaft, the femur has an anteroposteriorly compressed elliptical cross section. Although anteroposteriorly longer than the fibular distal condyle, the tibial distal condyle is mediolaterally narrower, as is the case in many other titanosauriforms (Wilson, 2002; Poropat *et al*., 2016). The fibular condyle is divided posteriorly into two well-developed condyles, but poor preservation means that we cannot be certain whether a ridge is present within this division, such as that seen in *Diamantinasaurus* and *Magyarosaurus* (Poropat *et al*., 2015a). As in many derived titanosaurs (Wilson, 2002), the fibular condyle extends further distally than the tibial condyle. The distal articular surface is anteroposteriorly convex, but it is not possible to determine whether the distal condyles extended onto the anterior surface.

Tibia

One left tibia (IANIGLA-PV 074/2) and three right (IANIGLA-PV 073/2, 073/3, 074/1) tibiae are preserved (Fig. 20A–N). The sole left tibia belongs to a larger individual than the remaining tibiae (see Table 6 for measurements). Although IANIGLA-PV 073/2 is complete, it has undergone extreme anteroposterior compression, whereas IANIGLA-PV 074/1 is much less deformed, but is missing most of its distal end. The proximal end of the third tibia is missing, and the distal end is slightly incomplete. As such, anatomical information on the tibia of *Mendozasaurus* is limited.

The proximal end is anteroposteriorly longer than mediolaterally wide, and the prominent cnemial crest projects primarily anteriorly, curving slightly laterally. There is no tuberculum fibularis, but a small 'second cnemial crest' is present. Posterior to this, there is an anterolateral expansion of the proximal end, although this is not as pronounced as it is in *Uberabatitan* (Salgado & Carvalho, 2008).

Fibula

A left (IANIGLA-PV 074/3) and a right (IANIGLA-PV 074/4) fibula, probably from the same individual, are preserved (Fig. 20O–R; see Table 6 for measurements). The left element is largely complete, with the exception of small pieces missing in places, including part of the anterior margin of the proximal end. The right element is distally incomplete, and much of the medial surface is not preserved.

In lateral view (Fig. 20O), the fibula is sinuous, a morphology that *Mendozasaurus* shares with a wide array of somphospondylans (Canudo, Royo-Torres & Cuenca-Bescós, 2008; D'Emic, 2012). The medial surface is flat for most of the length of the fibula (Fig. 20R), whereas the lateral surface is anteroposteriorly convex. Proximally, the medial surface is striated, with a weak ridge delimiting the ventral margin of this striated region, directed anteroventrally from the posterodorsal corner of the proximal end. As in most

somphospondylans (D'Emic, 2012; Mannion *et al*., 2013), an anteromedial crest is present at the proximal end. An anterolateral trochanter is also present (González Riga, 2003): there is a ridge on the lateral surface, a short distance from the anterior margin, situated above the level of the lateral trochanter, with an associated groove anterior to this ridge. A comparable feature has also been noted in several other titanosaurs, including *Jainosaurus* (Wilson *et al*., 2011), *Laplatasaurus* (González Riga, 2003) and *Uberabatitan* (Salgado & Carvalho, 2008: fig. 19g).

The lateral trochanter consists of a rugose area, comprising two parallel ridges, as is the case in many somphospondylans (Upchurch, 1998; Powell, 2003; Mannion *et al*., 2013). It is restricted to the proximal half of the fibula. Although fairly well developed, it does not project beyond the lateral margin of the remainder of the fibula, in contrast with the hypertrophied lateral trochanters that characterise the fibulae of some derived titanosaurs, such as *Laplatasaurus* (Powell, 2003) and *Uberabatitan* (Salgado & Carvalho, 2008).

The anterior margin of the distal third forms a ridge. Distally, the fibula expands strongly laterally, as well as medially and a little anteroposteriorly. There is no concavity on the medial surface of the distal end. In distal view, the fibula has a rounded, subtriangular outline, with the apex of this triangle pointing anteriorly, as characterises many titanosaurs (Upchurch *et al*., 2015).

Astragalus

The right astragalus (IANIGLA-PV 155; Fig. 21A–F) has undergone extreme dorsoventral compression (see Table 6 for measurements). It clearly decreases in dorsoventral height and anteroposterior length towards its medial margin, as in all derived eusauropods (Upchurch, 1998), and differs from derived titanosaurs (Wilson, 2002) in that it is not pyramidal. Little more anatomical information can be provided with confidence. No calcaneum is preserved, but we cannot be certain that its absence is genuine.

Pes

A total of twelve metatarsals and ten pedal phalanges are preserved (Figs 22–24; see Tables 7 and 8 for measurements). Although we cannot be certain, it is possible that these are the pedal elements of just two individuals. It seems likely that IANIGLA-PV 077/1–5 represent metatarsals I–V of a right pes of one individual (with a left metatarsal V [IANIGLA-PV 153] also preserved), along with a complete set of right pedal phalanges (IANIGLA-PV 077/6–10, 078/1–2 and 079), and two left phalanges (IANIGLA-PV 077/11 and 077/12). IANIGLA-PV 077/12 is extremely proximodistally compressed (Fig. 22AH–AM). The remaining pedal remains are from a larger individual and comprise: right metatarsals I (IANIGLA-PV 100/1), III (IANIGLA-PV 100/3; interpreted by González Riga & Astini [2007] as a titanosaur metacarpal and numbered as IANIGLA-PV 100), and the proximal end of V (IANIGLA-PV 100/5); and left metatarsals I (IANIGLA-PV 100/2; very poorly preserved and incomplete), IV (IANIGLA-PV 100/4) and V (IANIGLA-PV 100/6).

If our interpretation of the number of individuals represented by pedal remains is correct, then metatarsal IV is the longest element in the metatarsus, followed by metatarsals III, V, II, and I. Although metatarsal IV is often the longest element in the pes (see González Riga *et al*., 2016: table 2), there is variation between taxa, e.g. metatarsal III is the longest in *Opisthocoelicaudia* (Borsuk-Białynicka, 1977). Furthermore, the order of

decreasing size appears to be highly variable. Following our reconstruction of the pes, the phalangeal formula of *Mendozasaurus* is 2-2-2-2-0 (González Riga *et al*., 2016). The same formula has been described in several other titanosaurs, including the 'Invernada titanosaur' (González Riga, Calvo & Porfiri, 2008) and *Notocolossus* (González Riga *et al*., 2016), and fits the general trend of increased pedal phalangeal loss in titanosaurs compared with other sauropods (Upchurch, 1998; Wilson & Sereno, 1998; Bonnan, 2005; Nair & Salisbury, 2012; González Riga *et al*., 2016).

The proximal end of metatarsal I is 'D'-shaped, with an approximately flat lateral margin, and a pointed dorsolateral projection (Fig. 23D, AN). Whereas the proximal end is not bevelled relative to the long axis of the shaft, the distal end is, as a result of the lateral distal condyle extending further distally than the medial one, which is the condition in most eusauropods (Wilson, 2002). There are no foramina on the dorsal surface, nor is there a rugosity on the dorsolateral margin of the distal end of the metatarsal (or any subsequent metatarsals), such as that seen in many diplodocoids (Upchurch, 1998). The distal end lacks a distinct ventrolateral process, and does not extend further laterally than the proximal end. In this regard, the first metatarsal of *Mendozasaurus* differs from those of most diplodocoids (Upchurch, 1998) and several other eusauropods (Mannion *et al*., 2013), including a number of titanosauriforms (D'Emic *et al*., 2011). In distal view, the metatarsal has a semi-circular outline (Fig. 23B, AL).

The proximal end of metatarsal II is a little deformed, but its long axis is oriented dorsoventrally, with a mildly concave lateral margin (Fig. 23J). The distal end is bevelled, such that the lateral distal condyle extends further distally than the medial one. In distal view, the metatarsal has an almost semi-circular outline, with a mildly concave ventral margin and a convex dorsal margin (Fig. 23H).

In proximal view, metatarsal III has a dorsoventrally compressed trapezoidal outline (Fig. 23P, AU), tapering dorsoventrally along the ventromedial margin to a small point. The proximal articular surface is gently 'domed'. In dorsal view, the medial margin of the metatarsal is strongly concave (Fig. 23M, AR). As in metatarsals I and II, the distal end of metatarsal III is bevelled. In distal view, the metatarsal is slightly taller dorsoventrally at its medial than lateral margin (Fig. 23N, AS), and the distal articular surface extends onto the dorsal surface, with a medial bias. There is no midline foramen on the ventral surface, close to the distal end, such as that observed in *Epachthosaurus* (UNPSJB-PV 920: PDM & SFP pers. obs. 2013).

Metatarsal IV is trapezoidal-shaped in proximal view (Fig. 23V, BA), with the ventral margin the shortest, and a ventrolaterally facing lateral margin. In contrast with several titanosauriforms (D'Emic *et al*., 2011; D'Emic, 2012), there is no medial embayment for reception of metatarsal III. In dorsal view (Fig. 23S, AX), the lateral margin of the metatarsal is concave, with a mildly concave medial margin. In distal view (Fig. 23T, AY), the metatarsal has a transversely elongate, elliptical outline, with a flattened medial margin, and very subtly concave ventral margin. The distal articular surface is dorsoventrally convex, especially towards the ventral margin.

In dorsal view, metatarsal V is funnel-shaped (Fig. 23Y, AE, BD, BI), with only a slight transverse expansion of the distal end relative to the midshaft. The proximal end is dorsally expanded relative to the shaft (Fig. 23AB, AH, BF, BL), contrasting with the dorsoventrally compressed proximal ends seen in the fifth metatarsals of some derived titanosaurs, e.g. *Alamosaurus* and *Saltasaurus* (Poropat *et al*., 2016). At the medial margin, the proximal end thins dorsoventrally to form a small flange, presumably for articulation with metatarsal IV.

The lateral and medial margins of the proximal third are concave in dorsal view, with this concavity more pronounced along the lateral side. The ventral surface is transversely concave proximally, and mainly flat distally, and there is a rugose tubercle at approximately midlength, situated close to the lateral margin. A comparable ventral tubercle (or ridge) is present on the fifth metatarsals of the titanosaurs *Epachthosaurus* (UNPSJB-PV 920: PDM & SFP pers. obs. 2013), *Neuquensaurus* (MLP CS 1180: PDM pers. obs. 2013), and *Saltasaurus* (PVL 4017-121: PDM & SFP pers. obs. 2013) (see also Poropat *et al*., 2016). The distal end of metatarsal V of *Mendozasaurus* thickens dorsoventrally towards its lateral margin, where there is also a slight lateral expansion.

Phalanx I-1 (IANIGLA-PV 077/6) is complete and only slightly distorted (Fig. 24A–F). In proximal view (Fig. 24D), it has an approximate 'D'-shape, with a gently convex dorsal margin. The proximal articular surface is irregularly flat. Both the dorsal (Fig. 24A) and ventral (Fig. 24E) surfaces are anteroposteriorly concave, but whereas the dorsal surface is transversely convex, the ventral surface is fairly flat transversely. The distal end is very slightly bevelled, as a result of the medial margin being very slightly longer proximodistally than the lateral margin. In distal view (Fig. 24B), the phalanx is dorsoventrally tallest along its medial margin, and the distal articular surface is dorsoventrally convex. A left phalanx I-1 (IANIGLA-PV 077/12; Fig. 24AH–AM) has been strongly crushed anteroposteriorly.

The proximal end of phalanx II-1 (IANIGLA-PV 077/7) has a transversely wide semi-circular outline (Fig. 24G–L), with a fairly flat ventral margin (Fig. 24J). Its proximal articular surface is flat, and the phalanx is slightly taller dorsoventrally along its medial margin compared to its lateral margin. Whereas the dorsal surface of the phalanx is transversely convex and gently concave proximodistally, the ventral surface is very mildly concave in both directions. In dorsal view (Fig. 24G), the medial margin is more strongly concave than the lateral margin, and the medial distal condyle extends very slightly further distally than the lateral condyle. The distal end has a similar morphology to that of the proximal end, but is dorsoventrally shorter (Fig. 24H). The distal articular surface is convex dorsoventrally, especially along its medial half, where it extends prominently onto the dorsal and ventral surfaces. A left phalanx II-1 (Fig. 24AN–AS) is also preserved.

Phalanx III-1 (IANIGLA-PV 077/8) is complete, but has undergone some deformation, such that the distal end curves upwards (Fig. 24A–F). It decreases in dorsoventral height towards its lateral margin. In proximal view (Fig. 24D), the phalanx has a transversely elongate D-shape, with a flat ventral margin (note that the apparent ventral concavity is a result of breakage). The proximal articular surface is fairly flat, and there is no proximoventral projection. The ventral surface is gently concave in both directions and lacks foramina (Fig. 24E). There is no well-defined separation of the distal end into distinct condyles, and no distal bevelling (Fig. 24B).

Phalanx IV-1 (IANIGLA-PV 077/9) has a transversely elongate, semi-circular proximal outline, with a flat ventral margin (Fig. 24AB–AG). The proximal articular surface is fairly flat (Fig. 24AE). Both the medial and lateral margins of the phalanx are concave in dorsal view (Fig. 24AB), and the medial distal condyle extends further distally than the lateral condyle. The distal end is much shorter dorsoventrally than the proximal end, and decreases in dorsoventral height laterally. The distal articular surface is gently convex dorsoventrally (Fig. 24AC).

Ungual claws are present on digits I–III (IANIGLA-PV 078/1, 078/2, 079; Figs 22A, 24S–AA). These are strongly compressed mediolaterally (Fig. 22A). In lateral view, they have a convex dorsal margin and concave ventral margin (Fig. 24U, X, AA). A ridge-like tubercle is

present along the ventral surface of the distal two-fifths of each ungual claw. Similar ventral ridges or tubercles are present in a wide array of titanosauriforms (Canudo *et al*., 2008; Mannion *et al*., 2013), including the titanosaurs *Dreadnoughtus* (Ullmann & Lacovara, 2016), *Epachthosaurus* (Martínez *et al*., 2004: fig. 13; UNPSJB-PV 920: PDM & SFP pers. obs. 2013), *Malawisaurus* (Gomani, 2005) and *Muyelensaurus* (MAU-PV-LL 58, 59, 144-146: PDM pers. obs. 2014). Phalanx IV-2 (IANIGLA-PV 077/10) is a reduced, proximodistally short ungual, with subcircular proximal and distal ends (Figs 22A, 24AT, AU).

OSTEODERMS

Four osteoderms (IANIGLA-PV 080/1–2, 081/1–2) were found (Figs 25, 26) associated with the anterior caudal vertebrae (González Riga, 2003). Two of them are large and have a subspherical shape (IANIGLA-PV 080/1–2; Fig. 25). Their internal side is slightly convex, whereas this convexity is more pronounced on their external side. They correspond to the morphotype 1 (ellipsoid shape) described by D'Emic *et al*. (2009). IANIGLA-PV 080/2 (Fig. 25G–L) is slightly crushed. It has a subconical shape, with its dorsal surface dominated by an apex at which fibres and grooves converge (Gonzalez Riga, 2003: fig. 7). IANIGLA-PV 080/1 (Fig. 25A–F) is better preserved than IANIGLA-PV 080/1. It has a subspherical shape with a less pronounced dorsal apex. Neither osteoderm appears to be hollow. These two osteoderms lack the cingulum present in the osteoderms of *Ampelosaurus* (Le Loeuff, 1995), and are different in shape and size to the osteoderms of any other titanosaur. Consequently, we regard their shape as an autapomorphy of *Mendozasaurus*. The other two osteoderms (IANIGLA-PV 081/1–2) are small and bulbous (Fig. 26).

PHYLOGENETIC ANALYSIS

DATA SET

We utilised the titanosauriform-focussed data matrix of Mannion *et al*. (2013), using the most recently revised version presented in Mannion *et al*. (2017). *Mendozasaurus neguyelap* was added as an OTU, along with the Argentinean titanosaurs *Argentinosaurus huinculensis* (Bonaparte & Coria, 1993; MCF-PVPH-1: PDM pers. obs. 2009), *Notocolossus gonzalezparejasi* (González Riga *et al*., 2016), *Patagotitan mayorum* (Carballido *et al*., 2017), *Pitekunsaurus macayai* (Filippi & Garrido, 2008; MAU-Pv-AG-446: PDM pers. obs. 2014), *Puertasaurus reuili* (Novas *et al*., 2005), and *Rinconsaurus caudamirus* (Calvo & González Riga, 2003; MAU-Pv-CRS specimens: PDM pers. obs. 2014), with which it overlaps anatomically. Several of these were also recovered as members of Lognkosauria by Carballido *et al*. (2017). We also revised the scores for *Tapuiasaurus* and the cervical vertebrae of *Alamosaurus*, following Wilson *et al*. (2016) and Tykoski & Fiorillo (2016), respectively (see Appendix). In scoring *Mendozasaurus*, we take a conservative approach to assessing the referral of elements to discrete individuals, and therefore do not use anatomical ratios relating to more than one element.

Seven characters were also added to this data matrix, comprising modified characters from previous studies (e.g. González Riga *et al*., 2009, 2016; Carballido *et al*., 2017), as well as one novel character emanating from our revision of *Mendozasaurus* and personal observations of other taxa. A complete list of new characters, including their sources, is provided in the Appendix. Our revised data matrix comprises 84 taxa scored for 423

characters (the TNT file and full character list are available in the Supplementary Information).

ANALYTICAL PROTOCOL AND RESULTS

Following the most recent version of this data matrix presented by Mannion *et al*. (2017), characters 11, 14, 15, 27, 40, 51, 104, 122, 147, 148, 177, 195, 205 and 259 were treated as ordered multistate characters, and eight unstable and highly incomplete taxa (*Astrophocaudia*, *Australodocus*, *Brontomerus*, *Fukuititan*, *Fusuisaurus*, *Liubangosaurus*, *Mongolosaurus*, *Tendaguria*) were excluded *a priori*, although *Malarguesaurus* was retained because it was approximately spatiotemporally contemporaneous with *Mendozasaurus*. The pruned data matrix was then analysed (with equal weighting of characters) using the 'Stabilize Consensus' option in the 'New Technology Search' in TNT vs. 1.1 (Goloboff, Farris & Nixon, 2008). Searches were carried out using sectorial searches, drift, and tree fusing, with the consensus stabilized five times, prior to using the resultant trees as the starting trees for a 'Traditional Search' using Tree Bisection-Reconstruction. This resulted in 1176 MPTs of 1755 steps and produced a fairly well resolved strict consensus tree, aside from a polytomy in basal Somphospondyli. The Pruned Trees option in TNT demonstrated that *Malarguesaurus* is the least stable OTU, and this taxon is recovered as a non-titanosaurian somphospondylan. Other than the newly added taxa, the topology does not differ significantly from that presented in Mannion *et al*. (2017).

We recover a diverse Lognkosauria: the giant titanosaurs *Notocolossus*, *Patagotitan* and *Puertasaurus* form a polytomy, which is the sister clade to *Argentinosaurus*, with *Futalognkosaurus* outside of this grouping. *Mendozasaurus* is recovered as the most basal member of Lognkosauria. This largely supports the recent analysis of Carballido *et al*. (2017), although *Notocolossus* was recovered as the sister taxon to Lognkosauria in that study. Here, Lognkosauria is the sister clade to Rinconsauria (*Muyelensaurus* + *Rinconsaurus*), mirroring several recent analyses that have also found a close (or sister taxon) relationship (Gallina & Apesteguía, 2011; Gallina & Otero, 2015; Salgado *et al*., 2015), with *Epachthosaurus* and *Pitekunsaurus* recovered as successive outgroups. In contrast with previous analyses to have included *Aeolosaurus*, along with representatives of Lognkosauria and Rinconsauria (e.g. Coria *et al*., 2013; Salgado *et al*., 2015), we find that *Aeolosaurus* is more closely related to Saltasauridae than to these taxa. The clade comprising *Epachthosaurus* + (Lognkosauria + Rinconsauria) is placed near the base of Lithostrotia. A basal lithostrotian position for Lognkosauria is consistent with several previous analyses (including González Riga *et al*., 2016), although unlike many early studies (e.g. Calvo *et al*., 2007), it is not the sister taxon to *Malawisaurus*. Bremer supports for the interrelationships of *Epachthosaurus* + (Lognkosauria + Rinconsauria) are between values of 1 and 2, whilst support for the placement of this clade within Lithostrotia is slightly stronger (Bremer support = 3). Unlike the recent analysis of Tykoski & Fiorillo (2016), we did not recover *Alamosaurus* as closely related to Lognkosauria; instead, *Alamosaurus* is recovered as a saltasaurid, with shared characters of the cervical vertebrae interpreted as either convergences or as more widespread features amongst Lithostrotia (see also Carballido *et al*., 2017). Following its updated scoring, *Tapuiasaurus* remains as a lithostrotian, with close affinities to *Nemegtosaurus*, contrasting with the basal somphospondylan placement recovered by Wilson *et al*. (2016).

DISCUSSION

LOGNKOSAURIA

Our diagnosis of *Mendozasaurus* is revised based on a comprehensive reappraisal of its anatomy, including previously undescribed remains. Some characters that were originally described as autapomorphies of *Mendozasaurus* (González Riga, 2005: 537) are revaluated. One of these is the relatively short centra of cervical and dorsal vertebrae. A newly described cervical vertebra demonstrates that the presacral centra of *Mendozasaurus* were not especially short anteroposteriorly, and that their apparent short length is a taphonomic artefact via anteroposterior compression.

With the inclusion of the additional materials referred to *Futalognkosaurus* by Calvo (2014), *Futalognkosaurus* and *Mendozasaurus* overlap anatomically via: (1) middle–posterior cervical vertebrae; (2) anterior dorsal vertebrae; (3) anterior caudal vertebrae and chevrons; (4) the upper forelimb, as well as some metacarpals; and (5) the femur, fibula and some pedal elements. However, much of the skeleton of *Futalognkosaurus* awaits description, limiting detailed anatomical comparisons. The clade Lognkosauria is defined as the most recent common ancestor of *Mendozasaurus neguyelap* and *Futalognkosaurus dukei* and all its descendants (Calvo *et al*., 2007). Whereas prior studies restricted it to these two taxa (e.g. González Riga & Ortiz David, 2014; González Riga *et al*., 2016), our analysis and that of Carballido *et al*. (2017) demonstrate a richer Lognkosauria, augmented by *Argentinosaurus*, *Drusilasaura*, *Patagotitan*, *Puertasaurus*, *Quetecsaurus*, and possibly *Notocolossus*.

Following our analysis, Lognkosauria is diagnosed by eight synapomorphies, although none of these are unique to this clade. The high posterior-most cervical and anterior-most dorsal neural spines relative to posterior centrum height (C19) is a reversal to the plesiomorphic sauropod state, but several other derived somphospondylans also have high neural spines, including *Alamosaurus* (Tykoski & Fiorillo, 2016), *Isisaurus* (Jain & Bandyopadhyay, 1997) and *Ligabuesaurus* (Bonaparte *et al*., 2006). The presence of a deep spinodiapophyseal fossa on the lateral surface, at the base of the neural spine, in posterior cervical vertebrae (C417), is shared with *Alamosaurus* (Tykoski & Fiorillo, 2016) and possibly *Isisaurus* (Jain & Bandyopadhyay, 1997). *Alamosaurus* also shares with Lognkosauria (Tykoski & Fiorillo, 2016) the presence of laterally expanded posterior cervical neural spines, resulting from the expansion of the lateral lamina (C418). A low average Elongation Index value in anterior caudal centra (<0.6) is a reversal to the plesiomorphic sauropod state (C26) (though note that *Notocolossus* has the derived state), but several other titanosaurs also revert to shorter centra, e.g. *Malawisaurus* (Gomani, 1999), *Opisthocoelicaudia* (Borsuk-Białynicka, 1977) and *Savannasaurus* (Poropat *et al*., 2016). A ‘D’-shaped scapular blade (C217) is widespread amongst neosauropods, including the titanosaurs *Diamantinasaurus* (Poropat *et al*., 2015a) and *Opisthocoelicaudia* (Borsuk-Białynicka, 1977). As well as characterising Lognkosauria, a radius that is mediolaterally wider at its distal than proximal end (C46) is also a feature of several macronarians, including the titanosaurs *Alamosaurus* and *Rapetosaurus* (Curry Rogers, 2005). A femur with distal condyles of subequal width (C389) is a reversal to the plesiomorphic state, and also characterises several titanosaurs, e.g. *Opisthocoelicaudia* (Borsuk-Białynicka, 1977). Finally, Lognkosauria shares a proximally reduced metatarsal V (C74) with the titanosaur *Malawisaurus* and a number of non-titanosaurian neosauropods (Mannion *et al*., 2013).

NUMBER OF INDIVIDUALS OF *MENDOZASAURUS*

It is clear that multiple sauropods were preserved at the *Mendozasaurus* type site (Fig. 2) because several elements are duplicated (e.g. there are three right tibiae and two sets of right metatarsals), whereas other bones are size incongruent. González Riga (2003) suggested that the specimens recovered from the *Mendozasaurus* type site represented three individuals, along with additional indeterminate, fragmentary titanosaur specimens, as well as a small maniraptoran theropod (González Riga & Astini, 2007).

Herein, based on new materials and a full revision, we suggest that the remains of at least four *Mendozasaurus* individuals were preserved together. The fact that there are two right tibiae identical in size, one right tibia that is smaller, and one left tibia that is larger, indicates a minimum of four individuals: one larger (size class A), two intermediate (size class B), and one smaller (size class C), but it is not possible to unequivocally assign one of them to the preserved axial skeleton.

It is possible that all of the preserved vertebrae pertain to a single adult individual. The caudal vertebrae and chevrons, which were preserved as a partially articulated series, and the cervical vertebrae, which were concentrated in one section of the site (Fig. 2), support this notion. The idea that IANIGLA-PV 084, a large cervical vertebra, pertains to a larger individual (González Riga, 2003) is not supported herein—it is likely that it is one of the posteriormost cervical vertebrae, which are expected to be the largest in the cervical series.

The two femora (IANIGLA-PV 073/1 and 073/4) are sufficiently similar dimensionally and morphologically that they could pertain to the same individual. On the other hand, the tibiae evince the presence of at least four individuals, since two right tibiae, effectively identical in size, are preserved, along with a smaller right tibia and a left tibia that is markedly larger. It is probable that one of these tibiae pertains to the same individual as the femora. The tibia to femur length ratio is 0.63 in *Dreadnoughtus* (Lacovara *et al*., 2014) and 0.64 in *Epachthosaurus* (Martínez *et al*., 2004), whereas this ratio is 0.58 in *Opisthocoelicaudia* (Borsuk-Białynicka, 1977) and 0.52 in *Neuquensaurus* (Salgado *et al*., 2005). In *Mendozasaurus*, this ratio would be 0.65 using the largest tibia (IANIGLA-PV 074/2), and 0.55 using one of the intermediate-sized tibiae (IANIGLA-PV 073/2). Given that *Mendozasaurus* appears to be more closely related to *Epachthosaurus* than to those titanosaurs with a lower ratio, we tentatively suggest that the largest tibia pertains to the same individual as the femora (size class A).

Determining which size class the fibula belongs to is difficult. Whereas the ratio of the length of the fibula to tibia is 0.86 in *Dreadnoughtus* (Lacovara et al., 2014), it is slightly greater than 1.0 in *Epachthosaurus* (Martínez *et al*., 2004) and *Opisthocoelicaudia* (Borsuk-Białynicka, 1977). For *Mendozasaurus*, this ratio would be 0.92 using the largest tibia (IANIGLA-PV 074/2) and 1.08 using one of the intermediate-sized tibiae (IANIGLA-PV 073/2). We tentatively suggest that the fibula, astragalus and largest set of metatarsals (IANIGLA-PV 100/1-6) belong to size class A.

As noted in the Description, the two humeri, which are congruent both dimensionally and morphologically, and are probably a pair, appear to be from a smaller individual than the femora. The ratio of the intermediate-sized tibia (IANIGLA-PV 073/2) to humerus length is 0.74–0.77, which is comparable with that of *Dreadnoughtus* (0.75 [Lacovara *et al*., 2014]) and *Epachthosaurus* (0.74 [Martínez *et al*., 2004]). As such, we regard these elements as likely belonging to a similarly sized (or the same) individual, belonging to size class B. It is

probable that the sternal plate, scapula, ulna and radius all come from the same size class, and possibly pertain to the same individual, as the humeri. This is supported through the following comparisons. The ratio of the maximum dimensions of the humerus to scapula is 0.85 in *Opisthocoelicaudia* (Borsuk-Białynicka, 1977), and 0.92 in both *Alamosaurus* (Gilmore, 1946) and *Dreadnoughtus* (Lacovara *et al*., 2014). This ratio would be 0.92–0.95 in *Mendozasaurus* if the humeri and scapula are from the same individual. The radius to humerus length ratio is 0.59 in *Dreadnoughtus* (Lacovara et al., 2014) and *Epachthosaurus* (Martínez *et al*., 2004), 0.60 in *Futalognkosaurus* (Calvo, 2014), and 0.63 in *Opisthocoelicaudia* (Borsuk-Białynicka, 1977). This ratio would be 0.63–0.65 in *Mendozasaurus* if the radius and humeri are from the same individual.

Nearly all of the elements pertaining to the manus (metacarpals [IANIGLA-PV 074/1–5] and phalanges) can likely be attributed to the same sized individual (size class B) as the pectoral and forelimb elements outlined above. The longest metacarpal to radius length ratio would thus be 0.48 in *Mendozasaurus*, comparable to many titanosauriforms (Poropat *et al*., 2015b), including *Futalognkosaurus* (0.50 [Calvo, 2014]). The exception is IANIGLA-PV 154, which is only two-thirds the size of another morphologically similar metacarpal (IANIGLA-PV 074/5), and thus represents size class C. We attribute the remaining metatarsals and pedal phalanges to size class B.

In summary, it is possible that one individual (size class B) was the source of much of the material at the *Mendozasaurus* type site (i.e. the vertebrae, chevrons, scapula, sternal plate, humeri, ulna and radius, five of the metacarpals and manual phalanges, one right tibia, a complete right foot, and a left metatarsal V). However, the presence of a second right tibia, identical in size, complicates matters. A larger individual (size class A) is represented by femora and the left tibia (and possibly the fibula, astragalus, and a second set of metatarsals), whereas a single metacarpal indicates the presence of a smaller individual (size class C).

THE EVOLUTIONARY HISTORY OF *MENDOZASAURUS* AND LITHOSTROTIAN TITANOSAURS

Our analysis recovers a diverse clade of Late Cretaceous South American titanosaurs (*Argentinosaurus*, *Epachthosaurus*, *Futalognkosaurus*, *Mendozasaurus*, *Muyelensaurus*, *Notocolossus*, *Patagotitan*, *Pitekunsaurus*, *Puertasaurus*, *Rinconsaurus*) that is the sister taxon to a near-globally widespread clade. Whether or not this South American clade is endemic remains to be seen. It will be interesting in future to incorporate other Gondwanan titanosaurian taxa into this data matrix. For example, the Maastrichtian Indian taxon *Jainosaurus* shares with *Mendozasaurus* the presence of an anterolateral trochanter on the fibula (Wilson *et al*., 2011). Given that *Jainosaurus* is thought to be closely related to the Argentinean genus *Antarctosaurus* (Wilson *et al*., 2009) and the Malagasy taxon *Vahiny* (Curry Rogers & Wilson, 2014), with the latter also sharing some features with *Muyelensaurus* and *Pitekunsaurus* (Curry Rogers & Wilson, 2014), this might ultimately lead to the recovery of a large clade of South American and Indo-Madagascan titanosaurs.

The sister clade to this South American group consists of taxa from Asia (*Jiangshanosaurus*, *Nemegtosaurus*, *Opisthocoelicaudia*), India (*Isisaurus*), Madagascar (*Rapetosaurus*), North America (*Alamosaurus*), and South America (*Aeolosaurus*, *Saltasaurus*, *Tapuiasaurus*), and the African titanosaur *Malawisaurus* lies outside these two clades. When combined with information on the timing of Pangaean fragmentation and the existence of plausible dispersal routes, this near-global distribution supports the hypothesis

that most titanosaurian clades were widespread by the Early–middle Cretaceous (e.g. Gorscak & O'Connor, 2016; Poropat *et al*., 2016).

CONCLUSIONS

A detailed description of all remains pertaining to the early Late Cretaceous Argentinean titanosaurian sauropod dinosaur *Mendozasaurus neguyelap* enables a revised diagnosis for the genus. An expanded phylogenetic analysis recovers *Mendozasaurus* and several other taxa as part of a rich Lognkosauria that is placed within a diverse clade of South American lithostrotian titanosaurs. The sister clade to this South American group is composed of a near-global array of titanosaurs, which supports recent work that has argued for a widespread distribution of most titanosaurian clades by the Early–middle Cretaceous.

REFERENCES

Apesteguía S. 2005. Evolution of the titanosaur metacarpus. In: Tidwell V, Carpenter K, eds. *Thunder-lizards: the sauropodomorph dinosaurs*. Bloomington; Indianapolis: Indiana University Press, 321–345.

Bonaparte JF, Coria RA. 1993. Un nuevo y gigantesco saurópodo titanosaurio de la Formación Río Limay (Albiano-Cenomaniano) de la Provincia del-Neuquen, Argentina. *Ameghiniana* **30:** 271–282.

Bonaparte JF, González Riga BJ, Apesteguía S. 2006. *Ligabuesaurus leanzai* gen. et sp. nov. (Dinosauria, Sauropoda), a new titanosaur from the Lohan Cura Formation (Aptian, Lower Cretaceous) of Neuquén, Patagonia, Argentina. *Cretaceous Research* **27:** 364–376.

Bonnan MF. 2005. Pes anatomy in sauropod dinosaurs: implications for functional morphology, evolution, and phylogeny. In: Tidwell V, Carpenter K, eds. *Thunder-lizards: the sauropodomorph dinosaurs*. Bloomington; Indianapolis: Indiana University Press, 346–380.

Borsuk-Białynicka M. 1977. A new camarasaurid sauropod *Opisthocoelicaudia skarzynskii* gen. n., sp. n. from the Upper Cretaceous of Mongolia. *Palaeontologica Polonica* **37:** 5–63.

Calvo JO. 2014. New fossil remains of *Futalognkosaurus dukei* (Sauropoda, Titanosauria) from the Late Cretaceous of Neuquén, Argentina. *4th International Palaeontological Congress Abstract Volume* **4:** 325A.

Calvo JO, González Riga BJ. 2003. *Rinconsaurus caudamirus* gen. et sp. nov., a new titanosaurid (Dinosauria, Sauropoda) from the Late Cretaceous of Patagonia, Argentina. *Revista Geologica de Chile* **30:** 333–353.

Calvo JO, Salgado L. 1995. *Rebbachisaurus tessonei* sp. nov. a new Sauropoda from the Albian-Cenomanian of Argentina; new evidence on the origin of the Diplodocidae. *Gaia* **11:** 13–33.

Calvo JO, Porfiri JD, González Riga BJ, Kellner AWA. 2007. A new Cretaceous terrestrial ecosystem from Gondwana with the description of a new sauropod dinosaur. *Anais da Academia Brasileira de Ciências* **79:** 529–541.

Calvo JO, González Riga BJ, Porfiri JD. 2008a. A new titanosaur sauropod from the Late Cretaceous of Neuquén, Patagonia, Argentina. *Arquivos do Museu Nacional, Rio de Janeiro* **65:** 485–504.

Calvo JO, Porfiri JD, González Riga BJ, Kellner AWA. 2008b. Anatomy of *Futalognkosaurus dukei* Calvo, Porfiri, González Riga & Kellner, 2007 (Dinosauria, Titanosauridae) from the

Neuquén Group (Late Cretaceous), Patagonia, Argentina. *Arquivos do Museu Nacional, Rio de Janeiro* **65:** 511–526.

Canudo JI, Royo-Torres R, Cuenca-Bescós G. 2008. A new sauropod: *Tastavinsaurus sanzi* gen. et sp. nov. from the Early Cretaceous (Aptian) of Spain. *Journal of Vertebrate Paleontology* **28:** 712–731.

Carballido JL, Sander PM. 2014. Postcranial axial skeleton of *Europasaurus holgeri* (Dinosauria, Sauropoda) from the Upper Jurassic of Germany: implications for sauropod ontogeny and phylogenetic relationships of basal Macronaria. *Journal of Systematic Palaeontology* **12:** 335–387.

Carballido JL, Rauhut OWM, Pol D, Salgado L. 2011a. Osteology and phylogenetic relationships of *Tehuelchesaurus benitezii* (Dinosauria, Sauropoda) from the Upper Jurassic of Patagonia. *Zoological Journal of the Linnean Society* **163:** 605–662.

Carballido JL, Pol D, Cerda I, Salgado L. 2011b. The osteology of *Chubutisaurus insignis* del Corro, 1975 (Dinosauria: Neosauropoda) from the 'middle' Cretaceous of central Patagonia, Argentina. *Journal of Vertebrate Paleontology* **31:** 93–110.

Carballido JL, Salgado L, Pol D, Canudo JI, Garrido A. 2012. A new basal rebbachisaurid (Sauropoda, Diplodocoidea) from the Early Cretaceous of the Neuquén Basin; evolution and biogeography of the group. *Historical Biology* **24:** 631–654.

Carballido JL, Pol D, Otero A, Cerda IA, Salgado L, Garrido AC, Ramezani J, Cúneo NR, Krause JM. 2017. A new giant titanosaur sheds light on body mass evolution among sauropod dinosaurs. *Proceedings of the Royal Society of London B* **284:** 20171219.

Coria RA, Filippi LS, Chiappe LM, García R, Arcucci AB. 2013. *Overosaurus paradasorum* gen. et sp. nov., a new sauropod dinosaur (Titanosauria: Lithostrotia) from the Late Cretaceous of Neuquén, Patagonia, Argentina. *Zootaxa* **3683:** 357–376.

Curry Rogers K. 2005. Titanosauria: a phylogenetic overview. In: Curry Rogers K, Wilson JA, eds. *The sauropods: evolution and paleobiology*. Berkeley, Los Angeles: University of California Press, 50–103.

Curry Rogers K. 2009. The postcranial osteology of *Rapetosaurus krausei* (Sauropoda: Titanosauria) from the Late Cretaceous of Madagascar. *Journal of Vertebrate Paleontology* **29:** 1046–1086.

Curry Rogers K, Wilson JA. 2014. *Vahiny depereti*, gen. et sp. nov., a new titanosaur (Dinosauria, Sauropoda) from the Upper Cretaceous Maevarano Formation, Madagascar. *Journal of Vertebrate Paleontology* **34:** 606–617.

D'Emic MD. 2012. The early evolution of titanosauriform sauropod dinosaurs. *Zoological Journal of the Linnean Society* **166:** 624–671.

D'Emic MD, Wilson JA. 2011. New remains attributable to the holotype of the sauropod dinosaur *Neuquensaurus australis*, with implications for saltasaurine systematics. *Acta Palaeontologica Polonica* **56:** 61–73.

D'Emic MD, Wilson JA, Chatterjee S. 2009. The titanosaur (Dinosauria: Sauropoda) osteoderm record: review and first definitive specimen from India. *Journal of Vertebrate Paleontology* **29:** 165–177.

D'Emic MD, Wilson JA, Williamson TE. 2011. A sauropod dinosaur pes from the latest Cretaceous of North America and the validity of *Alamosaurus sanjuanensis* (Sauropoda, Titanosauria). *Journal of Vertebrate Paleontology* **31:** 1072–1079.

D'Emic MD, Mannion PD, Upchurch P, Benson RBJ, Pang Q, Cheng Z. 2013. Osteology of *Huabeisaurus allocotus* (Sauropoda: Titanosauriformes) from the Upper Cretaceous of China. *PLoS ONE* **8:** e69375.

Filippi LS, Garrido AC. 2008. *Pitekunsaurus macayai* gen. et sp. nov., nuevo titanosaurio (Saurischia, Sauropoda) del Cretácico Superior de la Cuenca Neuquina, Argentina. *Ameghiniana* **45:** 575–590.

Filippi LS, García RA, Garrido AC. 2011. A new titanosaur sauropod dinosaur from the Upper Cretaceous of North Patagonia, Argentina. *Acta Palaeontologica Polonica* **56:** 505–520.

Gallina PA. 2011. Notes on the axial skeleton of the titanosaur *Bonitasaura salgadoi* (Dinosauria–Sauropoda). *Anais da Academia Brasileira de Ciências* **83:** 235–245.

Gallina PA, Apesteguía S. 2011. Cranial anatomy and phylogenetic position of the titanosaurian sauropod *Bonitasaura salgadoi*. *Acta Palaeontologica Polonica* **56:** 45–60.

Gallina PA, Apesteguía S. 2015. Postcranial anatomy of *Bonitasaura salgadoi* (Sauropoda, Titanosauria) from the Late Cretaceous of Patagonia. *Journal of Vertebrate Paleontology* **35:** e924957.

Gallina PA, Otero A. 2015. Reassessment of *Laplatasaurus araukanicus* (Sauropoda: Titanosauria), from the Late Cretaceous of Patagonia, Argentina. *Ameghiniana* (doi: 10.5710/AMGH.08.06.2015.2911).

García RA, Salgado L, Fernández MS, Cerda IA, Paulina Carabajal A, Otero A, Coria RA, Fiorelli LE. 2014. Paleobiology of Titanosaurs: Reproduction, Development, Histology, Pneumaticity, Locomotion and Neuroanatomy from the South American Fossil Record. *Ameghiniana* **52:** 29–68.

Garrido AC. 2010. Estratigrafía del Grupo Neuquén, Cretácico Superior de la Cuenca Neuquina (Argentina): nueva propuesta de ordenamiento litoestratigráfico. *Revista del Museo Argentino de Ciencias Naturales* **12:** 121–177.

Gilmore CW. 1946. Reptilian fauna of the North Horn Formation of central Utah. *United States Geological Survey Professional Paper* **210-C:** 29–53.

Goloboff PA, Farris JS, Nixon KC. 2008. TNT, a free program for phylogenetic analysis. *Cladistics* **24:** 1–13.

Gomani EM. 1999. Sauropod caudal vertebrae from Malawi, Africa. *National Science Museum Monographs* **15:** 235–248.

Gomani EM. 2005. Sauropod dinosaurs from the Early Cretaceous of Malawi. *Palaeontologia Electronica* **8:** 1–37.

González Riga BJ. 2003. A new titanosaur (Dinosauria, Sauropoda) from the Upper Cretaceous of Mendoza Province, Argentina. *Ameghiniana* **40:** 155–172.

González Riga BJ. 2005. Nuevos restos fósiles de *Mendozasaurus neguyelap* (Sauropoda, Titanosauridae) del Cretácico tardío de Patagonia. *Ameghiniana* **43:** 535–548.

González Riga BJ. 2010. Paleobiology of South American titanosaurs. In: Calvo J, Porfiri J, González Riga BJ, Dos Santos D, eds. *Paleontología y Dinosaurios desde America Latina*. Universidad Nacional de Cuyo, EDIUNC, 125–141.

González Riga BJ. 2011. Speeds and stance of titanosaur sauropods: analysis of *Titanopodus* tracks from the Late Cretaceous of Mendoza, Argentina. *Anais da Academia Brasileira de Ciências* **83:** 279–290.

González Riga BJ, Astini RA. 2007. Preservation of large titanosaur sauropods in overbank fluvial facies: A case study in the Cretaceous of Argentina. *Journal of South American Earth Sciences* **23:** 290–303.

González Riga BJ, Calvo JO. 2009. A new wide-gauge sauropod track site from the Late Cretaceous of Mendoza, Neuquén Basin, Argentina. *Palaeontology* **52:** 631–640.

González Riga BJ, Ortiz David L. 2014. A New Titanosaur (Dinosauria, Sauropoda) from the Upper Cretaceous (Cerro Lisandro Formation) of Mendoza Province, Argentina. *Ameghiniana* **51:** 3–25.

González Riga BJ, Calvo JO, Porfiri J. 2008. An articulated titanosaur from Patagonia (Argentina): new evidence of neosauropod pedal evolution. *Palaeoworld* **17:** 33–40.

González Riga BJ, Previtera E, Pirrone CA. 2009. *Malarguesaurus florenciae* gen. et sp. nov., a new titanosauriform (Dinosauria, Sauropoda) from the Upper Cretaceous of Mendoza, Argentina. *Cretaceous Research* **30:** 135–148.

González Riga, B. J., Ortíz David L. D., Tomaselli M. B., Candeiro C. R. A., Coria J. P. and Prámparo M. 2015. Sauropod and theropod dinosaur tracks from the Upper Cretaceous of Mendoza (Argentina): trackmakers and anatomical evidences. *Journal of South American Earth Sciences* **61:** 134–141.

González Riga BJ, Lamanna MC, Ortiz David LD, Calvo JO, Coria JP. 2016. A gigantic new dinosaur from Argentina and the evolution of the sauropod hind foot. *Scientific Reports* **6:** 19165.

Gorscak E, O'Connor PM. 2016. Time-calibrated models support congruency between Cretaceous continental rifting and titanosaurian evolutionary history. *Biology Letters* **12:** 20151047.

Gorscak E, O'Connor PM, Roberts EM, Stevens NJ. 2017. The second titanosaurian (Dinosauria: Sauropoda) from the middle Cretaceous Galula Formation, southwestern Tanzania, with remarks on African titanosaurian diversity. *Journal of Vertebrate Paleontology* **57:** e1343250.

Harris JD. 2007. The appendicular skeleton of *Suuwassea emilieae* (Sauropoda: Flagellicaudata) from the Upper Jurassic Morrison Formation of Montana (USA). *Geobios* **40:** 501–522.

Jain SL, Bandyopadhyay S. 1997. New titanosaurid (Dinosauria: Sauropoda) from the Late Cretaceous of Central India. *Journal of Vertebrate Paleontology* **17:** 114–136.

Jesus Faria CC, González Riga B, Candeiro CRA, Marinho TS, Ortiz David L, Simbras FM, Castanho RB, Muniz FP, Costa Pereira PVLG. 2015. Cretaceous sauropod diversity and taxonomic succession in South America. *Journal of South American Earth Sciences* **61:** 154–163.

Kellner AWA, Campos DA, Trotta MNF. 2005. Description of a titanosaurid caudal series from the Bauru Group, Late Cretaceous of Brazil. *Arquivos do Museu Nacional, Rio de Janeiro* **63:** 529–564.

Kellner AWA, Campos DA, Azevedo SAK, Trotta MNF, Henriques DDR, Craik MMT, Silva HP. 2006. On a new titanosaur sauropod from the Bauru Group, Late Cretaceous of Brazil. *Boletim do Museu Nacional, Nova Série, Geologia* **74:** 1–31.

Lacovara KJ, Lamanna MC, Ibiricu LM, Poole JC, Schroeter ER, Ullmann PV, Voegele KK, Boles ZM, Carter AM, Fowler EK, Egerton VM, Moyer AE, Coughenour CL, Schein JP, Harris JD, Martínez RD, Novas FE. 2014. A Gigantic, Exceptionally Complete Titanosaurian Sauropod Dinosaur from Southern Patagonia, Argentina. *Scientific Reports* **4:** 6196.

Le Loeuff J. 1995. *Ampelosaurus atacis* (nov, gen., nov. sp.), un nouveau Titanosauridae (Dinosauria, Sauropoda) du Crétacé supérieur de la Haute Vallée de l'Aude (France). *Comptes Rendus de l'Académie des Sciences à Paris, Série IIA* **321:** 693–699.

Mannion PD, Calvo JO. 2011. Anatomy of the basal titanosaur (Dinosauria, Sauropoda) *Andesaurus delgadoi* from the mid-Cretaceous (Albian-early Cenomanian) Río Limay

Formation, Neuquén Province, Argentina: implications for titanosaur systematics. *Zoological Journal of the Linnean Society* **163:** 155–181.

Mannion PD, Otero A. 2012. A reappraisal of the Late Cretaceous Argentinean sauropod dinosaur *Argyrosaurus superbus*, with a description of a new titanosaur genus. *Journal of Vertebrate Paleontology* **32:** 614–638.

Mannion PD, Allain, R, Moine O. 2017. The earliest known titanosauriform sauropod dinosaur and the evolution of Brachiosauridae. *PeerJ* **5:** e3217.

Mannion PD, Upchurch P, Barnes RN, Mateus O. 2013. Osteology of the Late Jurassic Portuguese sauropod dinosaur *Lusotitan atalaiensis* (Macronaria) and the evolutionary history of basal titanosauriforms. *Zoological Journal of the Linnean Society* **168:** 98–206.

Marsh OC. 1878. Principal characters of American Jurassic dinosaurs. Part I. *American Journal of Science* **16:** 411–416.

Martínez RD, Giménez O, Rodríguez J, Luna M, Lamanna MC. 2004. An articulated specimen of the basal titanosaurian (Dinosauria: Sauropoda) *Epachthosaurus sciuttoi* from the early Late Cretaceous Bajo Barreal Formation of Chubut province, Argentina. *Journal of Vertebrate Paleontology* **24:** 107–120.

Mateus O, Jacobs LL, Schulp AS, Polcyn MJ, Tavares TS, Neto AB, Morais ML, Antunes MT. 2011. *Angolatitan adamastor*, a new sauropod dinosaur and the first record from Angola. *Anais da Academia Brasileira de Ciências* **83:** 1–13.

Nair JP, Salisbury SW. 2012. New anatomical information on *Rhoetosaurus brownei* Longman, 1926, a gravisaurian sauropodomorph dinosaur from the Middle Jurassic of Queensland, Australia. *Journal of Vertebrate Paleontology* **32:** 369–394.

Novas F, Salgado L, Calvo J, Agnolin F. 2005. Giant titanosaur (Dinosauria, Sauropoda) from the Late Cretaceous of Patagonia. *Revista del Museo Argentino de Ciencias Naturales Nueva Serie* **7:** 37–41.

Otero A. 2010. The appendicular skeleton of *Neuquensaurus*, a Late Cretaceous saltasaurine sauropod from Patagonia, Argentina. *Acta Palaeontologica Polonica* **55:** 399–426.

Poropat SF, Upchurch P, Mannion PD, Hocknull SA, Kear BP, Sloan T, Sinapius GHK, Elliott DA. 2015a. Revision of the sauropod dinosaur *Diamantinasaurus matildae* Hocknull et al. 2009 from the middle Cretaceous of Australia: implications for Gondwanan titanosauriform dispersal. *Gondwana Research* **27:** 995–1033.

Poropat SF, Mannion PD, Upchurch P, Hocknull SA, Kear BP, Elliott DA. 2015b. Reassessment of the non-titanosaurian somphospondylan *Wintonotitan wattsi* (Dinosauria: Sauropoda: Titanosauriformes) from the mid-Cretaceous Winton Formation, Queensland, Australia. *Papers in Palaeontology* **1:** 59–106.

Poropat SF, Mannion PD, Upchurch P, Hocknull SA, Kear BP, Kundrát M, Tischler TT, Sloan T, Sinapius GHK, Elliott JA, Elliott DA. 2016. New Australian sauropods shed light on Cretaceous dinosaur palaeobiogeography. *Scientific Reports* **6:** 34467.

Powell JE 1987. The Late Cretaceous fauna of Los Alamitos, Patagonia, Argentina. Part VI. The titanosaurids. *Revista del Museo Argentino de Ciencias Naturales 'Bernardino Rivadavia'* **3:** 147–153.

Powell JE. 2003. Revision of South American titanosaurid dinosaurs: palaeobiological, palaeobiogeographical and phylogenetic aspects. *Records of the Queen Victoria Museum* **111:** 1–173.

Salgado L, Carvalho IS. 2008. *Uberabatitan ribeiroi*, a new titanosaur from the Marília Formation (Bauru Group, Upper Cretaceous), Minas Gerais, Brazil. *Palaeontology* **51:** 881–901.

Salgado, L, Apesteguía, S, Heredia, SE. 2005. A new specimen of *Neuquensaurus australis*, a Late Cretaceous saltasaurine titanosaur from north Patagonia. *Journal of Vertebrate Paleontology* **25:** 623–634.

Salgado L, Coria RA, Calvo JO. 1997. Evolution of titanosaurid sauropods. I: phylogenetic analysis based on the postcranial evidence. *Ameghiniana* **34:** 3–32.

Salgado L, Gallina PA, Paulina Carabajal A. 2015. Redescription of *Bonatitan reigi* (Sauropoda: Titanosauria), from the Campanian–Maastrichtian of the Río Negro Province (Argentina). *Historical Biology* **27:** 525–548.

Santucci RM, Arruda-Campos AC. 2011. A new sauropod (Macronaria, Titanosauria) from the Adamantina Formation, Bauru Group, Upper Cretaceous of Brazil and the phylogenetic relationships of Aeolosaurini. *Zootaxa* **3085:** 1–33.

Sanz JL, Powell JE, Le Loueff J, Martinez R, Pereda Suberbiola X. 1999. Sauropod remains from the Upper Cretaceous of Laño (northcentral Spain). Titanosaur phylogenetic relationships. *Estudios del Museo de Ciencias Naturales de Alava* **14:** 235–255.

Smith JB, Lamanna MC, Lacovara KJ, Dodson P, Smith JR, Poole JC, Giegengack R, Attia Y. 2001. A giant sauropod dinosaur from an Upper Cretaceous mangrove deposit in Egypt. *Science* **292:** 1704–1706.

Tschopp E, Mateus O, Benson RBJ 2015. A specimen-level phylogenetic analysis and taxonomic revision of Diplodocidae (Dinosauria, Sauropoda). *PeerJ* **3:** e857.

Tykoski RS, Fiorillo AR. 2016. An articulated cervical series of *Alamosaurus sanjuanensis* Gilmore, 1922 (Dinosauria, Sauropoda) from Texas: new perspective on the relationships of North America's last giant sauropod. *Journal of Systematic Palaeontology* (doi: 10.1080/14772019.2016.1183150).

Ullmann PV, Lacovara KJ. 2016. Appendicular osteology of *Dreadnoughtus schrani*, a giant titanosaurian (Sauropoda, Titanosauria) from the Upper Cretaceous of Patagonia, Argentina. *Journal of Vertebrate Paleontology* **36:** e1225303.

Upchurch P. 1995. The evolutionary history of sauropod dinosaurs. *Philosophical Transactions of the Royal Society of London, Series B* **349:** 365–390.

Upchurch P. 1998. The phylogenetic relationships of sauropod dinosaurs. *Zoological Journal of the Linnean Society* **124:** 43–103.

Upchurch P, Barrett PM, Dodson P. 2004. Sauropoda. In: Weishampel DB, Dodson P, Osmólska H, eds. *The Dinosauria, 2nd edn*. Berkeley: University of California Press, 259–324.

Upchurch P, Mannion PD, Taylor MP. 2015. The Anatomy and Phylogenetic Relationships of "*Pelorosaurus*" *becklesii* (Neosauropoda, Macronaria) from the Early Cretaceous of England. *PLoS ONE* **10:** e0125819.

Whitlock JA, D'Emic MD, Wilson JA. 2011. Cretaceous diplodocids in Asia? Re-evaluating the phylogenetic affinities of a fragmentary specimen. *Palaeontology* **54:** 351–364.

Wilson JA. 1999. A nomenclature for vertebral laminae in sauropods and other saurischian dinosaurs. *Journal of Vertebrate Paleontology* **19:** 639–653.

Wilson JA. 2002. Sauropod dinosaur phylogeny: critique and cladistic analysis. *Zoological Journal of the Linnean Society* **136:** 217–276.

Wilson JA, Sereno PC. 1998. Early evolution and higher-level phylogeny of sauropod dinosaurs. *Society of Vertebrate Paleontology Memoir* **5:** 1–68.

Wilson JA, Barrett PM, Carrano MT. 2011. An associated partial skeleton of *Jainosaurus* cf. *septentrionalis* (Dinosauria: Sauropoda) from the Late Cretaceous of Chhota Simla, central India. *Palaeontology* **54:** 981–998.

Wilson JA, Martinez RN, Alcober O. 1999. Distal tail segment of a titanosaur (Dinosauria: Sauropoda) from the Upper Cretaceous of Mendoza, Argentina. *Journal of Vertebrate Paleontology* **19:** 591–594.

Wilson JA, D'Emic MD, Curry Rogers KA, Mohabey DM, Sen S. 2009. Reassessment of the sauropod dinosaur *Jainosaurus* (="*Antarctosaurus*") *septentrionalis* from the Upper Cretaceous of India. *Contributions from the Museum of Paleontology, University of Michigan* **32:** 17–40.

Wilson JA, D'Emic MD, Ikejiri T, Moacdieh EM, Whitlock JA. 2011. A nomenclature for vertebral fossae in sauropods and other saurischian dinosaurs. *PLoS ONE* **6:** e17114.

Wilson JA, Pol D, Carvalho AB, Zaher H. 2016. The skull of the titanosaur *Tapuiasaurus macedoi* (Dinosauria: Sauropoda) from the Lower Cretaceous of Brazil. *Zoological Journal of the Linnean Society* **178:** 611–662.

TABLES

Table 1. Measurements of presacral vertebrae (IANIGLA-PV 066, 076/1–4, 084/1) of *Mendozasaurus neguyelap*. Measurements with an asterisk have been heavily affected by crushing. A # sign denotes a measurement that is extrapolated based on only one half being complete. All measurements are in millimetres.

Dimension	076/5	076/3	076/1	084/1	076/4	066
Centrum length (including ball)	–	417	286	–	–	158
Centrum length (excluding ball)	–	~315	259	~480	–	128
Anterior centrum height	124	–	152	136	–	–
Anterior centrum width	144	–	211	276	–	–
Posterior centrum height	–	156*	184	–	–	189
Posterior centrum width	–	230*	238	–	–	263
Neural arch height	–	–	–	–	–	126
Neural spine height	–	–	440	–	261	252
Maximum mediolateral width of neural spine	–	–	390	389	–	76
Anteroposterior length of neural spine	–	–	–	–	–	42
Total width across diapophyses	–	–	730	–	840#	680

Table 2. Measurements of caudal vertebrae (IANIGLA-PV 065/1–22) of *Mendozasaurus neguyelap*. Abbreviations: **LIC**, length of centrum including condyle; **LEC**, length of centrum excluding condyle; **ACH**, anterior centrum height; **ACW**, anterior centrum width; **PCH**, posterior centrum height; **PCW**, posterior centrum width; **NAH**, neural arch height; **NSH**, neural spine height; **NSW**, neural spine width at base; **MNSW**, maximum neural spine width; **NSL**, neural spine length at base; **TWD**, transverse width across diapophyses. A # sign denotes a measurement that is extrapolated based on only one half being complete. Centrum heights do not include chevron facets. All measurements are in millimetres.

Cd	LIC	LEC	ACH	ACW	PCH	PCW	NAH	NSH	NSW	MNSW	NSL	TWD
I	–	–	–	–	208	229	82	260	87	99	70	370
II	197	140	220	154	183	135	–	–	–	–	–	270#
III	155	115	192	233	158	190	–	–	–	–	–	–
IV	215	147	–	–	174	–	70	190	32	57	95	–
V	–	–	–	–	–	–	–	–	–	–	–	–
VI	152	123	160	159	132	156	50	–	–	–	–	275
VII	–	129	127	–	145	–	40	128	23	–	72	–
VIII	–	120	124	162	130	153	–	–	–	–	–	208
IX	–	–	–	–	–	–	–	–	–	–	–	–
X	–	145	142	119	–	–	–	–	–	–	–	–
XI	–	148	119	~122	–	–	–	–	–	–	–	–
XII	–	147	118	119	129	118	33	80	26	–	92	–
XIII	–	161	–	–	111	116	23	74	21	–	110	–
XIV	150	143	116	116	116	100	15	80	21	–	100	–
XV	155	141	109	86	102	101	25	78	18	–	105	–

XVI	155	143	99	119	102	122	20	73	20	–	102	–
XVII	157	147	95	111	82	115	–	–	–	–	–	–
XVIII	160	149	85	113	80	107	–	–	–	–	–	–
XIX	143	131	95	105	91	~103	22	–	–	–	68	–
XX	159	143	94	90	86	92	–	–	–	–	–	–
XXI	137	126	92	102	77	93	–	–	–	–	–	–
XXII	–	–	–	–	93	~85	–	–	–	–	–	–

Table 3. Measurements of chevrons (IANIGLA-PV 065/23–25) of *Mendozasaurus neguyelap*. All measurements are in millimetres.

Dimension	065/23	065/24	065/25
Proximodistal height	332	307	291
Haemal canal depth	148	125	120
Proximal ramus anteroposterior length	63	58	57
Proximal ramus maximum mediolateral width	39	33	36
Maximum anteroposterior length of distal blade	69	74	68

Table 4. Measurements of pectoral girdle and upper forelimb elements (IANIGLA-PV 067–070) of *Mendozasaurus neguyelap*. Measurements with an asterisk have been affected by crushing. All measurements are in millimetres.

Element	Dimension	Measurement
Right scapula (068)	Proximodistal length	1200
	Anteroposterior length of acromion	395
	Dorsoventral height of acromion (as preserved)	545
	Minimum dorsoventral height of scapular blade	179
	Maximum dorsoventral height of scapular blade (as preserved)	296
Right sternal plate (067)	Anteroposterior length	861
	Maximum mediolateral width at approximate midlength	415
Right humerus (069/1)	Proximodistal length	1142
	Proximal end maximum mediolateral width	350
	Distance from proximal end to distal tip of deltopectoral crest	500
	Midshaft mediolateral width	153
	Midshaft anteroposterior length	72
	Midshaft minimum circumference	412
	Distal end mediolateral width	340
	Distal end maximum anteroposterior length	135
Left humerus (069/2)	Proximodistal length	1100
	Proximal end maximum mediolateral width	377
	Distance from proximal end to distal tip of deltopectoral crest	470
	Midshaft mediolateral width	162
	Midshaft anteroposterior length	83

	Midshaft minimum circumference	421
	Distal end mediolateral width (as preserved)	310
	Distal end maximum anteroposterior length	132
Right radius (070/2)	Proximodistal length	717
	Proximal end mediolateral width	160
	Proximal end maximum anteroposterior length	62*
	Midshaft mediolateral width	90
	Midshaft maximum anteroposterior length	61*
	Distal end mediolateral width	185
	Distal end maximum anteroposterior length	62*
Right ulna (070/1)	Proximodistal length (as preserved)	737
	Proximal end mediolateral width (as preserved)	173
	Distal end maximum mediolateral width	108
	Distal end maximum anteroposterior length	189

Table 5. Measurements of metacarpals (IANIGLA-PV 071/1–5, 154) of *Mendozasaurus neguyelap*. All measurements are in millimetres.

Dimension	I (071/4)	II (071/3)	III (071/1)	IV (071/2)	V (071/5)	I (154)
Proximodistal length	330	333	333	341	306	234
Proximal end maximum diameter	109	90	121	116	119	102
Proximal end diameter perpendicular to long axis	41	64	68	44	43	51
Midshaft maximum diameter	46	56	47	50	57	50
Midshaft diameter perpendicular to long axis	44	37	28	29	31	29
Distal end mediolateral width	78	101	100	90	103	75
Distal end dorsoventral height	70	54	54	60	55	54

Table 6. Measurements of hindlimb elements (IANIGLA-PV 073, 074, 155) of *Mendozasaurus neguyelap*. Measurements with an asterisk have been affected by crushing. All measurements are in millimetres.

Element	Dimension	Measurement
Left femur (073/4)	Proximodistal length	1530
	Distance from proximal end to distal tip of fourth trochanter	780
	Midshaft mediolateral width	195
	Midshaft anteroposterior length	103
	Midshaft minimum circumference	520
	Distal end anteroposterior length on tibial condyle	231

	Distal end anteroposterior length on fibular condyle	210
	Distal end mediolateral width on tibial condyle	162
	Distal end mediolateral width on fibular condyle	189
Right tibia (073/2)	Proximodistal length	845
	Mediolateral width of cnemial crest	132
	Midshaft maximum diameter	139*
	Distal end maximum diameter	214*
Right tibia (074/1)	Proximodistal length (as preserved)	847
	Proximal end maximum mediolateral width	185
	Proximal end maximum anteroposterior length	249
	Midshaft maximum diameter	130
	Midshaft diameter perpendicular to maximum diameter	70
	Distal end mediolateral width (as preserved)	122
Right tibia (073/3)	Proximodistal length (as preserved)	720
	Midshaft maximum diameter	128
	Distal end maximum mediolateral width (as preserved)	195
	Distal end maximum anteroposterior length	152
Left tibia (074/2)	Proximodistal length	990
	Proximal end maximum mediolateral width	375
	Midshaft maximum diameter	145
Left fibula (074/3)	Proximodistal length	914
	Proximal end maximum anteroposterior length	208
	Proximal end maximum mediolateral width	80
	Distance from proximal end to distal tip of lateral trochanter	~450
	Midshaft anteroposterior length	99
	Midshaft mediolateral width	60
	Distal end maximum anteroposterior length	169
	Distal end maximum mediolateral width	131
Right fibula (074/4)	Proximodistal length (as preserved)	633
	Midshaft anteroposterior length	93
	Midshaft mediolateral width	58
Right astragalus (155)	Mediolateral width	219*
	Anteroposterior length	159*

Table 7. Measurements of metatarsals (IANIGLA-PV 077/1–5, 100/1–6, 153) of *Mendozasaurus neguyelap*. Specimens 077/1–4 have all undergone significant distortion. Measurements with an asterisk have been affected by crushing, and those with the symbol # are incomplete. All measurements are in millimetres.

Dimension	I (077/1)	II (077/2)	III (077/3)	IV (077/4)	V (077/5)	I (100/1)	II (100/2)	III (100/3)	IV (100/4)	V (100/5)	V (100/6)	V (153)

Proximodistal length	135	158	181	212	169	145	142	195	232	126 #	187	159
Proximal end maximum diameter	74	97	–	108	121	127	118 #	101 #	98	128	132 #	136
Proximal end diameter perpendicular to long axis	68	63	–	–	36*	78	56	74	86	54	54	28
Midshaft mediolateral width	–	42	–	–	63	–	86	49	41	52	70	57
Midshaft dorsoventral height	–	39	–	–	–	–	44	38	40	34	–	22
Distal end mediolateral width	–	91	83	66	77	112	114	89	93	–	93#	63
Distal end dorsoventral height	–	65	58	49	36*	64	45	66	56	–	32	20

Table 8. Measurements of pedal phalanges (IANIGLA-PV 077/6–12, 078/1–2, 079) of *Mendozasaurus neguyelap*. Measurements with an asterisk have been affected by crushing. All measurements are in millimetres.

Dimension	**I-1 (077/ 6)**	**I-1 (077/ 12)**	**II-1 (077/ 7)**	**II-1 (077/ 11)**	**III-1 (077/ 8)**	**IV-1 (077/ 9)**	**I-2 (078/ 1)**	**II-2 (078/ 2)**	**III-2 (079)**	**IV-2 (077/ 10)**
Proximodistal length	55	26*	58	58	52	79	133	122	121	35
Proximal end mediolateral width	61	66	77	66	70	72	21	–	19*	55
Proximal end dorsoventral height	58	45	47	55	50	40	79	73	65	51
Midshaft mediolateral width	56	64	61	53	–	52	–	–	–	–
Distal end mediolateral width	62	55	71	55	62	63	–	–	–	–
Distal end dorsoventral height	47	48	35	40	–	23	–	–	–	–

Table 9. Measurements of osteoderms (IANIGLA-PV 080, 081) of *Mendozasaurus neguyelap*. We interpret the maximum diameter to be the anteroposterior length. All measurements are in millimetres.

Dimension	**080/1**	**080/2**	**081/1**	**082/2**
Maximum proximodistal height	143	160	71	69
Maximum diameter	189	184	81	71
Diameter perpendicular to maximum diameter	113	101	42	34

FIGURE CAPTIONS

Figure 1. A) Map showing the locality where *Mendozasaurus neguyelap* was found. B) Stratigraphic column of the Late Cretaceous strata of Neuquen Group with indication of the fossiliferous level of the Sierra Barrosa Formation.

Figure 2. Quarry map of Arroyo Seco showing the fossil accumulation of *Mendozasaurus neguyelap* with the holotype caudal sequence highlighted (modified from González Riga & Astini, 2007).

Figure 3. Life restoration of *Mendozasaurus neguyelap* based on the largest adult individual (femur length: 1530 mm). Artwork by Bernardo Gonzaléz Riga.

Figure 4. *Mendozasaurus neguyelap* cervical vertebra (IANIGLA-PV 076/5) in A) anterior and B) left anterolateral views. Scale bar = 100 mm.

Figure 5. *Mendozasaurus neguyelap* cervical vertebra (IANIGLA-PV 076/3) in A) posterior, B) right lateral, C) anterior, D) dorsal, and E) ventral views. Scale bar = 100 mm.

Figure 6. *Mendozasaurus neguyelap* cervical vertebra (IANIGLA-PV 076/1) in A) anterior, B) left lateral, C) posterior, D) right lateral, E) ventral, and F) dorsal views. Scale bar = 150 mm.

Figure 7. *Mendozasaurus neguyelap* cervical vertebra (IANIGLA-PV 084/1) in A) right lateral, B) dorsal, C) anterior, D) posterior (neural spine only), and E) left lateral views. Scale bar = 250 mm.

Figure 8. *Mendozasaurus neguyelap* dorsal vertebra (IANIGLA-PV 066) in A) anterior, B) left lateral (reversed), C) posterior, D) right lateral, E) ventral, and F) dorsal views. Scale bar = 200 mm.

Figure 9. *Mendozasaurus neguyelap* caudal vertebrae: Caudal vertebra I (IANIGLA-PV 066/1) in A) anterior, B) left lateral (right lateral reversed), C) dorsal, and D) posterior views; caudal vertebra II (IANIGLA-PV 066/2) in E) anterior, F) left lateral, and G) posterior views; caudal vertebra III (IANIGLA-PV 066/3) in H) anterior, I) dorsal, and J) left lateral views; caudal vertebra IV (IANIGLA-PV 066/4) in K) anterior, L) left lateral (right lateral reversed), and M) posterior views; caudal vertebra VI (IANIGLA-PV 066/6) in N) anterior, O) dorsal, P) left lateral, and Q) posterior views; caudal vertebra VII (IANIGLA-PV 066/7) in R) left lateral view; caudal vertebra VIII (IANIGLA-PV 066/8) in S) anterior, and T) left lateral views; caudal vertebra XVI (IANIGLA-PV 066/16) in U) anterior, V) dorsal, W) left lateral, and X) posterior views; caudal vertebra XVIII (IANIGLA-PV 066/18) in Y) anterior, Z) dorsal, AA) left lateral, and AB) posterior views; and caudal vertebrae V–XIX (IANIGLA-PV 066/5–18) in AC) dorsal, and AC) left lateral views. Scale bar = 200 mm.

Figure 10. Comparisons of middle caudal vertebrae of titanosaurs: A) *Mendozasaurus neguyelap* caudal XVI, B) *Dreadnoughtus schrani* caudal XV, C) *Epachthosaurus sciuttoi* caudal X, D) *Baurutitan britoi* caudal XIV (right lateral reversed), E) *Andesaurus delgadoi* caudal XX, F) *Malawisaurus dixeyi* caudal VII, and G) *Narambuenatitan palomoi* middle caudal. Not to scale.

Figure 11. *Mendozasaurus neguyelap* chevrons: IANIGLA 065/23 in A) anterior, B) left lateral, C) proximal, D) posterior, and E) right lateral views; IANIGLA 065/24 in F) anterior, G) left lateral, H) proximal, I) posterior, and J) right lateral views; IANIGLA 065/25 in K) anterior, L) left lateral, M) proximal, N) posterior, and O) right lateral views. Scale bar = 100 mm.

Figure 12. *Mendozasaurus neguyelap* pectoral girdle elements: right scapula (IANIGLA-PV 068) in A) lateral, and B) medial views; and right sternal plate (IANIGLA-PV 067) in dorsal (internal) view. Scale bar = 150 mm.

Figure 13. Comparisons of right scapulae of sauropods: A) *Mendozasaurus neguyelap*, B) *Ligabuesaurus leanzai*, C) *Dreadnoughtus schrani*, D) *Pitekunsaurus macayai*, E) *Opisthocoelicaudia skarzynskii*, F) *Rapetosaurus krausei*, and G) *Muyelensaurus pecheni*. Not to scale.

Figure 14. *Mendozasaurus neguyelap* humeri: right humerus (IANIGLA-PV 069/1) in A) proximal, B) anterior, C) distal, D) medial, E) posterior, and F) lateral views; and left humerus (IANIGLA-PV 069/2) in G) anterior, H) distal, I) proximal, and J) posterior views. Scale bar = 250 mm.

Figure 15. Comparisons of right humeri of sauropods: A) *Mendozasaurus neguyelap*, B) *Angolatitan adamastor*, C) *Narambuenatitan palomoi* (left reversed); D) *Paralititan stromeri*; E) *Rapetosaurus krausei* (left reversed); F) *Petrobrasaurus puestohernandezi*; G) *Andesaurus delgadoi*; H) *Notocolossus gonzalezparejasi*; and I) *Dreadnoughtus schrani* (left reversed). Not to scale.

Figure 16. *Mendozasaurus neguyelap* antebrachial elements: right radius (IANIGLA-PV 070/2) in A) proximal, B) anterior, C) posterior, and D) distal views; and right ulna (IANIGLA-PV 070/1) in E) anterior, F) distal, G) proximal, and H) posterior views. Scale bar = 250 mm.

Figure 17. *Mendozasaurus neguyelap* composite right metacarpus in proximal end view, incorporating left metacarpal I (IANIGLA-PV 071/4; reversed), right metacarpal II (IANIGLA-PV 071/3), right metacarpal III (IANIGLA-PV 071/1), left metacarpal IV (IANIGLA-PV 071/2; reversed) and left metacarpal V (IANIGLA-PV 071/5; reversed).

Figure 18. *Mendozasaurus neguyelap* metacarpals: left metacarpal I (IANIGLA-PV 071/4) in A) proximal, B) ventral, C) distal, D) medial, and E) dorsal views; right metacarpal II (IANIGLA-PV 071/3) in F) dorsal, G) distal, H) medial, I) proximal, J) ventral, and K) lateral views; right metacarpal III (IANIGLA-PV 071/1) in L) dorsal, M) distal, N) medial, O) proximal, P) ventral, and Q) lateral views; left metacarpal IV (IANIGLA-PV 071/2) in R) dorsal, S) proximal, T) lateral, U) ventral, V) distal, and W) medial views; left metacarpal V (IANIGLA-PV 71/5 in X) dorsal, Y) proximal, Z) lateral, AA) ventral, AB) medial, and AC) distal views; and small right metacarpal I or left metacarpal V (IANIGLA-PV 154) in AD) dorsal, AE) proximal, AF) lateral, AG) ventral, AH) medial, and AI) distal views. Scale bar = 150 mm.

Figure 19. *Mendozasaurus neguyelap* femora: left femur (IANIGLA-PV 073/4) in A) medial, B) proximal, C) anterior, D) lateral, E) posterior, and F) distal views; and right femur (IANIGLA-PV 073/1) in G) anterior view. Scale bar = 400 mm.

Figure 20. *Mendozasaurus neguyelap* crural elements: right tibia (IANIGLA-PV 073/3) in A) lateral, B) distal, and C) medial views; right tibia (IANIGLA-PV 073/2) in D) lateral, E) distal, F) proximal, and G) medial views; right tibia (IANIGLA-PV 074/1) in H) lateral, I) proximal, and J) medial views; left tibia (IANIGLA-PV 074/2) in K) lateral, L) distal, M) proximal, and N) medial views; and left fibula (IANIGLA-PV 074/3) in O) lateral, P) distal, Q) proximal, and R) medial views. Scale bar = 400 mm.

Figure 21. *Mendozasaurus neguyelap* right astragalus (IANIGLA-PV 155) in A) anterior, B) distal, C) medial, D) proximal, E) posterior, and F) lateral views. Scale bar = 200 mm.

Figure 22. *Mendozasaurus neguyelap* pedal elements: right pes (metatarsals = IANIGLA-PV 077/1–5, non-ungual phalanges = IANIGLA-PV 077/6–10, ungual phalanges = IANIGLA-PV 078/1–2 & 079) in A) dorsal view; and rearticulated right metatarsals I–V (IANIGLA-PV 077/1–5) in B) dorsal, C) proximal, and D) distal views. Roman numerals correspond to pedal digit number. Scale bar = 100 mm.

Figure 23. *Mendozasaurus neguyelap* metatarsals: right metatarsal I (IANIGLA-PV 077/1) in A) dorsal, B) distal, C) medial, D) proximal, E) ventral, and F) lateral views; right metatarsal II (IANIGLA-PV 077/2) in G) dorsal, H) distal, I) medial, J) proximal, K) ventral, and L) lateral views; right metatarsal III (IANIGLA-PV 077/3) in M) dorsal, N) distal, O) medial, P) proximal, Q) ventral, and R) lateral views; right metatarsal IV (IANIGLA-PV 077/4) in S) dorsal, T) distal, U) medial, V) proximal, W) ventral, and X) lateral views; right metatarsal V (IANIGLA-PV 077/5) in Y) dorsal, Z) distal, AA) medial, AB) proximal, AC) ventral, and AD) lateral views; left metatarsal V (IANIGLA-PV 153) in AE) dorsal, AF) distal, AG) lateral, AH) proximal, AI) ventral, and AJ) medial views; large right metatarsal I (IANIGLA-PV 100/1) in AK) dorsal, AL) distal, AM) medial, AN) proximal, AO) ventral, and AP) lateral views; large left metatarsal I (IANIGLA-PV 100/2) in AQ) dorsal view; large right metatarsal III (IANIGLA-PV 100/3) in AR) dorsal, AS) distal, AT) medial, AU) proximal, AV) ventral, and AW) lateral views; left metatarsal IV (IANIGLA-PV 100/4) in AX) dorsal, AY) distal, AZ) lateral, BA) proximal, BB) ventral, and BC) medial views; right metatarsal V (IANIGLA-PV 100/5) in BD) dorsal, BE) medial, BF) proximal, BG) ventral, and BH) lateral views; and large left metatarsal V (IANIGLA-PV 100/6) in BI) dorsal, BJ) distal, BK) lateral, BL) proximal, BM) ventral, and BN) medial views. Scale bar = 150 mm.

Figure 24. *Mendozasaurus neguyelap* pedal phalanges: right pedal phalanx I-1 (IANIGLA-PV 077/6) in A) dorsal, B) distal, C) medial, D) proximal, E) ventral, and F) lateral views; right pedal phalanx II-1 (IANIGLA-PV 077/7) in G) dorsal, H) distal, I) medial, J) proximal, K) ventral, and L) lateral views; right pedal phalanx III-1 (IANIGLA-PV 077/8) in M) dorsal, N) distal, O) medial, P) proximal, Q) ventral, and R) lateral views; right pedal ungual phalanx I-2 (IANIGLA-PV 078/1) in S) medial, T) proximal, and U) lateral views; right pedal ungual phalanx II-2 (IANIGLA-PV 078/2) in V) medial, W) proximal, and X) lateral views; right pedal ungual phalanx III-2 (IANIGLA-PV 079) in Y) medial, Z) proximal, and AA) lateral views; right pedal phalanx IV-1 (IANIGLA-PV 077/9) in AB) dorsal, AC) distal, AD) medial, AE) proximal, AF) ventral, and AG) lateral views; left pedal phalanx I-1 (IANIGLA-PV 77/12) in AH) dorsal, AI) distal, AJ) lateral, AK) proximal, AL) ventral, and AM) medial views; left pedal phalanx II-1 (IANIGLA-PV 77/11) in AN) dorsal, AO) distal, AP) lateral, AQ) proximal, AR) ventral, and AS)

medial views; and pedal phalanx IV-2 (IANIGLA-PV 77/10) in AT) dorsal and AU) lateral views. Scale bar = 100 mm.

Figure 25. *Mendozasaurus neguyelap* large osteoderms: IANIGLA-PV 080/1 in A) anterior, B) left lateral, C) ventral, D) posterior, E) dorsal, and F) right lateral views; and IANIGLA-PV 080/2 in G) anterior, H) left lateral, I) ventral, J) posterior, K) dorsal, and L) right lateral views. Scale bar = 200 mm.

Figure 26. *Mendozasaurus neguyelap* small osteoderms: IANIGLA-PV 081/1 in A) anterior, B) left lateral, C) ventral, D) posterior, E) dorsal, and F) right lateral views; and IANIGLA-PV 081/2 in G) anterior, H) left lateral, I) ventral, J) posterior, K) dorsal, and L) right lateral views. Scale bar = 50 mm.

Figure 27. Strict consensus cladogram of 1176 MPTs. Note that this tree was produced following the a priori exclusion of eight unstable taxa (see text for details).

Figure 28. Time-calibrated phylogenetic tree showing geographic distribution and stratigraphic range (including uncertainty) of Titanosauria, based on the agreement subtree of the strict consensus. Titanosaur silhouette drawn by Scott Hartman and available at Phylopic under a Creative Commons Attribution-NonCommerical 3.0 Unported license (https://creativecommons.org/licenses/by-nc/3.0/).

APPENDIX – ADDITIONAL CHARACTERS AND SCORE CHANGES

The following seven characters have been added to the end of the character data matrix presented in Mannion *et al*. (2017) and are thus numbered as C417–423.

C417. Posterior cervical neural arches, spinodiapophyseal fossa, at base of lateral surface of neural spine: absent or shallow fossa (0); deep fossa (1) (González Riga, 2005; González Riga *et al*., 2009; modified here; see Figs 4, 6, 7).

C418. Posterior cervical neural spines, dorsal half laterally expanded as a result of expansion of the lateral lamina (spinodiapophyseal lamina?): absent (0); present (1) (González Riga, 2005; González Riga *et al*., 2009; Gallina, 2011; González Riga & Ortiz David, 2014; modified here; see Figs 4, 6, 7).

C419. Anteriormost caudal neural spines, medial spinoprezygapophyseal laminae (mSPRLs) merge into the prespinal lamina (PRSL) close to the base of the spine: absent (0); present (1) (Calvo *et al*., 2008b; Carballido *et al*., 2017; modified here; note that in *Patagotitan* these might be the only SPRLs, whereas *Futalognkosaurus* appears to have more typical lateral SPRLs too).

C420. Metacarpals, metacarpal V, dorsomedial margin of distal third forms a prominent ridge or flange: absent (0); present (1) (new character; see Fig. 18AB).

C421. Metatarsals, ratio of metatarsal III to metatarsal I proximodistal length: 1.3 or greater (0); less than 1.3 (1) (González Riga *et al*., 2016; modified and polarity reversed here).

C422. Metatarsals, ratio of metatarsal III to metatarsal IV proximodistal length: 1.0 or greater (0); less than 1.0 (1) (González Riga *et al*., 2016; modified here).

C423. Pedal digit III, number of phalanges: 3 or more (0); 2 or fewer (1) (González Riga *et al*., 2008, 2016; Nair & Salisbury, 2012).

Taxon scores for C1–416 follow those in the data matrix of Mannion *et al*. (2017), with the following changes made to our *Alamosaurus* and *Tapuiasaurus* OTUs based on Tykoski & Fiorillo (2016) and Wilson *et al*. (2016), respectively (the first number denotes the character, and the number/symbol in parentheses denotes the new score):

Alamosaurus: 15 (1); 19 (0); 127 (?); 139 (1); 140 (1); 328 (0); 401 (0); 405 (1)

Tapuiasaurus: 2 (1); 78 (0); 84 (0); 92 (1); 93 (1); 94 (0); 95 (0/1); 96 (1); 98 (0); 99 (0); 102 (0); 116 (0); 122 (2); 132 (0); 139 (1); 140 (1); 166 (1); 296 (1); 298 (1); 303 (1); 304 (1); 307 (1); 308 (0); 309 (1); 315 (1); 399 (1); 401 (0)

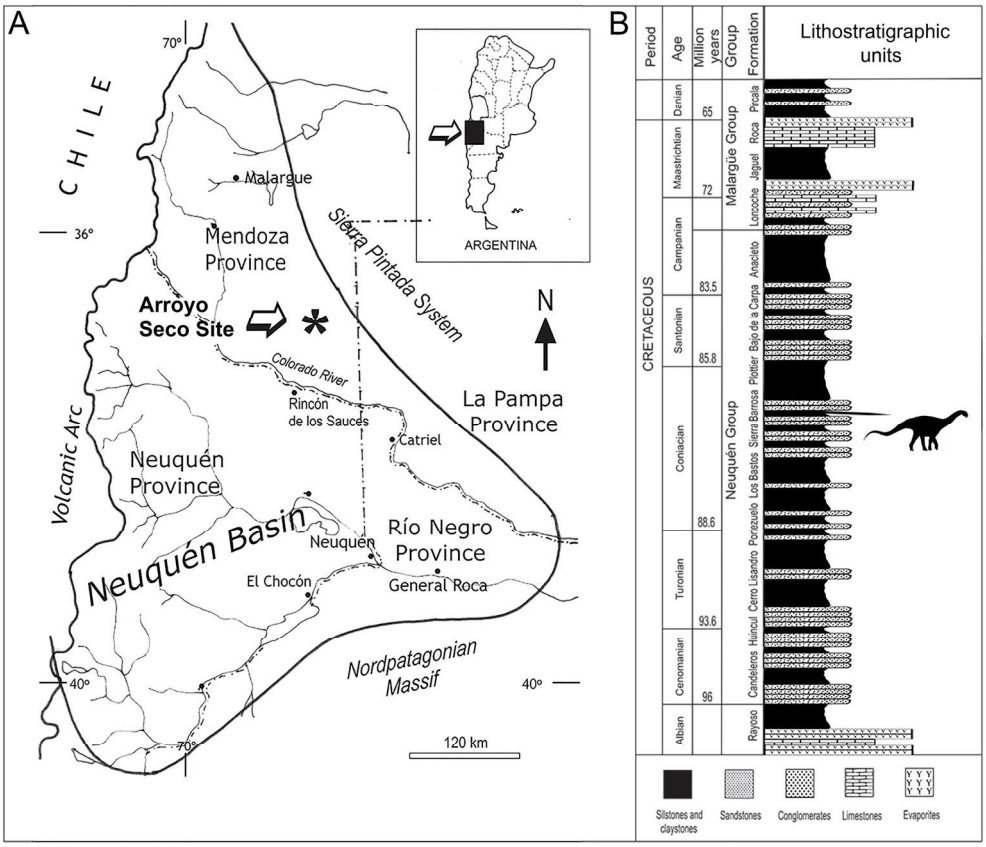

Figure 1. A) Map showing the locality where Mendozasaurus neguyelap was found. B) Stratigraphic column of the Late Cretaceous strata of Neuquen Group with indication of the fossiliferous level of the Sierra Barrosa Formation.

85x72mm (600 x 600 DPI)

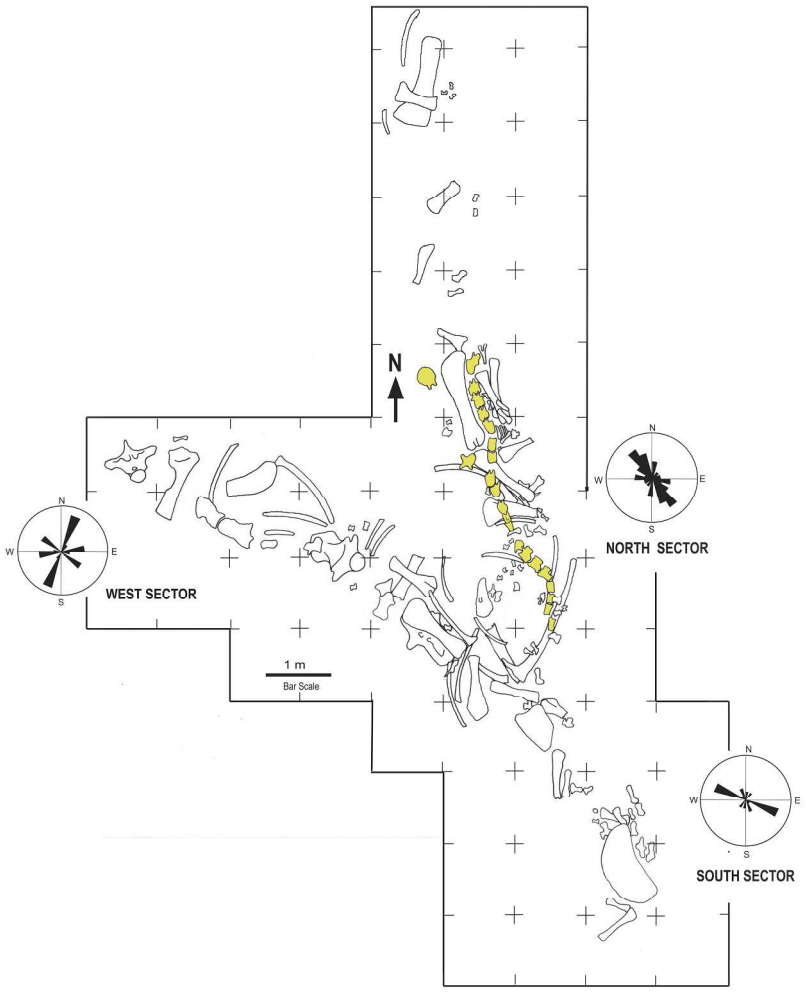

Figure 2. Quarry map of Arroyo Seco showing the fossil accumulation of Mendozasaurus neguyelap with the holotype caudal sequence highlighted (modified from González Riga & Astini, 2007).

700x700mm (100 x 100 DPI)

Figure 3. Life restoration of Mendozasaurus neguyelap based on the largest adult individual (femur length: 1530 mm). Artwork by Bernardo Gonzaléz Riga.

241x171mm (300 x 300 DPI)

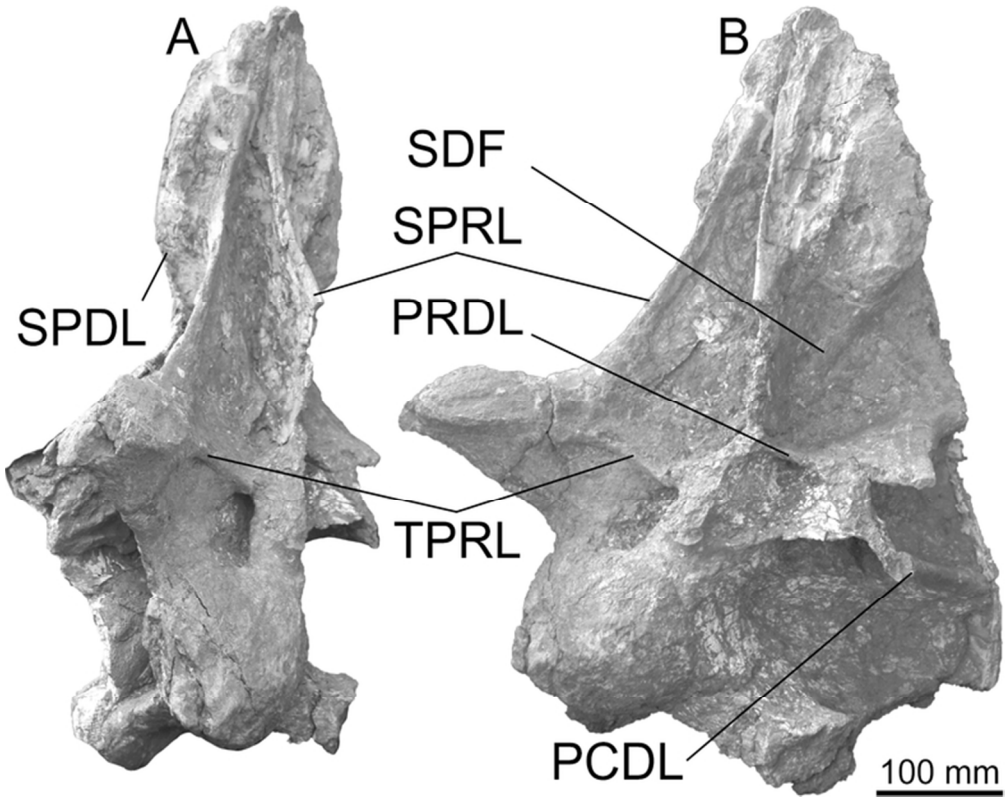

Figure 4. Mendozasaurus neguyelap cervical vertebra (IANIGLA-PV 076/5) in A) anterior and B) left anterolateral views. Scale bar = 100 mm.

66x52mm (300 x 300 DPI)

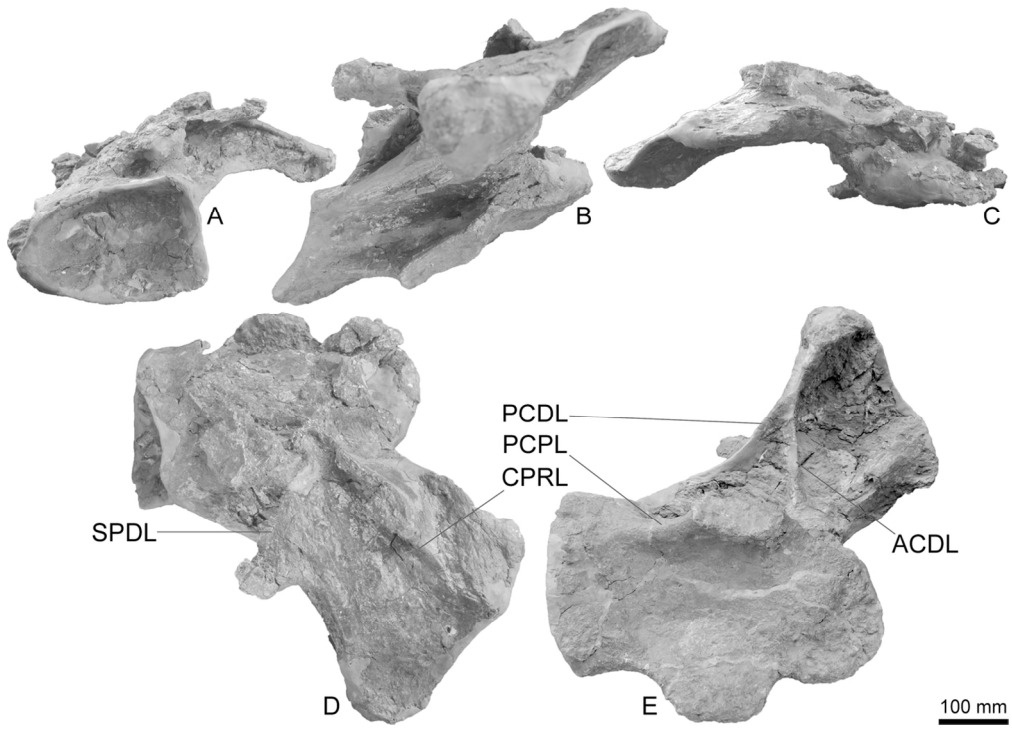

Figure 5. Mendozasaurus neguyelap cervical vertebra (IANIGLA-PV 076/3) in A) posterior, B) right lateral, C) anterior, D) dorsal, and E) ventral views. Scale bar = 100 mm.

121x86mm (300 x 300 DPI)

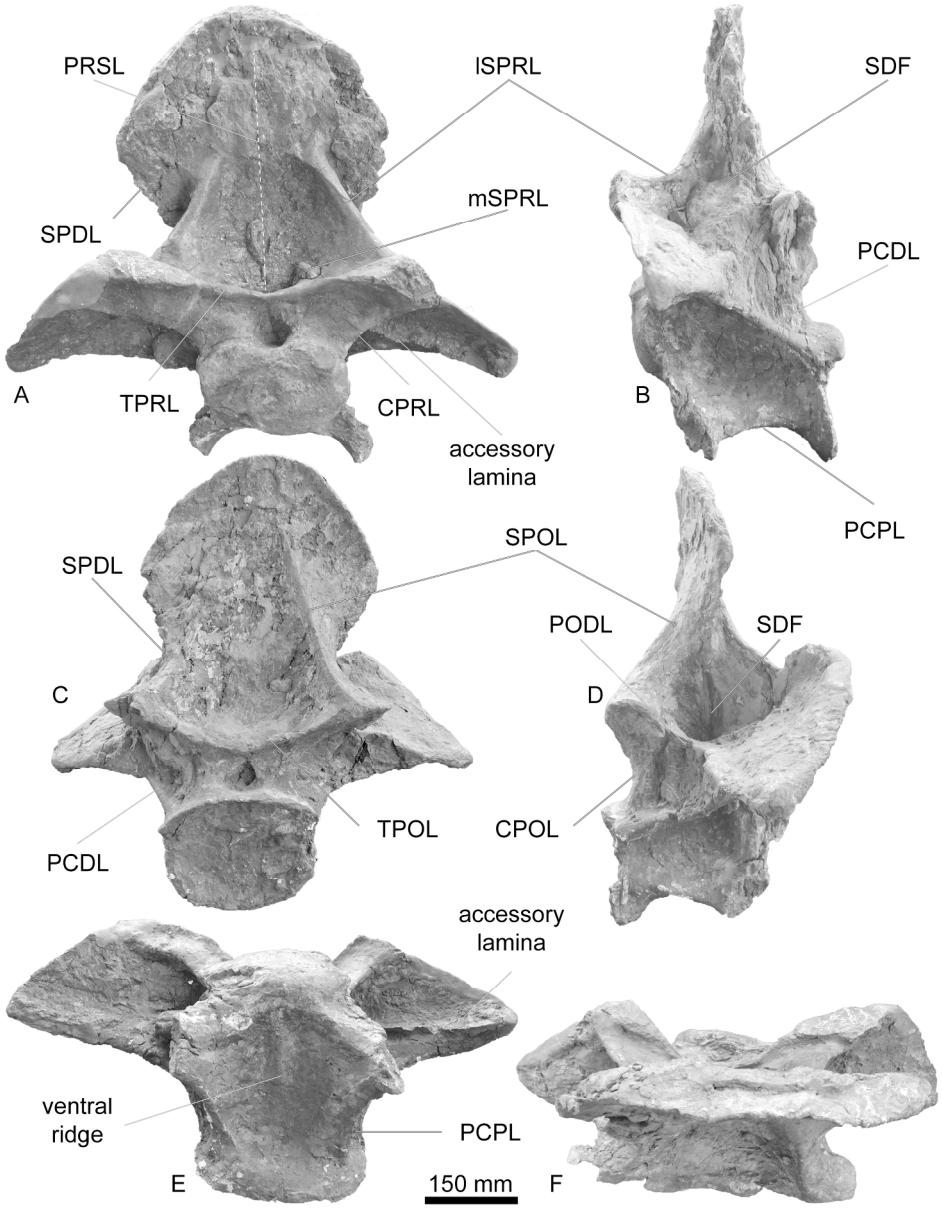

Caption : Figure 6. Mendozasaurus neguyelap cervical vertebra (IANIGLA-PV 076/1) in A) anterior, B) left lateral, C) posterior, D) right lateral, E) ventral, and F) dorsal views. Scale bar = 150 mm.

215x277mm (300 x 300 DPI)

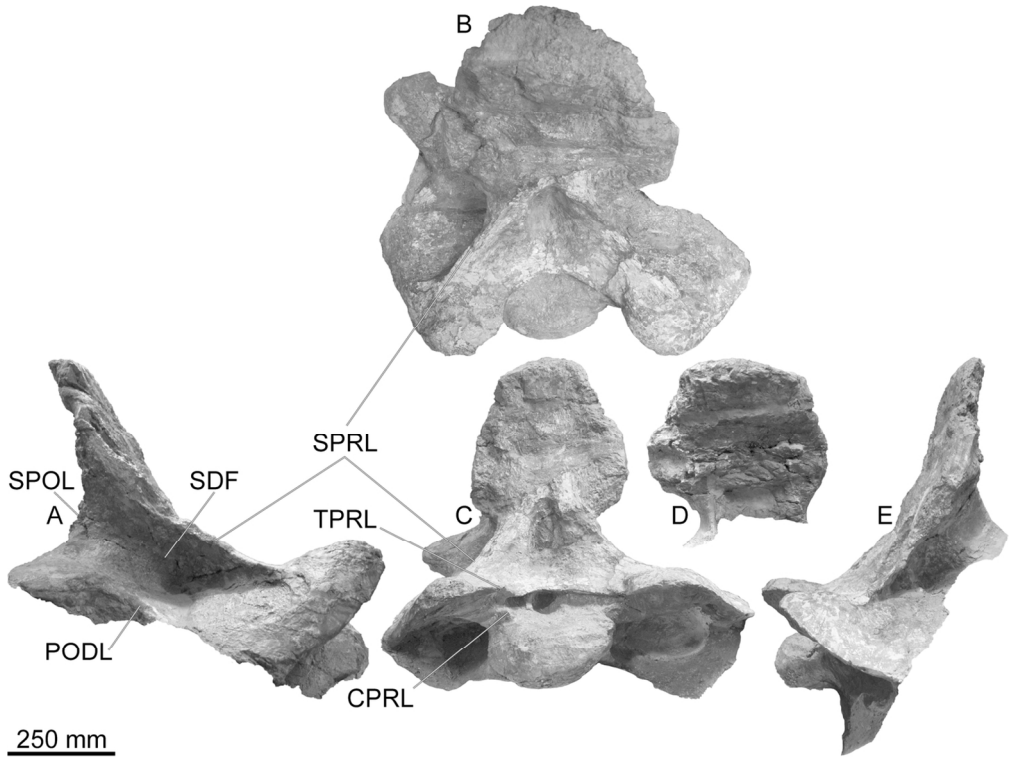

Figure 7. Mendozasaurus neguyelap cervical vertebra (IANIGLA-PV 084/1) in A) right lateral, B) dorsal, C) anterior, D) posterior (neural spine only), and E) left lateral views. Scale bar = 250 mm.

126x94mm (300 x 300 DPI)

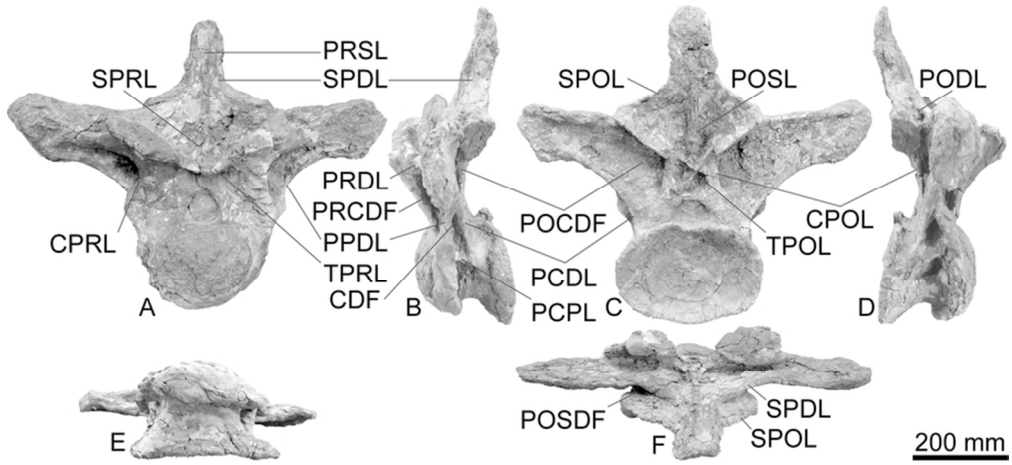

Figure 8. Mendozasaurus neguyelap dorsal vertebra (IANIGLA-PV 066) in A) anterior, B) left lateral (reversed), C) posterior, D) right lateral, E) ventral, and F) dorsal views. Scale bar = 200 mm.

77x35mm (300 x 300 DPI)

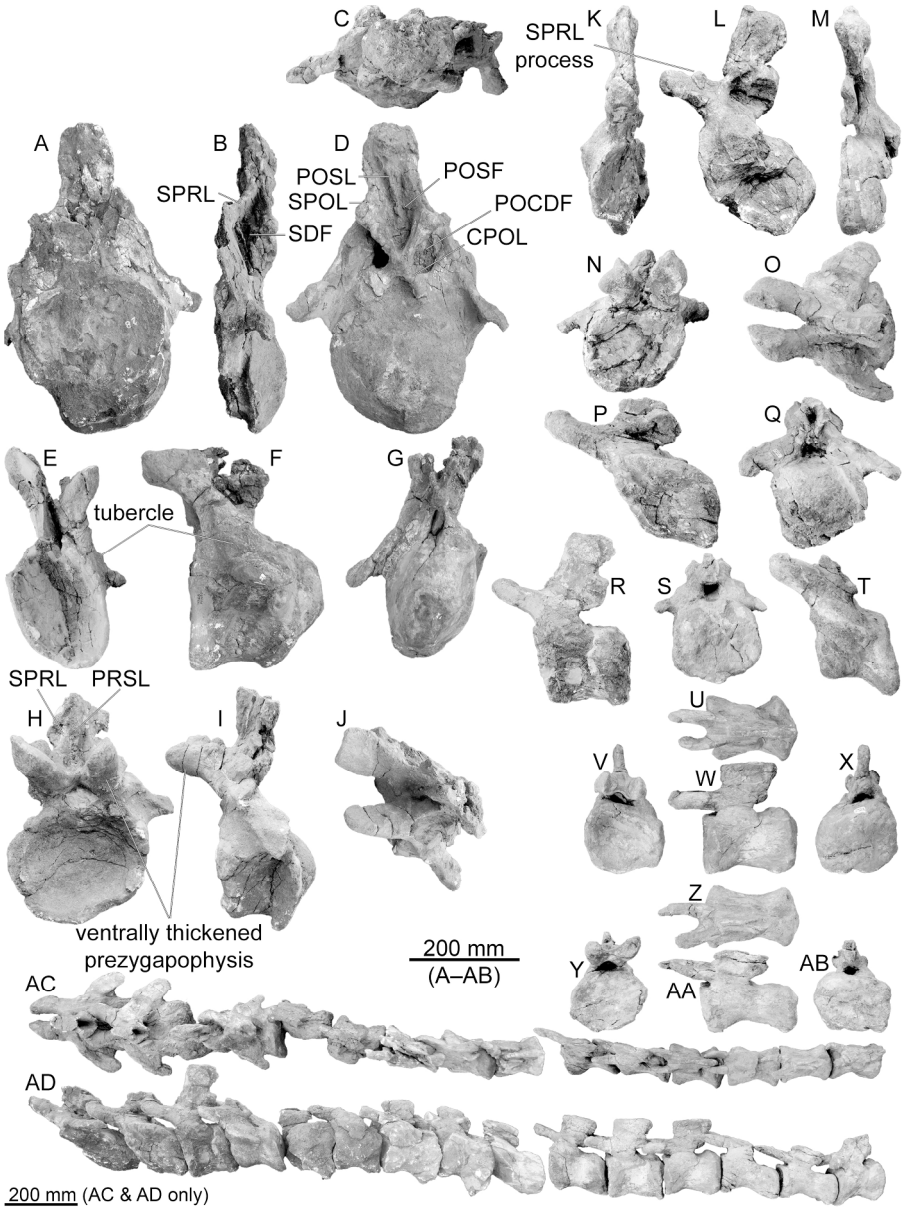

Caption : Figure 9. Mendozasaurus neguyelap caudal vertebrae: Caudal vertebra I (IANIGLA-PV 066/1) in A) anterior, B) left lateral (right lateral reversed), C) dorsal, and D) posterior views; caudal vertebra II (IANIGLA-PV 066/2) in E) anterior, F) left lateral, and G) posterior views; caudal vertebra III (IANIGLA-PV 066/3) in H) anterior, I) dorsal, and J) left lateral views; caudal vertebra IV (IANIGLA-PV 066/4) in K) anterior, L) left lateral (right lateral reversed), and M) posterior views; caudal vertebra VI (IANIGLA-PV 066/6) in N) anterior, O) dorsal, P) left lateral, and Q) posterior views; caudal vertebra VII (IANIGLA-PV 066/7) in R) left lateral view; caudal vertebra VIII (IANIGLA-PV 066/8) in S) anterior, and T) left lateral views; caudal vertebra XVI (IANIGLA-PV 066/16) in U) anterior, V) dorsal, W) left lateral, and X) posterior views; caudal vertebra XVIII (IANIGLA-PV 066/18) in Y) anterior, Z) dorsal, AA) left lateral, and AB) posterior views; and caudal vertebrae V–XIX (IANIGLA-PV 066/5–18) in AC) dorsal, and AC) left lateral views. Scale bar = 200 mm.

224x301mm (300 x 300 DPI)

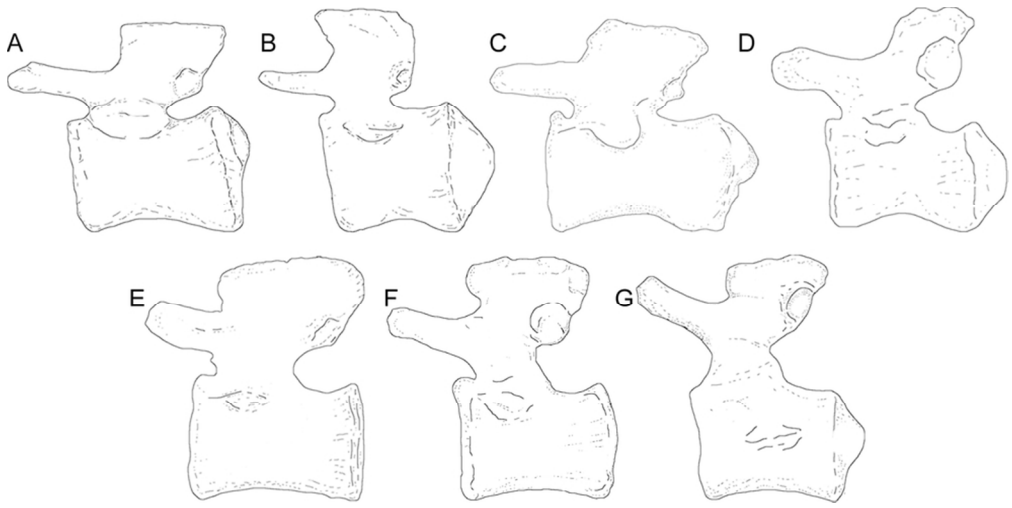

Figure 10. Comparisons of middle caudal vertebrae of titanosaurs: A) Mendozasaurus neguyelap caudal 16, B) Dreadnoughtus schrani caudal 15, C) Epachthosaurus sciuttoi caudal 10, D) Baurutitan britoi caudal 14 (right lateral reversed), E) Andesaurus delgadoi caudal 20, F) Malawisaurus dixeyi caudal 7, and G) Narambuenatitan palomoi middle caudal. Not to scale.

83x41mm (300 x 300 DPI)

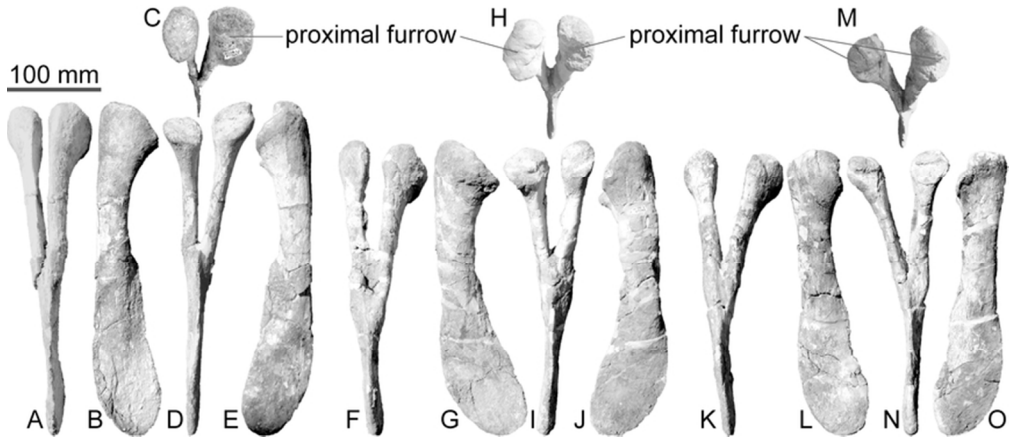

Figure 11. Mendozasaurus neguyelap chevrons: IANIGLA 065/23 in A) anterior, B) left lateral, C) proximal, D) posterior, and E) right lateral views; IANIGLA 065/24 in F) anterior, G) left lateral, H) proximal, I) posterior, and J) right lateral views; IANIGLA 065/25 in K) anterior, L) left lateral, M) proximal, N) posterior, and O) right lateral views. Scale bar = 100 mm.

72x31mm (300 x 300 DPI)

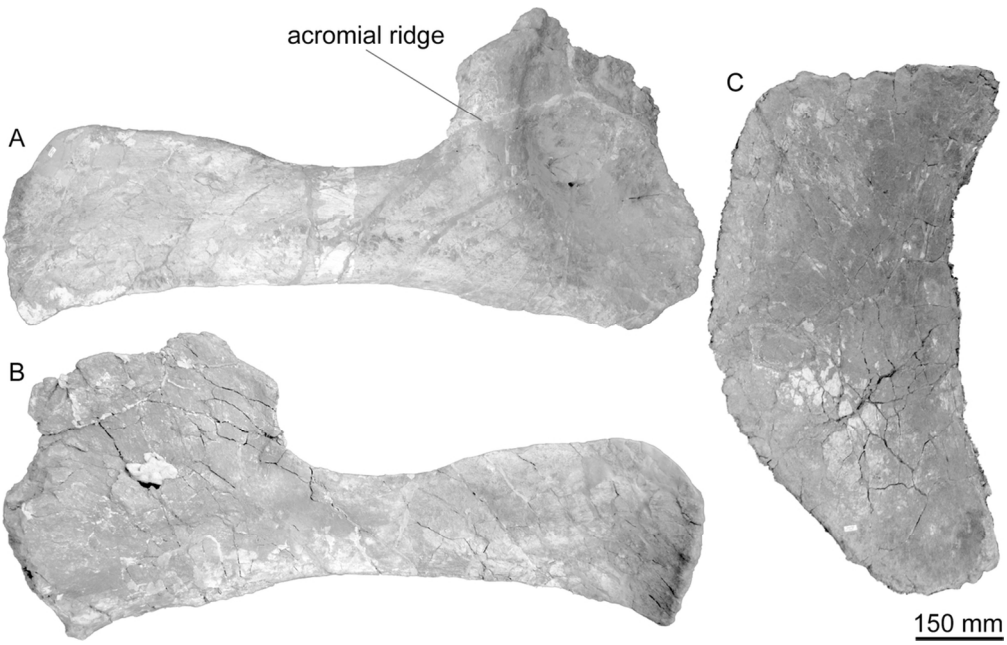

Figure 12. Mendozasaurus neguyelap pectoral girdle elements: right scapula (IANIGLA-PV 068) in A) lateral, and B) medial views; and right sternal plate (IANIGLA-PV 067) in dorsal (internal) view. Scale bar = 150 mm.

106x67mm (300 x 300 DPI)

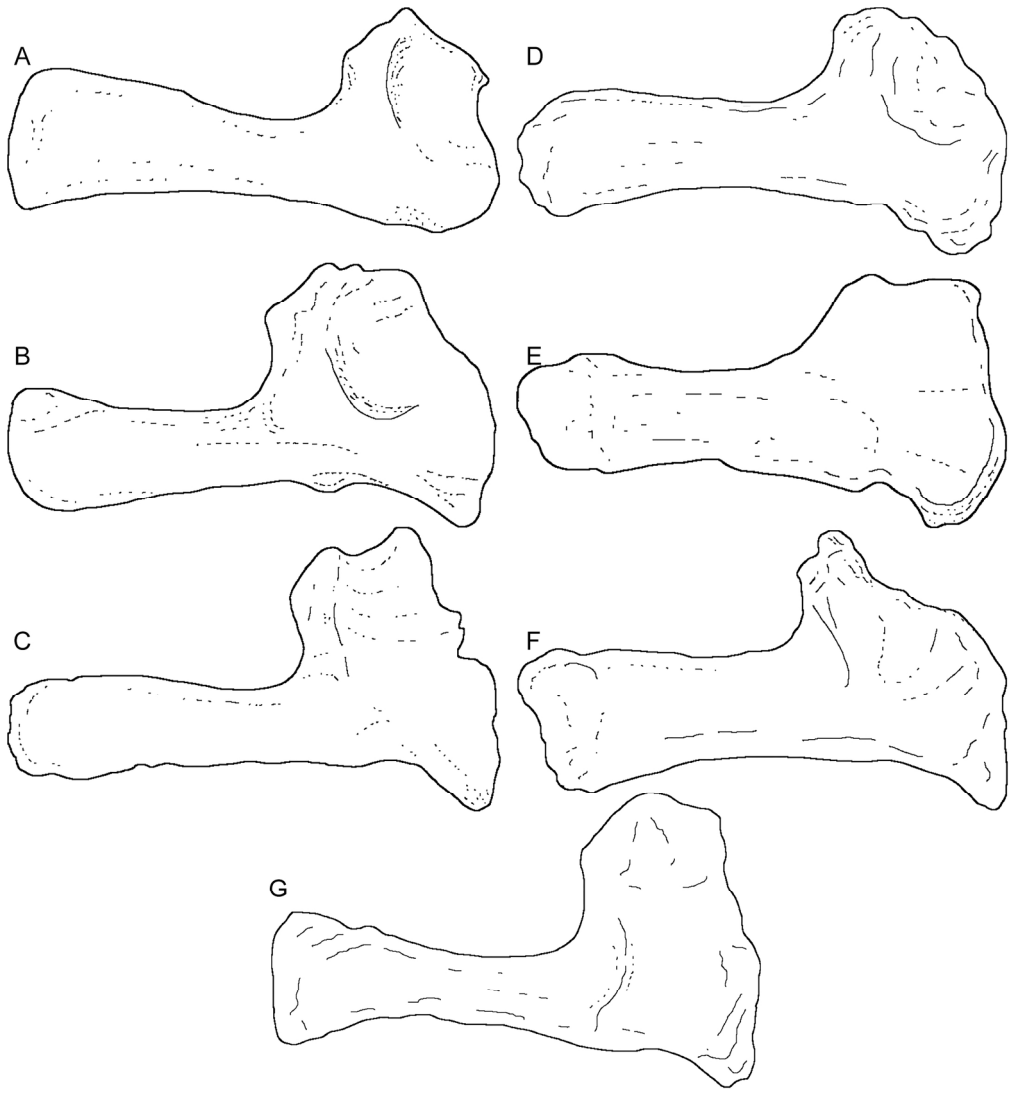

Figure 13. Comparisons of right scapulae of sauropods: A) Mendozasaurus neguyelap, B) Ligabuesaurus leanzai, C) Dreadnoughtus schrani, D) Pitekunsaurus macayai, E) Opisthocoelicaudia skarzynskii, F) Rapetosaurus krausei, and G) Muyelensaurus pecheni. Not to scale.

182x197mm (300 x 300 DPI)

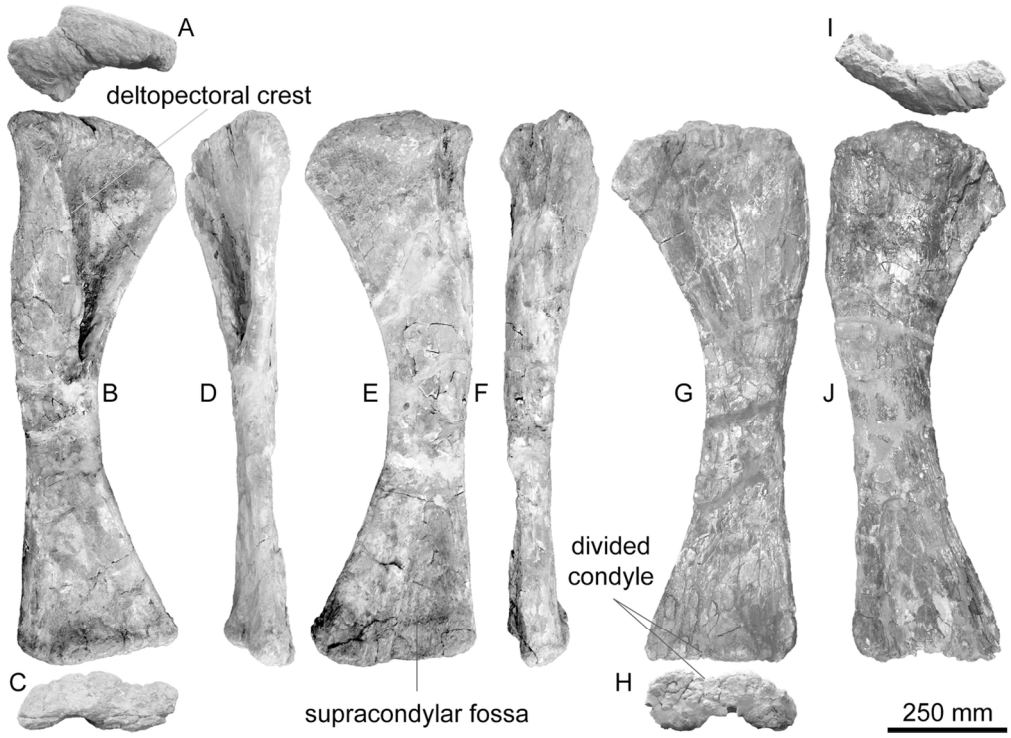

Figure 14. Mendozasaurus neguyelap humeri: right humerus (IANIGLA-PV 069/1) in A) proximal, B) anterior, C) distal, D) medial, E) posterior, and F) lateral views; and left humerus (IANIGLA-PV 069/2) in G) anterior, H) distal, I) proximal, and J) posterior views. Scale bar = 250 mm.

122x89mm (300 x 300 DPI)

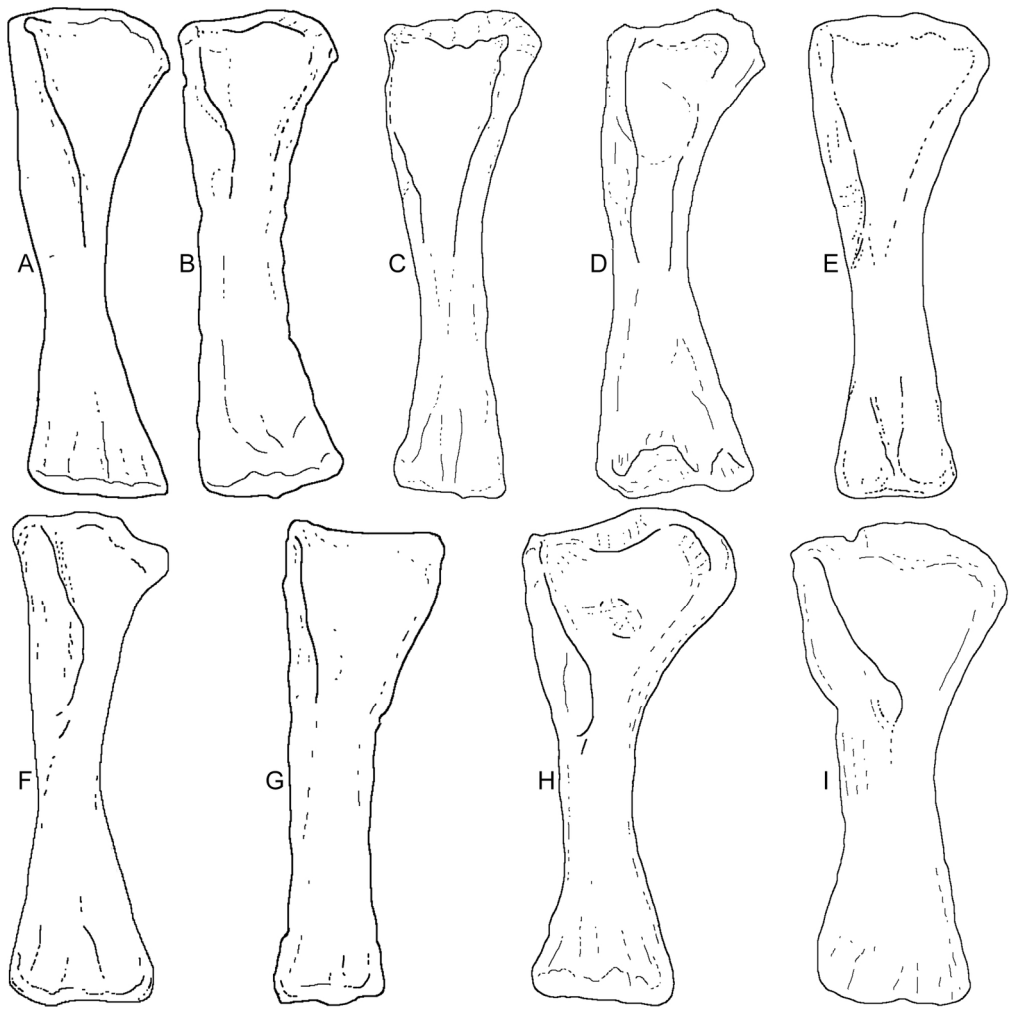

Figure 15. Comparisons of right humeri of sauropods: A) Mendozasaurus neguyelap, B) Angolatitan adamastor, C) Narambuenatitan palomoi (left reversed); D) Paralititan stromeri; E) Rapetosaurus krausei (left reversed); F) Petrobrasaurus puestohernandezi; G) Andesaurus delgadoi; H) Notocolossus gonzalezparejasi; and I) Dreadnoughtus schrani (left reversed). Not to scale.

168x168mm (300 x 300 DPI)

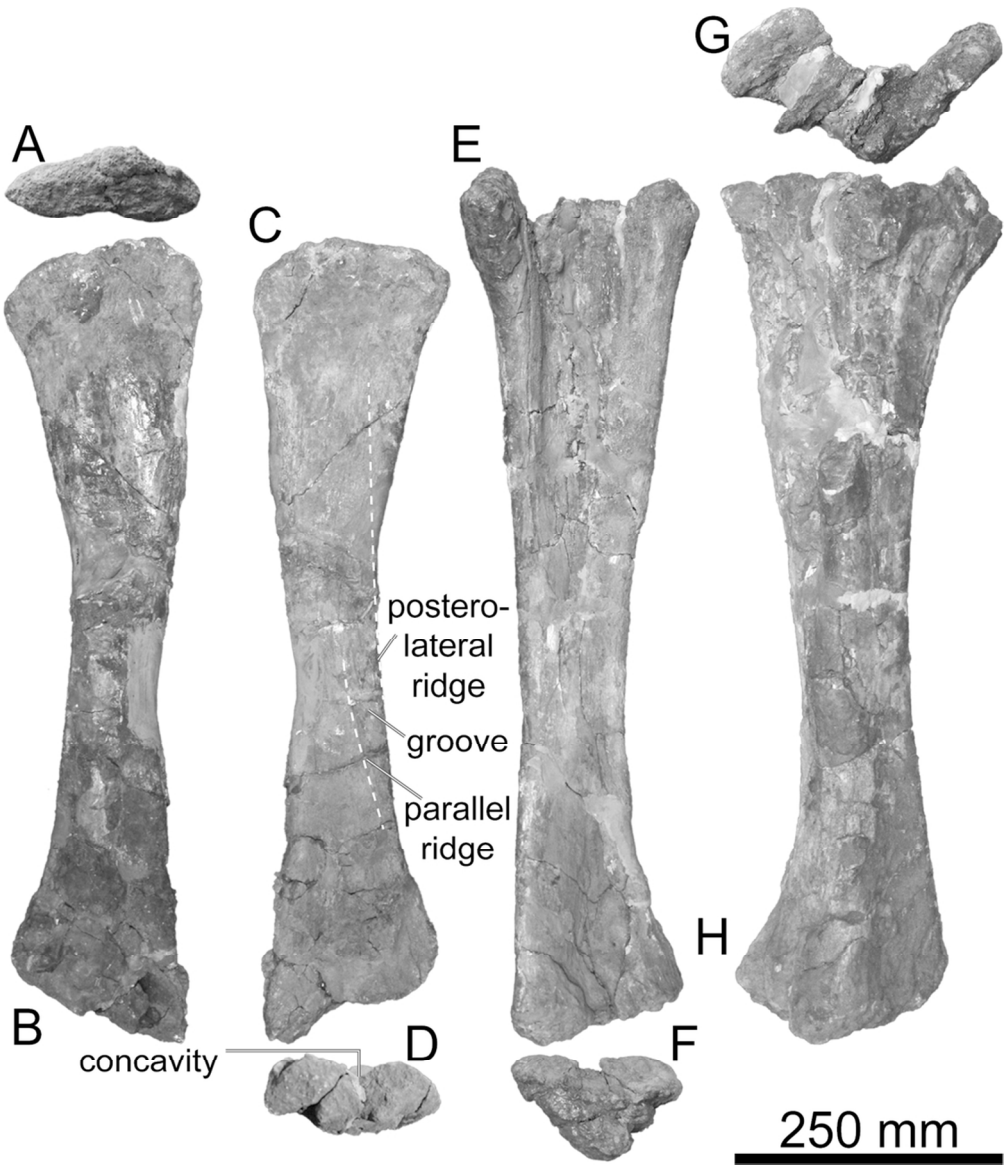

Figure 16. Mendozasaurus neguyelap antebrachial elements: right radius (IANIGLA-PV 070/2) in A) proximal, B) anterior, C) posterior, and D) distal views; and right ulna (IANIGLA-PV 070/1) in E) anterior, F) distal, G) proximal, and H) posterior views. Scale bar = 250 mm.

97x113mm (300 x 300 DPI)

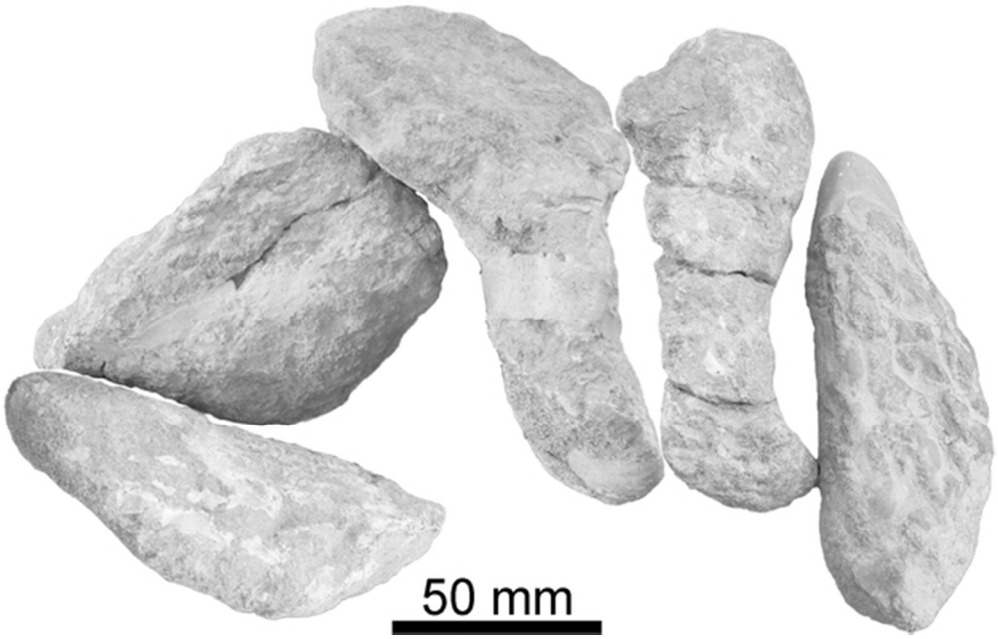

Figure 17. Mendozasaurus neguyelap composite right metacarpus in proximal end view, incorporating left metacarpal I (IANIGLA-PV 071/4; reversed), right metacarpal II (IANIGLA-PV 071/3), right metacarpal III (IANIGLA-PV 071/1), left metacarpal IV (IANIGLA-PV 071/2; reversed) and left metacarpal V (IANIGLA-PV 071/5; reversed).

53x33mm (300 x 300 DPI)

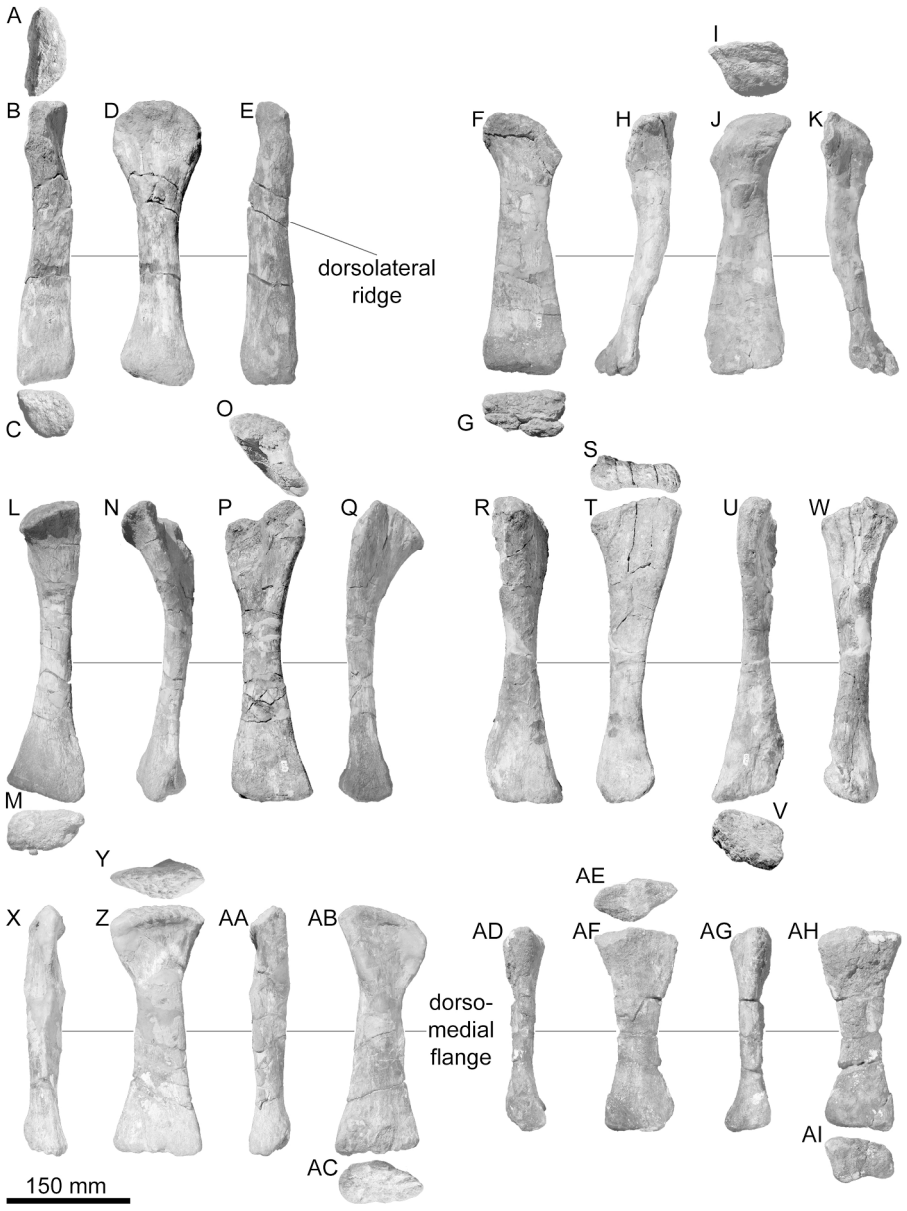

Caption : Figure 18. Mendozasaurus neguyelap metacarpals: left metacarpal I (IANIGLA-PV 071/4) in A) proximal, B) ventral, C) distal, D) medial, and E) dorsal views; right metacarpal II (IANIGLA-PV 071/3) in F) dorsal, G) distal, H) medial, I) proximal, J) ventral, and K) lateral views; right metacarpal III (IANIGLA-PV 071/1) in L) dorsal, M) distal, N) medial, O) proximal, P) ventral, and Q) lateral views; left metacarpal IV (IANIGLA-PV 071/2) in R) dorsal, S) proximal, T) lateral, U) ventral, V) distal, and W) medial views; left metacarpal V (IANIGLA-PV 71/5 in X) dorsal, Y) proximal, Z) lateral, AA) ventral, AB) medial, and AC) distal views; and small right metacarpal I or left metacarpal V (IANIGLA-PV 154) in AD) dorsal, AE) proximal, AF) lateral, AG) ventral, AH) medial, and AI) distal views. Scale bar = 150 mm.

224x301mm (300 x 300 DPI)

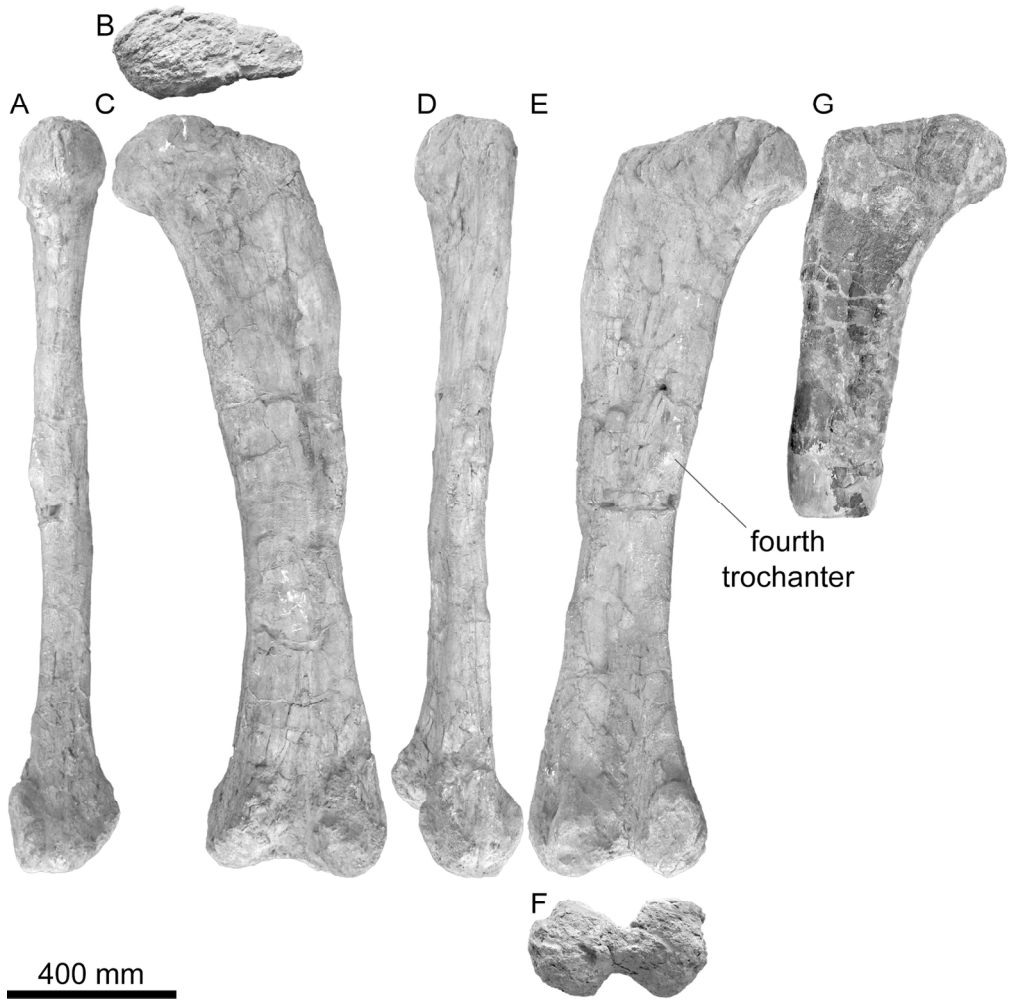

Figure 19. Mendozasaurus neguyelap femora: left femur (IANIGLA-PV 073/4) in A) medial, B) proximal, C) anterior, D) lateral, E) posterior, and F) distal views; and right femur (IANIGLA-PV 073/1) in G) anterior view. Scale bar = 400 mm.

143x141mm (300 x 300 DPI)

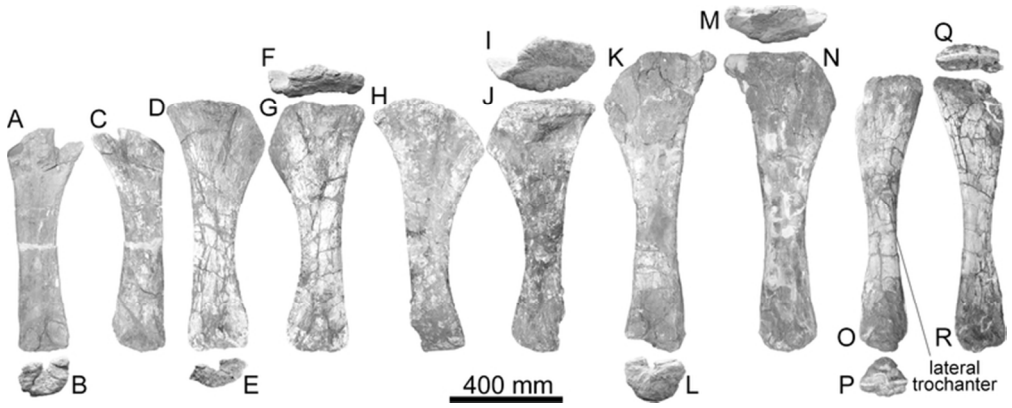

Figure 20. Mendozasaurus neguyelap crural elements: right tibia (IANIGLA-PV 073/3) in A) lateral, B) distal, and C) medial views; right tibia (IANIGLA-PV 073/2) in D) lateral, E) distal, F) proximal, and G) medial views; right tibia (IANIGLA-PV 074/1) in H) lateral, I) proximal, and J) medial views; left tibia (IANIGLA-PV 074/2) in K) lateral, L) distal, M) proximal, and N) medial views; and left fibula (IANIGLA-PV 074/3) in O) lateral, P) distal, Q) proximal, and R) medial views. Scale bar = 400 mm.

67x26mm (300 x 300 DPI)

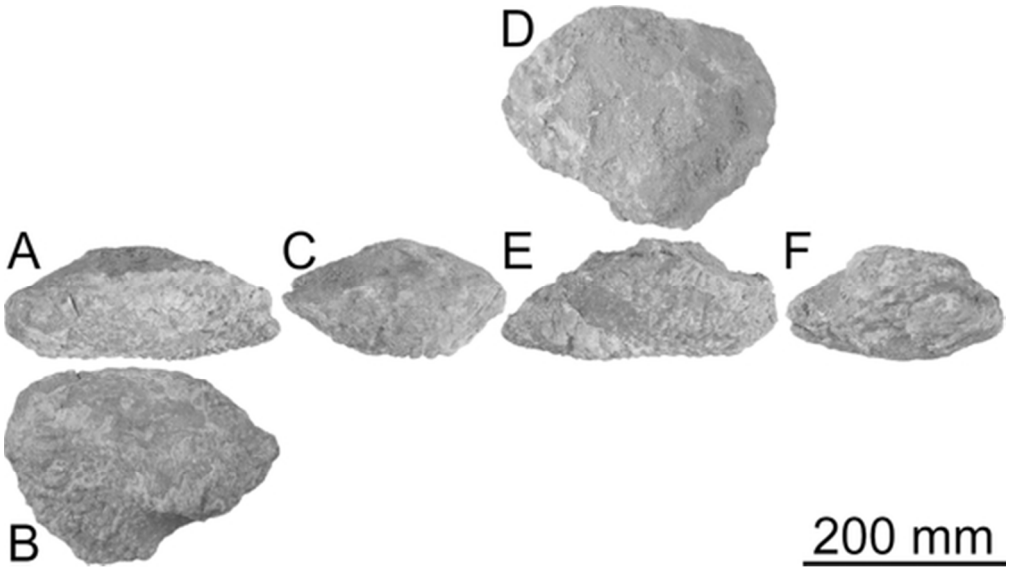

Figure 21. Mendozasaurus neguyelap right astragalus (IANIGLA-PV 155) in A) anterior, B) distal, C) medial, D) proximal, E) posterior, and F) lateral views. Scale bar = 200 mm.

46x26mm (300 x 300 DPI)

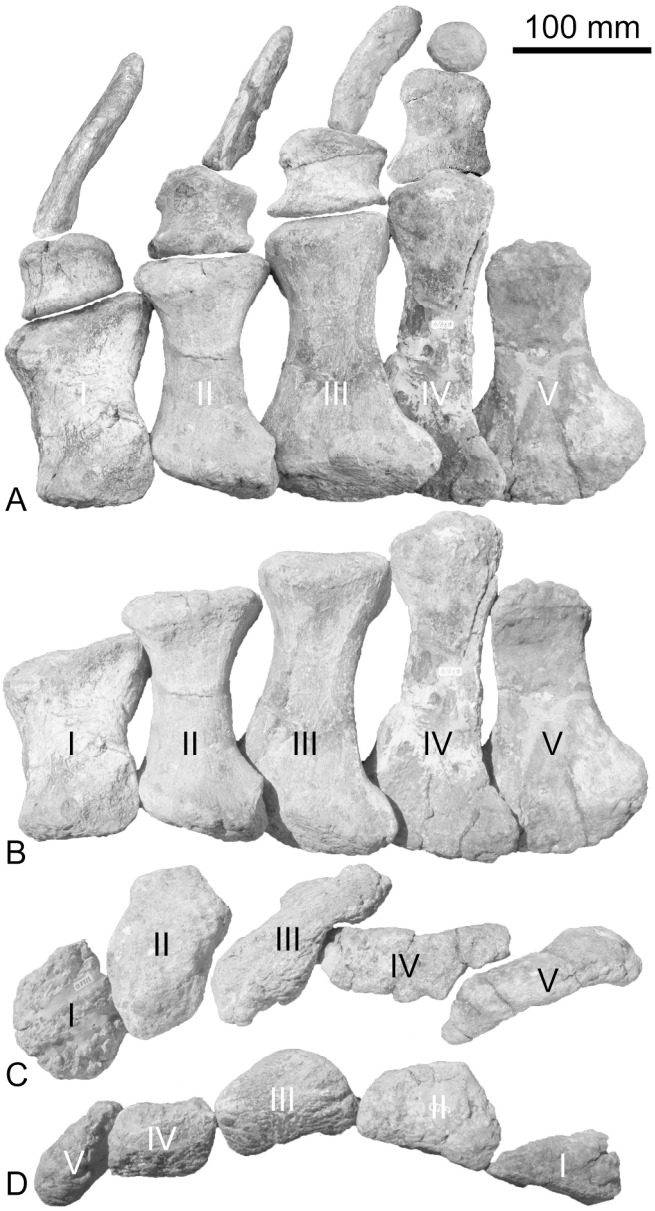

Figure 22. Mendozasaurus neguyelap pedal elements: right pes (metatarsals = IANIGLA-PV 077/1–5, non-ungual phalanges = IANIGLA-PV 077/6–10, ungual phalanges = IANIGLA-PV 078/1–2 & 079) in A) dorsal view; and rearticulated right metatarsals I–V (IANIGLA-PV 077/1–5) in B) dorsal, C) proximal, and D) distal views. Roman numerals correspond to pedal digit number. Scale bar = 100 mm.

156x288mm (300 x 300 DPI)

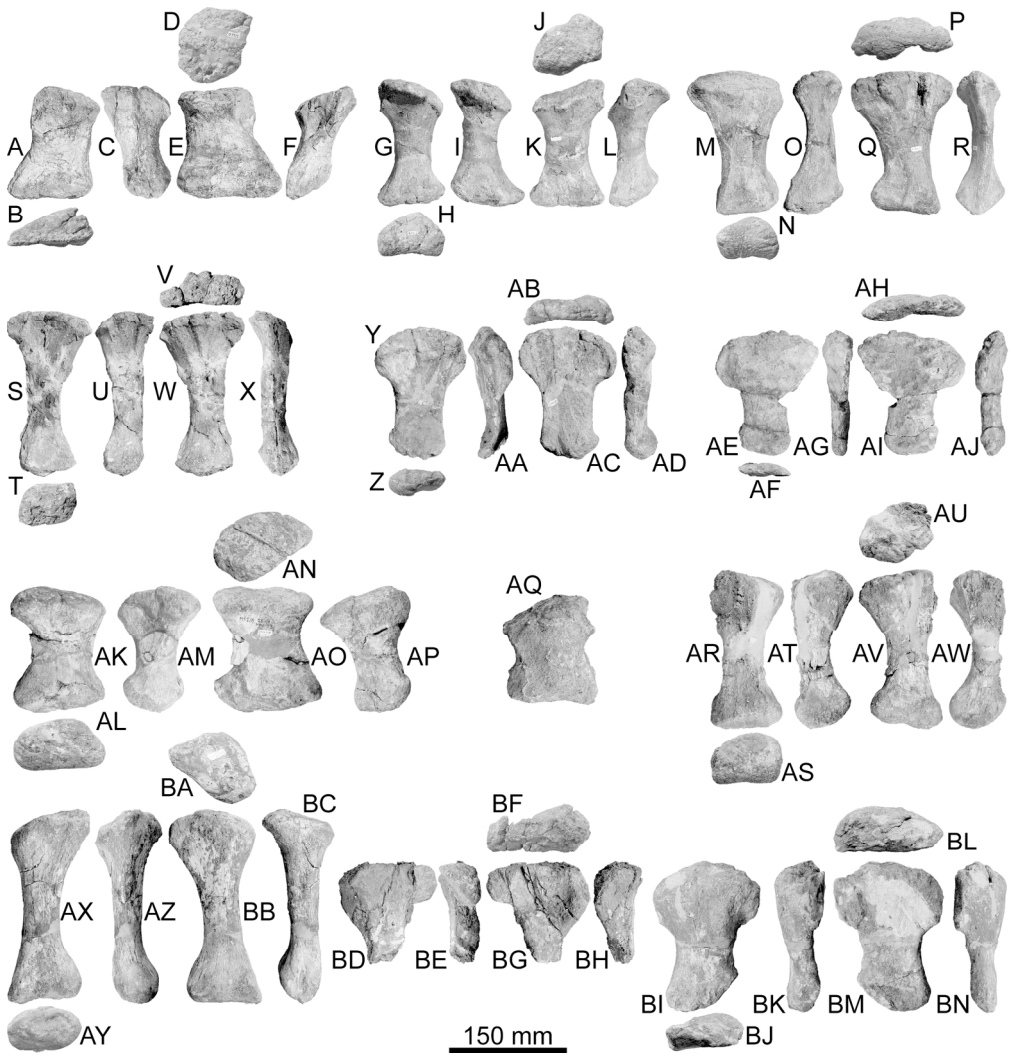

Figure 23. Mendozasaurus neguyelap metatarsals: right metatarsal I (IANIGLA-PV 077/1) in A) dorsal, B) distal, C) medial, D) proximal, E) ventral, and F) lateral views; right metatarsal II (IANIGLA-PV 077/2) in G) dorsal, H) distal, I) medial, J) proximal, K) ventral, and L) lateral views; right metatarsal III (IANIGLA-PV 077/3) in M) dorsal, N) distal, O) medial, P) proximal, Q) ventral, and R) lateral views; right metatarsal IV (IANIGLA-PV 077/4) in S) dorsal, T) distal, U) medial, V) proximal, W) ventral, and X) lateral views; right metatarsal V (IANIGLA-PV 077/5) in Y) dorsal, Z) distal, AA) medial, AB) proximal, AC) ventral, and AD) lateral views; left metatarsal V (IANIGLA-PV 153) in AE) dorsal, AF) distal, AG) lateral, AH) proximal, AI) ventral, and AJ) medial views; large right metatarsal I (IANIGLA-PV 100/1) in AK) dorsal, AL) distal, AM) medial, AN) proximal, AO) ventral, and AP) lateral views; large left metatarsal I (IANIGLA-PV 100/2) in AQ) dorsal view; large right metatarsal III (IANIGLA-PV 100/3) in AR) dorsal, AS) distal, AT) medial, AU) proximal, AV) ventral, and AW) lateral views; left metatarsal IV (IANIGLA-PV 100/4) in AX) dorsal, AY) distal, AZ) lateral, BA) proximal, BB) ventral, and BC) medial views; right metatarsal V (IANIGLA-PV 100/5) in BD) dorsal, BE) medial, BF) proximal, BG) ventral, and BH) lateral views; and large left metatarsal V (IANIGLA-PV 100/6) in BI) dorsal, BJ) distal, BK) lateral, BL) proximal, BM) ventral, and BN) medial views. Scale bar = 150 mm.

176x185mm (300 x 300 DPI)

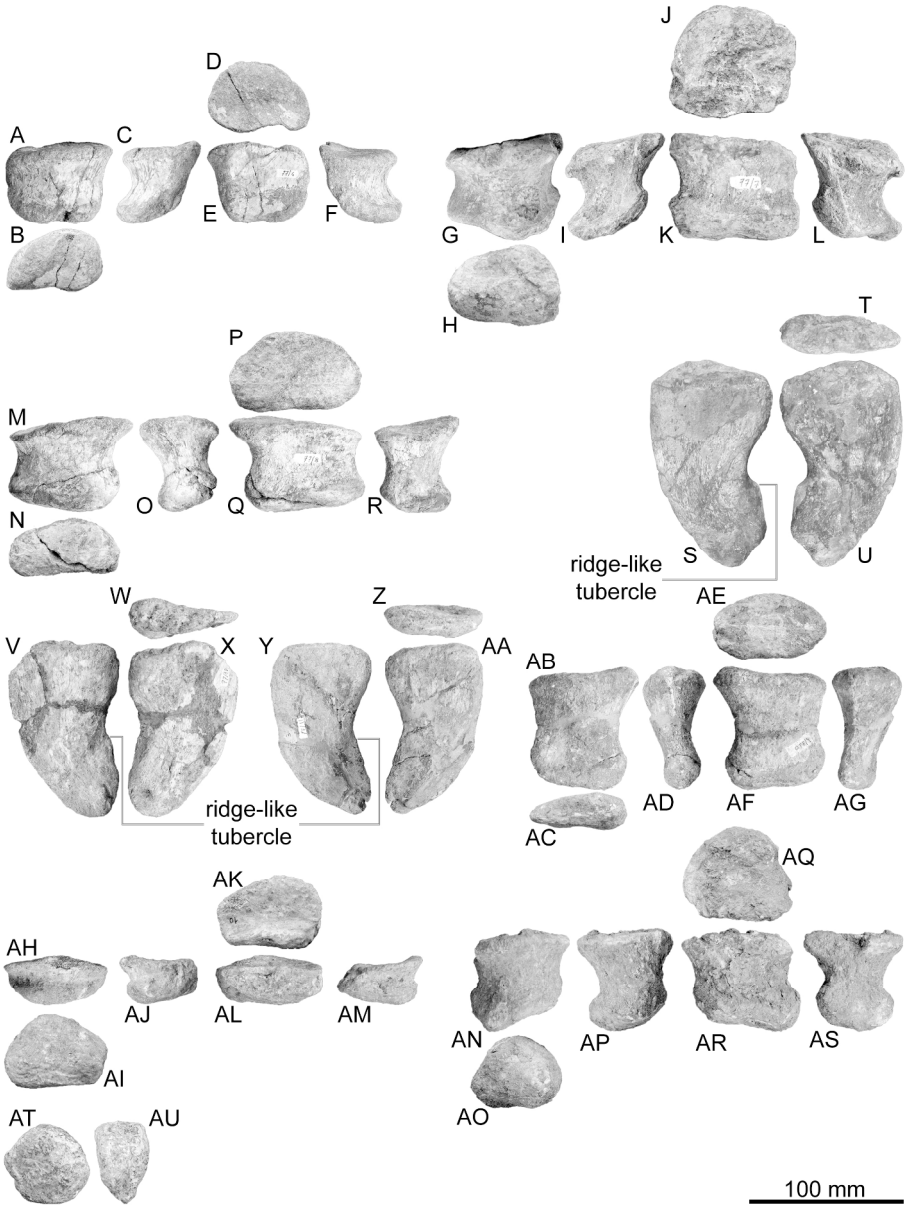

Figure 24. Mendozasaurus neguyelap pedal phalanges: right pedal phalanx I-1 (IANIGLA-PV 077/6) in A) dorsal, B) distal, C) medial, D) proximal, E) ventral, and F) lateral views; right pedal phalanx II-1 (IANIGLA-PV 077/7) in G) dorsal, H) distal, I) medial, J) proximal, K) ventral, and L) lateral views; right pedal phalanx III-1 (IANIGLA-PV 077/8) in M) dorsal, N) distal, O) medial, P) proximal, Q) ventral, and R) lateral views; right pedal ungual phalanx I-2 (IANIGLA-PV 078/1) in S) medial, T) proximal, and U) lateral views; right pedal ungual phalanx II-2 (IANIGLA-PV 078/2) in V) medial, W) proximal, and X) lateral views; right pedal ungual phalanx III-2 (IANIGLA-PV 079) in Y) medial, Z) proximal, and AA) lateral views; right pedal phalanx IV-1 (IANIGLA-PV 077/9) in AB) dorsal, AC) distal, AD) medial, AE) proximal, AF) ventral, and AG) lateral views; left pedal phalanx I-1 (IANIGLA-PV 77/12) in AH) dorsal, AI) distal, AJ) lateral, AK) proximal, AL) ventral, and AM) medial views; left pedal phalanx II-1 (IANIGLA-PV 77/11) in AN) dorsal, AO) distal, AP) lateral, AQ) proximal, AR) ventral, and AS) medial views; and pedal phalanx IV-2 (IANIGLA-PV 77/10) in AT) dorsal and AU) lateral views. Scale bar = 100 mm.

223x297mm (300 x 300 DPI)

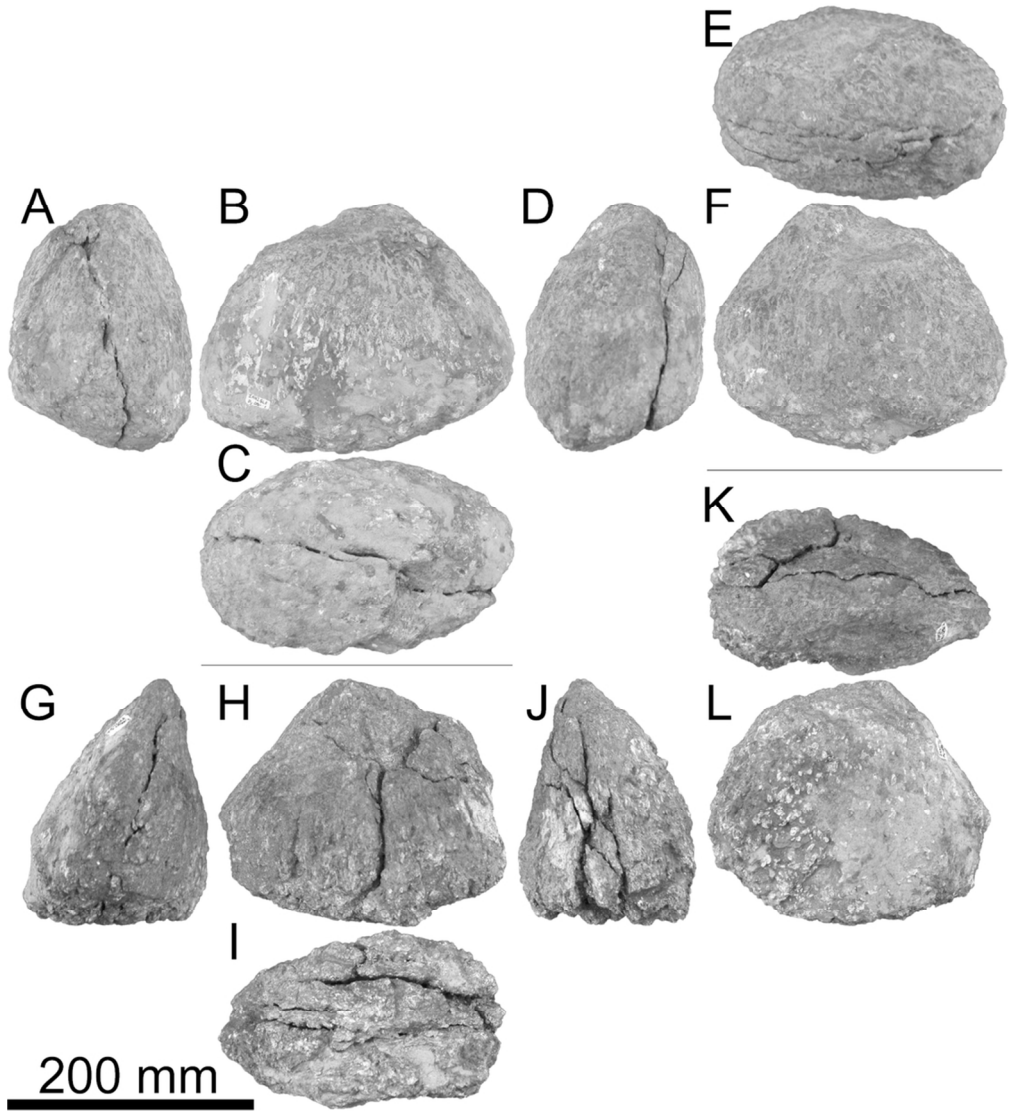

Figure 25. Mendozasaurus neguyelap large osteoderms: IANIGLA-PV 080/1 in A) anterior, B) left lateral, C) ventral, D) posterior, E) dorsal, and F) right lateral views; and IANIGLA-PV 080/2 in G) anterior, H) left lateral, I) ventral, J) posterior, K) dorsal, and L) right lateral views. Scale bar = 200 mm.

93x103mm (300 x 300 DPI)

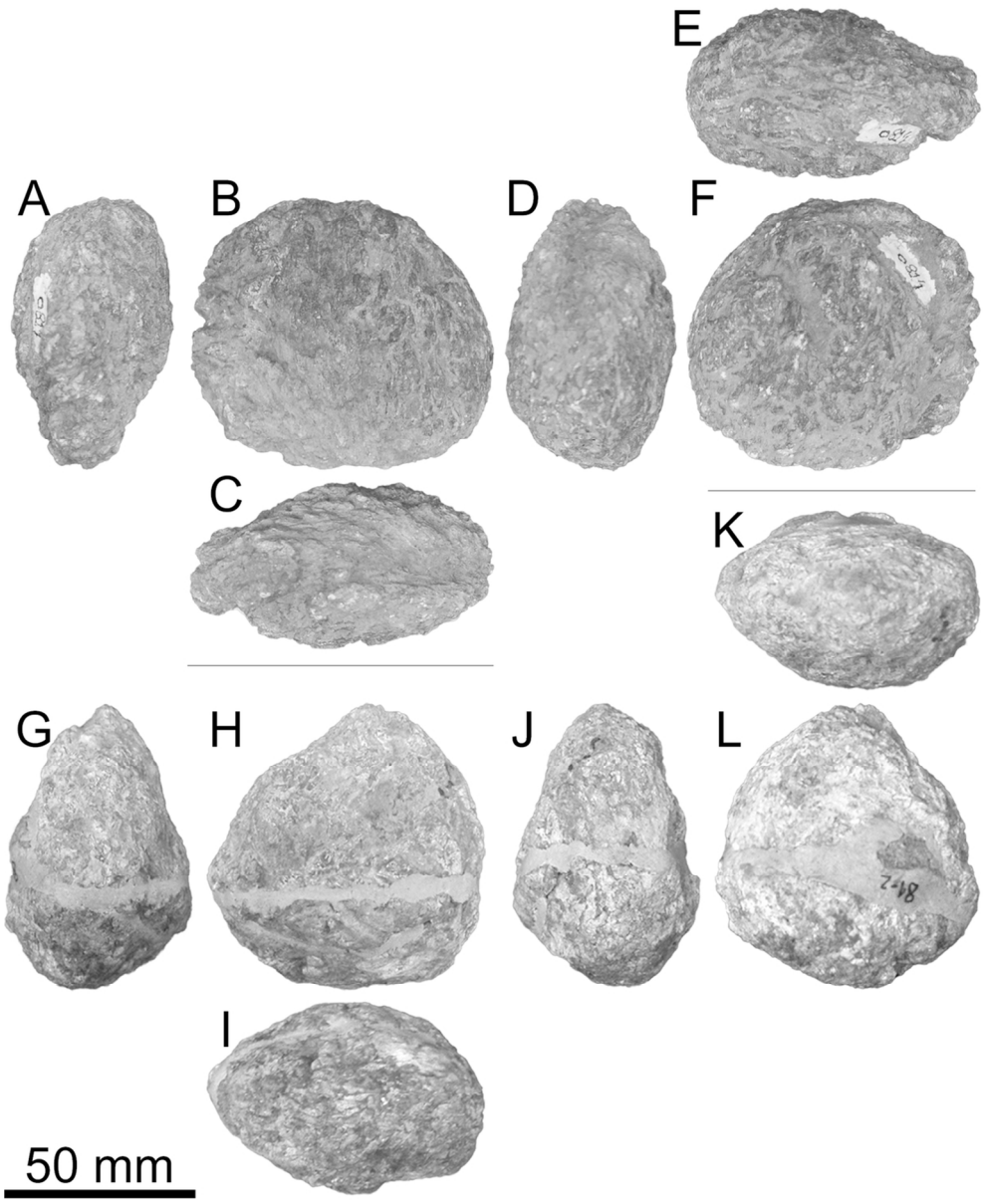

Figure 26. Mendozasaurus neguyelap small osteoderms: IANIGLA-PV 081/1 in A) anterior, B) left lateral, C) ventral, D) posterior, E) dorsal, and F) right lateral views; and IANIGLA-PV 081/2 in G) anterior, H) left lateral, I) ventral, J) posterior, K) dorsal, and L) right lateral views. Scale bar = 50 mm.

103x125mm (300 x 300 DPI)

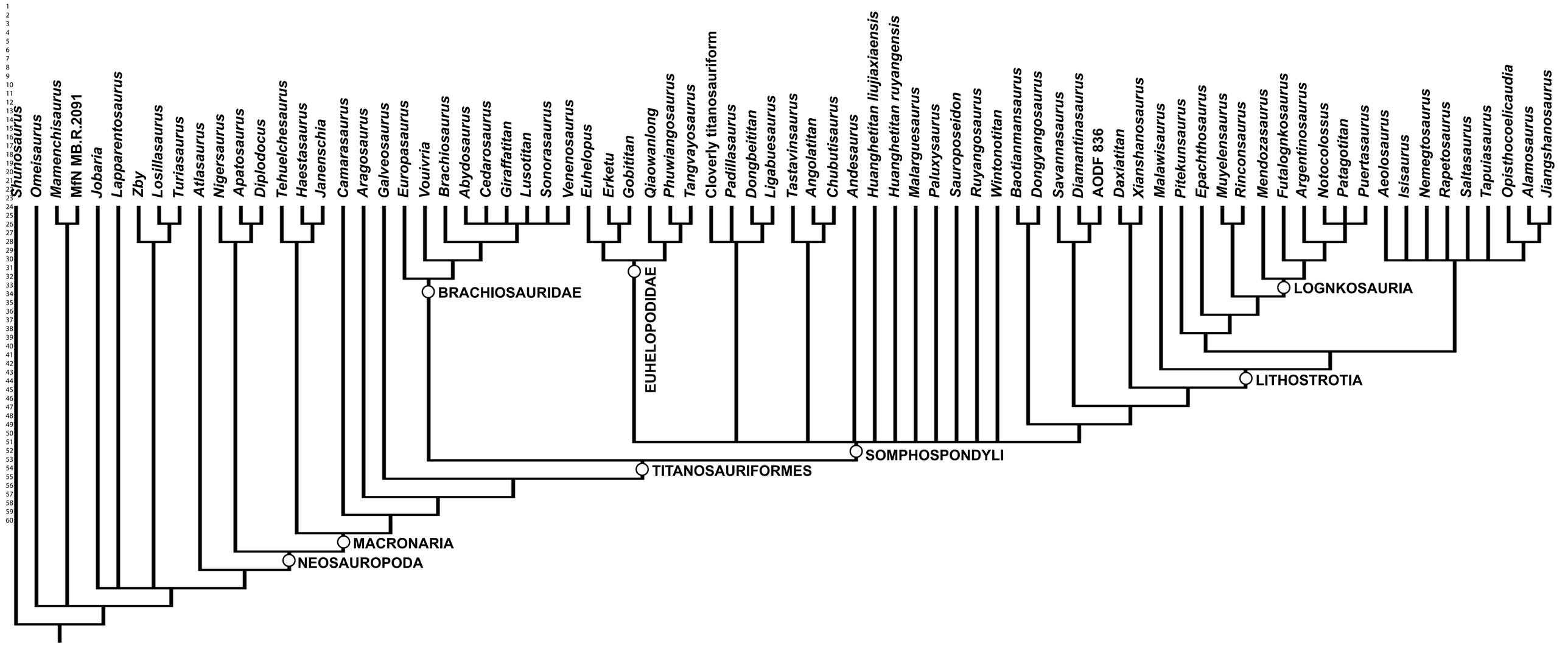
Shunosaurus
Omeisaurus
Mamenchisaurus
MfN MB.R.2091
Jobaria
Lapparentosaurus
Zby
Losillasaurus
Turiasaurus
Atlasaurus
Nigersaurus
Apatosaurus
Diplodocus
Tehuelchesaurus
Haestasaurus
Janenschia
Camarasaurus
Aragosaurus
Galveosaurus
Europasaurus
Vouivria
Brachiosaurus
Abydosaurus
Cedarosaurus
Giraffatitan
Lusotitan
Sonorasaurus
Venenosaurus
Euhelopus
Erketu
Gobititan
Qiaowanlong
Phuwiangosaurus
Tangvayosaurus
Cloverly titanosauriform
Padillasaurus
Dongbeititan
Ligabuesaurus
Tastavinsaurus
Angolatitan
Chubutisaurus
Andesaurus
Huanghetitan liujiaxiaensis
Huanghetitan ruyangensis
Malarguesaurus
Paluxysaurus
Sauroposeidon
Ruyangosaurus
Wintonotitan
Baotianmansaurus
Dongyangosaurus
Savannasaurus
Diamantinasaurus
AODF 836
Daxiatitan
Xianshanosaurus
Malawisaurus
Pitekunsaurus
Epachthosaurus
Muyelensaurus
Rinconsaurus
Mendozasaurus
Futalognkosaurus
Argentinosaurus
Notocolossus
Patagotitan
Puertasaurus
Aeolosaurus
Isisaurus
Nemegtosaurus
Rapetosaurus
Saltasaurus
Tapuiasaurus
Opisthocoelicaudia
Alamosaurus
Jiangshanosaurus
BRACHIOSAURIDAE
EUHELOPODIDAE
LOGNKOSAURIA
LITHOSTROTIA
SOMPHOSPONDYLI
TITANOSAURIFORMES
MACRONARIA
NEOSAUROPODA

CRETACEOUS

EARLY

LATE

BERRIASIAN 145.0

VALANGINIAN 139.4

HAUTERIVIAN 133.9

BARREMIAN 130.8

APTIAN 126.3

ALBIAN 113.0

CENOMANIAN 100.5

TURONIAN 93.9

CONIACIAN 89.8

SANTONIAN 86.3

CAMPANIAN 83.6

MAASTRICHTIAN 72.1

AFRICA

ASIA

AUSTRALASIA

INDIA

NORTH AMERICA

SOUTH AMERICA

TITANOSAURIA

Andesaurus

Baotianmansaurus

Dongyangosaurus

Diamantinasaurus

Savannasaurus

Daxiatitan

Xianshanosaurus

Malawisaurus

Pitekunsaurus

Epachthosaurus

Muyelensaurus

RINCONSAURIA

Rinconsaurus

Mendozasaurus

Futalognkosaurus

LOGNKOSAURIA

Argentinosaurus

Notocolossus

Patagotitan

LITHOSTROTIA

Nemegtosaurus

Tapuiasaurus

Isisaurus

Opisthocoelicaudia

Alamosaurus

Jiangshanosaurus